

**Plasticity of neuronal response properties
in mouse visual cortex
assessed with two-photon calcium imaging**

Dissertation

zur Erlangung des Grades
eines Doktors der Naturwissenschaften

der Fakultät für Biologie
der Ludwig-Maximilians-Universität München

vorgelegt von
Anne Kristina Kreile
Master of Science
26. April 2012

Erstgutachter:

Professor Dr. Mark Hübener

Zweitgutachter:

Professor Dr. Benedikt Grothe

Promotionsgesuch eingereicht am:

26. April 2012

Datum der mündlichen Prüfung:

26. Juni 2012

Ehrenwörtliche Versicherung:

Ich versichere hiermit ehrenwörtlich, dass ich die Dissertation mit dem Titel “Plasticity of neuronal response properties in mouse visual cortex assessed with two-photon calcium imaging“ selbstständig und ohne unerlaubte Beihilfe angefertigt habe. Ich habe mich dabei keiner anderen als der von mir ausdrücklich bezeichneten Hilfen und Quellen bedient.

Erklärung:

Hiermit erkläre ich, dass ich mich nicht anderweitig einer Doktorprüfung ohne Erfolg unterzogen habe. Die Dissertation wurde in ihrer jetzigen oder ähnlichen Form bei keiner anderen Hochschule eingereicht und hat noch keinen sonstigen Prüfungszwecken gedient.

München, 26. April 2012

Anne Kreile

Meinen Eltern

Table of contents

L-1	List of figures	7
L-2	List of tables.....	9
1	Summary	11
2	Abbreviations	13
3	Introduction	15
3.1	Primary visual cortex and experience-dependent plasticity	15
3.1.1	The visual system and basic feature detection.....	15
3.1.2	Orientation selectivity in V1.....	17
3.1.3	Development and plasticity of neuronal response properties	18
3.1.4	Environmental enrichment in learning and plasticity	19
3.1.5	Experience-dependent plasticity of orientation preference	20
3.1.6	Permissive and instructive mechanisms in experience-dependent plasticity	21
3.1.7	Unraveling the role of the visual environment during experience-dependent plasticity	22
3.2	Interactions between V1 and higher visual areas in perception and learning	23
3.2.1	Investigating the role of V1 during learning.....	23
3.2.2	Higher visual areas.....	23
3.2.3	Theories of visual awareness.....	25

Table of contents

3.2.4	Visual perceptual learning	25
3.2.5	Attention	27
3.2.6	Reward signaling.....	27
3.2.7	Reinforcement learning.....	28
3.2.8	Operant conditioning and functional plasticity	30
3.3	Technical advances and impact of study.....	31
3.3.1	Benefits of two photon calcium imaging	31
3.3.2	Aims of study	32
4	Materials and Methods.....	35
4.1	Methods	35
4.1.1	Surgical procedures	35
4.1.1.1	Acute window implantation.....	35
4.1.1.2	Virus injection and chronic window implantation.....	36
4.1.2	Rearing and learning paradigms.....	37
4.1.2.1	Stripe Rearing	37
4.1.2.2	Environmental enrichment.....	38
4.1.2.3	Operant learning	38
4.1.2.3a	Operant chamber.....	38
4.1.2.3b	General training protocol.....	39
4.1.2.3c	Long training regime for single cell assessment of learning-induced changes.....	39
4.1.2.3d	Short training regime for repeated assessment of learning-induced changes in individual neurons.....	40
4.1.3	Two-photon calcium imaging.....	40
4.1.3.1	Anesthesia	40
4.1.3.2	Imaging	40
4.1.3.3	Visual stimulation.....	41
4.1.4	Data analysis	41
4.1.4.1	Analysis of two-photon calcium imaging data	41
4.1.4.1a	Cell detection	41
4.1.4.1b	Orientation tuning	42
4.1.4.1c	Determining stripe rearing effect and horizontal bias in neurons measured with OGB1-AM	42

4.1.4.1d	Determining response properties in repeatedly imaged neurons	43
4.1.4.2	Behavioral data.....	44
4.1.4.2a	Measures of task performance	44
4.1.4.2b	Measures of orientation discrimination performance	44
4.2	Materials.....	45
4.2.1	Cements, Glues & Gels	45
4.2.2	Drugs, Chemicals & Solutions	45
4.2.3	Further equipment.....	46
4.2.4	Instrumentation.....	46
4.2.5	Microscope setup components	47
4.2.6	Operant chamber.....	48
4.2.7	Software.....	49
4.2.8	Tools.....	50
4.2.9	Virus	51
4.3	Solutions	51
4.3.1	Cortex buffer (ACSF - artificial cerebral spinal fluid)	51
4.3.2	Dye buffer	51
5	Results.....	53
5.1	Experience-dependent plasticity of orientation preference in mouse V1.....	53
5.1.1	Stripe rearing using standing and moving gratings	53
5.1.2	Stripe rearing using cylinder lens goggles.....	54
5.1.3	Stripe rearing shifts the distribution of orientation preference towards the experienced orientation	55
5.1.4	Shifts in orientation preference of orthogonal rearing conditions are complementary	58
5.1.5	Fraction of responsive neurons is slightly decreased after stripe rearing.....	59

Table of contents

5.1.6	Stripe rearing effect varies with depth in layer 2/3 and is caused by instructive changes in lower layer 2/3	60
5.1.7	Absolute number of neurons tuned to the experienced orientation increases in lower layer 2/3.....	62
5.1.8	Can the drop in responsiveness explain the specific effect?.....	64
5.1.9	Stripe rearing effect is stable over a range of temporal and spatial frequencies	65
5.1.10	Horizontal bias changes with spatial frequency	67
5.1.11	Depth-dependent horizontal bias in layer 2/3 is also present in an enriched environment.....	68
5.1.12	Synopsis – experience-dependent plasticity of orientation preference	70
5.2	Plasticity of orientation tuning in mouse V1 induced by operant conditioning.....	71
5.2.1	An orientation discrimination task designed for mice.....	71
5.2.2	Mice improve in task performance during a single 10-hour training session.....	73
5.2.3	Mice increase accuracy during training and efficiency after introducing time pressure	77
5.2.4	Performance is limited by mice's orientation discrimination threshold.....	77
5.2.5	Training-induced changes in cortical orientation tuning	79
5.2.6	Adapted orientation discrimination task for combination with repeated calcium imaging	81
5.2.7	Repeated orientation preference measurements in individual neurons using GCaMP3.....	86
5.2.8	Good performers show increased plasticity in orientation preference before training	87
5.2.9	Modulations in response amplitude and tuning width correlate with performance	89
5.2.10	Specific changes of average tuning curves.....	92
5.2.11	Good performers gain more orientation-selective neurons during training	92
5.2.12	Synopsis – plasticity of orientation tuning induced by operant conditioning	95

6	Discussion.....	97
6.1	Experience-dependent plasticity in single V₁ neurons	98
6.1.1	Orientation selectivity in layer 2/3 of mouse V ₁	98
6.1.2	Design and effect of stripe rearing paradigm.....	99
6.1.3	Instructive and permissive environmental effects can be assessed with two-photon calcium imaging	100
6.1.4	Drop in responsiveness and its significance during experience-dependent plasticity	101
6.1.5	Instructive changes during experience-dependent plasticity.....	102
6.2	Plasticity of orientation tuning in individual V₁ neurons induced by learning.....	103
6.2.1	Visual discrimination learning in mice	104
6.2.2	Design of an effective learning paradigm for mice using operant conditioning....	104
6.2.3	Additional factors affecting task performance and learning	106
6.2.4	Elusive role of V ₁ in visual perceptual learning and memory	107
6.2.5	Repeated calcium imaging of orientation tuning in individual neurons using GCaMP ₃	108
6.2.6	Adapted training paradigm for repeated calcium imaging.....	109
6.2.7	Increased stability of orientation preference during training	110
6.2.8	Functional changes in individual neurons during training	111
6.2.9	Reward coding in V ₁	113
6.2.10	Learning-related plasticity in V ₁	114
6.3	Synopsis - experience-dependent and learning-induced plasticity in V₁ neurons	115
7	References.....	117
8	Acknowledgements	139

List of Figures

Figure 1:	The mouse visual system.....	16
Figure 2:	Permissive and instructive changes can explain the effects of stripe rearing	21
Figure 3:	Potential pathways for top-down signaling to V1.	29
Figure 4:	Stripe rearing using standing and moving gratings	54
Figure 5:	Stripe rearing using cylinder lens goggles.....	55
Figure 6:	Two-photon calcium imaging of orientation selectivity	56
Figure 7:	Orientation preference in the primary visual cortex of control and stripe-reared mice.....	58
Figure 8:	Shifts in distribution of preferred orientations after stripe rearing are complementary	60
Figure 9:	Effect of stripe rearing on the fraction of responsive neurons.....	61
Figure 10:	Horizontal bias and permissive effect depend on depth in layer 2/3	61
Figure 11:	Stripe rearing has a stronger effect on neurons in lower layer 2/3.....	62
Figure 12:	Global specific effect of stripe rearing at different depths of layer 2/3.....	63
Figure 13:	No correlation between change in responsiveness and specific stripe rearing effect.....	64
Figure 14:	Response properties in stripe-reared and control mice characterized with gratings of different spatial and temporal frequencies	66
Figure 15:	Enriched environment	68
Figure 16:	Distribution of preferred orientations of mice raised in an enriched environment.....	69
Figure 17:	Mouse solving a visual task in the operant chamber	71

List of Figures

Figure 18:	Mouse training protocol for the visual task	72
Figure 19:	Improvement within single training sessions	74
Figure 20:	Improvement over sessions	76
Figure 21:	Performance depends on the difference between target and non-target orientation	79
Figure 22:	Distribution of preferred orientations after training with a vertical target	80
Figure 23:	Tuning width and response amplitude after training on a vertical target	81
Figure 24:	Modified training protocol compatible with chronic calcium imaging	83
Figure 25:	Imaging orientation preference with the genetically encoded calcium indicator GCaMP ₃	84
Figure 26:	Repeated two-photon calcium imaging in mouse V ₁	85
Figure 27:	Changes in orientation preference of individual neurons over time in good and bad performers	87
Figure 28:	Changes in neuronal response properties before, during and after learning in good and bad performers	88
Figure 29:	Correlations between performance and learning-induced changes in neuronal response properties	90
Figure 30:	Changes in orientation tuning curves before, during and after training	91
Figure 31:	Learning induced changes in selectivity in individual neurons	93

List of tables

Table 1: Average performance assessed every two hours during training B in ten mice 73

Table 2: Average frequency of target and non-target responses assessed every five minutes during the first 20 minutes of training D in 14 mice..... 75

Table 3: Average performance assessed every two hours during training D in 14 mice 75

Table 4: Average performance during training and food retrieval phase assessed every 2.5 days in 14 mice.....78

Summary

Neurons in the mammalian primary visual cortex (V_1) respond to contours in the visual field, and, for most cells, response strength depends on contour orientation. This property, orientation selectivity, can develop without any visual input. However, orientation selectivity is plastic, and it can be modified by visual experience. In this thesis, I have investigated two types of functional plasticity, namely experience-dependent and learning-induced plasticity.

Experience-dependent plasticity of orientation preference can be induced by stripe rearing. In this paradigm, an animal is exposed to contours of only a single orientation, causing an over-representation of the experienced orientation in the visual cortex. Two competing hypotheses have been put forward to explain this effect: The permissive hypothesis proposes that neurons, which are not tuned to the experienced orientation, lose responsiveness, leaving only neurons, which are driven by the experienced orientation. In contrast, the instructive hypothesis suggests that neurons actively change their preferred orientation towards the experienced one. Accordingly, the permissive hypothesis predicts a drop in the number of responsive neurons, which would not be expected, if the instructive hypothesis was true. In order to solve this issue, I took advantage of two-photon calcium imaging, a method which allows reliably determining the fraction of responsive neurons. Mice were stripe reared for three weeks with goggles containing cylinder lenses. Subsequent two-photon calcium imaging using the synthetic calcium sensor OGB1-AM revealed a dominant role of instructive mechanisms during stripe rearing in layer 2/3 of mouse V_1 . More specifically, the stripe rearing effect was depth-dependent: In lower layer 2/3, the absolute number of neurons preferring the experienced orientation increased, indicating an instructive change. In upper layer 2/3, the fraction of responsive neurons dropped slightly, but this drop was not correlated with the

magnitude of the stripe rearing effect in individual mice. Thus, permissive effects cannot be completely excluded, but the slight decrease in responsiveness is unlikely to cause the overall stripe rearing effect. Rather, instructive effects, for example a change in the preferred orientation of individual neurons, underlie the stripe rearing effect in mouse visual cortex.

Learning-induced plasticity in the visual system can be elicited by a modified assignment of behavioral relevance to a visual stimulus. However, whether early sensory areas such as V1 are involved in learning is highly controversial. Hierarchical models of the visual system assign a mainly infrastructural role to V1, merely distributing incoming visual signals to higher cortical areas. Interactive models view V1 as part of a recurrent network, thus permitting top-down modifications of neuronal response properties in V1. In order to measure functional changes in V1 during learning, I trained mice on an orientation discrimination task using reward-based operant conditioning. Before and after training, I performed two-photon calcium imaging using the genetically encoded calcium indicator GCaMP3 to measure changes in orientation tuning in the same neurons over a period of 12 days. I found a clear correlation between the performance of individual mice on the task and changes in response amplitude in neurons with certain preferred orientations. This suggests that the task-specific, selective re-weighting of visual input during perceptual learning proposed by some models actually may occur already in V1. Furthermore, mice performing well on the task gained orientation-selective neurons, most of which were tuned to the rewarded and the orthogonal orientation. Similarly, in these mice, neurons preferring the orthogonal orientation increased tuning width during training. Taken together, these data support a facilitated categorization of visual stimuli based on the ratio of population activity in neurons preferring the target orientation and neurons preferring a wide range of non-target orientations. This interpretation is in line with the reverse hierarchy theory of visual perceptual learning, which predicts increasing feature separation during learning.

In this study, I have demonstrated that orientation tuning in mouse primary visual cortex is very dynamic. It can be altered by the visual environment and is modified by assignment of behavioral relevance to a visual feature. This high adaptability of neurons in V1 apparently plays a central role in optimizing proper detection and interpretation of features in the visual world.

Abbreviations

AAV	adeno-associated virus
AC.....	accuracy
ACSF	artificial cerebrospinal fluid
ANOVA	analysis of variance
BDNF	brain-derived neurotrophic factor
cpd	cycles per degree
DMSO	dimethyl sulfoxide
dO	differential orientation
dPO	differential preferred orientation
dpt.....	diopters
EF	efficiency
FEF	frontal eye field
fMRI	functional magnetic resonance imaging
GABA	γ -aminobutyric acid
HEPES.....	4-(2-hydroxyethyl)-1-piperazineethanesulfonic acid
HLS	hue, lightness and saturation
IT.....	inferior temporal cortex
LGN.....	lateral geniculate nucleus
LIP.....	lateral intraparietal area
LPFC.....	lateral prefrontal cortex

Abbreviations

LTD	long term depression
LTP	long term potentiation
MD	monocular deprivation
MST.....	medial superior temporal area
MT.....	middle temporal area
NA.....	numerical aperture
NMDA.....	N-Methyl-D-aspartate
NR2A.....	NMDA receptor subunit 2A
NR2B.....	NMDA receptor subunit 2B
OD	ocular dominance
OGB1-AM.....	Oregon Green BAPTA-1, AM
p	postnatal day
RD	response delay
REM	rapid-eye-movement
RY.....	reward yield
SEM.....	standard error of the mean
SR101.....	Sulforhodamine 101
V1.....	primary visual cortex
VPL.....	visual perceptual learning

Introduction

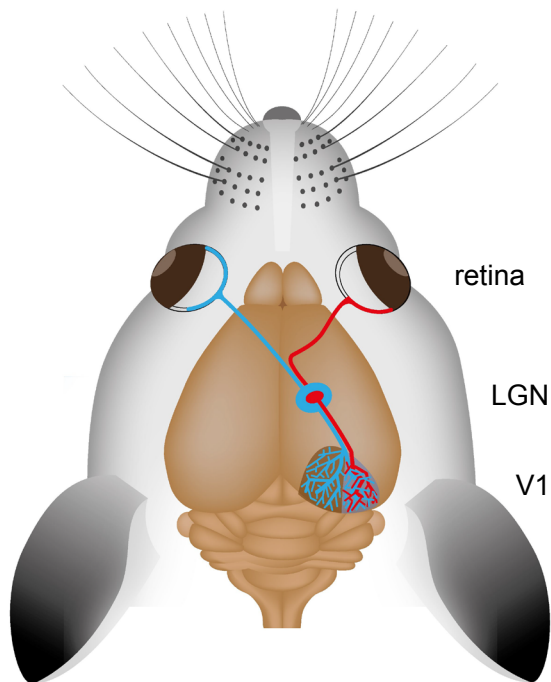
3.1 Primary visual cortex and experience-dependent plasticity

3.1.1 The visual system and basic feature detection

A large part of human perception of the world relies on vision. The mammalian visual system is a highly developed part of the brain which has been intensively investigated for decades. Especially the early processing stages for visual information have been described in great detail. Briefly, light is transduced into neuronal signals in the photoreceptors of the retina which, via several different cell types, pass signals on to retinal ganglion cells. About 90% of the retinal ganglion cells project via the thalamic lateral geniculate nucleus (LGN) to primary visual cortex (V₁)^{1, 2}, the first area in the cortex where visual information is processed. In V₁, excitatory neurons in six cortical layers are connected in a canonical circuit common to many cortical areas. Specifically, excitatory neurons in layer 4 receive input from LGN^{3, 4} and synapse onto layer 2/3 neurons⁵ which then connect to layer 5 neurons¹. Layer 5 neurons project to layer 6 neurons which then connect back to layer 4 neurons¹. The axonal projections originating from different layers differ in their main projection targets: Layer 2/3 sends out cortico-cortical projections^{5, 6}. Layer 5 is the main output layer with connections to subcortical structures⁷, mainly the superior colliculus^{6, 8, 9}, the lateral posterior nucleus of the thalamus¹⁰, and the pons¹¹. Layer 6 provides feedback connections to the LGN^{5, 6, 12, 13}. Layer 1 mainly contains distal tufts of pyramidal apical dendrites receiving feedback connections from other cortical regions and subcortical nuclei⁷.

In the visual system, neurons are driven by visual stimuli within a spatially defined area of the visual field, termed the receptive field¹⁴. Topography of the visual input is main-

tained through large parts of the visual system^{15, 16}, such that the receptive fields of neurons are arranged within an orderly retinotopic map in V1¹⁷. In V1, neurons can receive input from mainly the contralateral, the ipsilateral or both eyes and accordingly differ in ocular dominance. In primates^{18, 19}, cats²⁰ and ferrets²¹, ocular dominance is represented in a columnar structure. Mouse V1 is separated into a monocular and a smaller binocular area (Fig. 1). In monocular V1, neurons receive input from the contralateral eye, while neurons in binocular



V1 are driven by both eyes^{22, 23}. Most neurons in V1 respond to specific features of a visual stimulus such as orientation, direction, spatial and temporal frequency, and speed²⁴⁻²⁶. Thus, neurons in V1 are believed to act as basic feature detectors. In primates²⁷, cats²⁸ and ferrets²⁹, neurons are sharply tuned to stimulus orientation, and orientation preference is represented in an orderly map arranged in a pinwheel-like fashion^{30, 31}. Moreover, the retinotopic map, the ocular dominance map and

Figure 1: The mouse visual system. Schematic of the mouse visual system (from Levelt and Hübener³²²): Axons of retinal ganglion cells, processing visual input from the central (*red*) and the peripheral (*blue*) field of view, form the optic nerve. Ganglion cells in the nasal part of the retina (*blue*) send their axons across the midline to the contralateral hemisphere at the optic chiasm, while axons from a very small number of temporal ganglion cells (*red*) remain on the ipsilateral side of the brain. Retinal ganglion cell axons terminate in the lateral geniculate nucleus (LGN), where ipsilateral (*red*) and contralateral (*blue*) inputs remains segregated. From the LGN, neurons project to the primary visual cortex (V1), which is subdivided into a monocular (*blue*) and a binocular (*blue-red*) region. Monocular V1 receives input from the contralateral eye only, while binocular V1 processes input from both eyes.

the orientation selectivity map are arranged relative to each other in a way that optimal coverage of the stimulus space on the single neuron level is achieved^{32, 33}. In rodents, orientation tuning is equally precise²⁵. However, instead of an orderly map, orientation preference is organized in a salt-and-pepper arrangement^{22, 34, 35} with cells having very different preferred orientations located next to each other.

3.1.2 Orientation selectivity in V1

Orientation selectivity, beside ocular dominance, is a thoroughly characterized neuronal response property and a well-established model system for experience-dependent plasticity, which I employed in this study. Orientation-selective neurons, first described by Hubel and Wiesel²⁸, are best driven by stripes, contours or gratings of a particular orientation in the visual field. Orientation preference was proposed by Hubel and Wiesel to arise through patterned feedforward connectivity of neurons projecting from LGN to V1²⁸. Specifically, neurons in the retina and LGN mostly have concentric receptive fields with an antagonistic center-surround organization. According to Hubel and Wiesel²⁸, neurons in layer 4 of V1 receive input from LGN neurons, the receptive fields of which are arranged along one axis in visual space. Evidence for this hypothesis was provided only decades later^{29, 36, 37}. Still, other, only partially understood, mechanisms seem to contribute to the generation of orientation selectivity. Local connectivity – particularly lateral inhibition, but also excitatory connections – within V1 plays an important role in sharpening orientation tuning³⁸⁻⁴⁰. Excitatory neurons in V1 typically show horizontal connections preferably with neurons sharing the same orientation preference⁴¹⁻⁴³. Nevertheless, excitatory V1 neurons receive a relatively broad excitatory synaptic input⁴³⁻⁴⁵, which is strongest at its preferred orientation^{44, 46}. The inhibitory synaptic input to excitatory V1 neurons is tuned even more broadly^{25, 47-49} and is also strongest at their preferred orientation^{44, 46}. In mouse V1, the interplay of inhibitory and excitatory input has recently been shown to account for a sharpening of orientation tuning⁴⁴.

Two types of orientation selective neurons are known, which differ in the phase-dependence of their response to moving gratings: Simple cells have an elongated receptive field with separate ON and OFF fields arranged side by side. In contrast, complex cells typically

have a homogeneous receptive field without separate ON and OFF sub-fields and therefore show, other than simple cells, a phase-invariant response to moving gratings²⁸. Cat layer 2/3 almost exclusively contains complex cells. In addition, complex cells are found in layers 5 and 6. Layer 4 mainly contains simple cells, which are also located in layer 6 and deeper layer 3^{28, 50}.

Orientation tuning is typically different in excitatory and inhibitory neurons. In mice, most studies agreed on inhibitory neurons being much more broadly tuned than excitatory neurons^{25, 47, 48}. Consistent with this observation, inhibitory neurons receive strong synaptic input from nearby pyramidal cells with diverse stimulus preferences⁴⁹. Note, however, that another study detected a population of sharply tuned inhibitory neurons⁵¹. In addition, excitatory and inhibitory neurons differ in firing rate. Multiple recordings have shown, that putative inhibitory units typically have higher firing rates than putative excitatory units^{25, 52, 53}.

3.1.3 Development and plasticity of neuronal response properties

Orientation selectivity is not fully established from birth, but rather matures after eye-opening⁵⁴⁻⁵⁸. In principle, orientation selectivity can develop in the absence of any visual input. However, while the orientation map's spatial layout remains largely unaffected in dark-reared cats and ferrets⁵⁹⁻⁶¹, single neurons show immature, broad orientation tuning^{56, 59, 61}. In contrast, orientation tuning in mouse V1 is hardly affected by dark-rearing⁵⁴. During the critical period, a phase of enhanced plasticity in development^{62, 63}, orientation tuning is adjusted to binocular vision through alignment of orientation preference between synaptic inputs from the ipsi- and the contralateral eye⁶⁴. Thus, visual input is crucial for a full maturation of orientation selectivity.

A striking example demonstrating the importance of visual experience for maturation of neuronal response properties is the induction of direction selectivity by repeated presentation of moving gratings in ferrets^{65, 66}. However, direction selectivity in mouse V1 seems to develop independent of visual input⁵⁴. The influence of visual experience on neuronal response properties is largest during the critical period^{63, 67}. In mice, the critical period peaks around the age of postnatal day (p) 30 as revealed by monocular deprivation (MD) experi-

ments, the temporal closure of one eye, inducing ocular dominance (OD) plasticity⁶³. During development, the critical period is induced by a change in levels of the neurotrophic factor BDNF⁶⁸ and GABAergic inhibition⁶⁹ and is characterized by an exchange of NMDA receptor subunit NR2B to NR2A, which, however, is irrelevant to critical period expression in the visual cortex⁷⁰. Dark-rearing delays inhibitory maturation⁷¹, facilitates long-term potentiation (LTP, synaptic strengthening) and reduces long-term depression (LTD, synaptic weakening) in visual cortical neurons^{72, 73} leading to a prolonged critical period. OD plasticity can also be induced in adult mice; however, it is slower and is based on different mechanisms⁷⁴⁻⁷⁷. Compared to mice, adult cats and primates show substantially less adult plasticity⁷⁸.

3.1.4 Environmental enrichment in learning and plasticity

In addition to the specific visual experience, also the environment, in which an animal is raised, has a strong impact both on the maturation of the visual system and on neuronal plasticity in adult mice. Environmental enrichment as a testable scientific concept was introduced by Rosenzweig⁷⁹. To implement ‘a combination of complex inanimate and social stimulation’⁸⁰, animals are raised in large groups living in cages with spatial complexity and equipped with a variety of objects, such as toys, tunnels, nesting materials, shelters and stairs. Central to the concept of environmental enrichment is the opportunity for voluntary physical exercise such as in running wheels or on climbing devices⁸¹.

In response to environmental enrichment, the expression levels of several dozens of genes change, amongst them genes involved in neuronal structure, synaptic transmission and plasticity, neuronal excitability and neuroprotection^{82, 83}. In mice raised in an enriched environment, the maturation of the visual system is strongly accelerated⁸⁴, the critical period presumably closes earlier⁸⁵ and visual acuity in adult mice is higher compared to mice raised under standard housing conditions⁸⁶. The effects of dark-rearing on visual system development can be entirely prevented by concurrent environmental enrichment⁸⁷. In amblyopic adult rats, which had undergone monocular deprivation as juveniles, visual acuity and ocular dominance was completely recovered after environmental enrichment⁸⁸. A very high level of plasticity was induced in these adult rats, potentially caused by a marked reduction of

cortical inhibition⁸⁸. Consistent with these findings, environmental enrichment enhances learning and memory in mice^{89, 90}, an effect which I employed in this thesis during operant conditioning of mice.

3.1.5 Experience-dependent plasticity of orientation preference

As discussed above, orientation selectivity is plastic and modified by visual experience^{91, 92}. Three lines of experimental evidence motivated the assumption that experience-dependent plasticity of orientation tuning results in an optimization of orientation discrimination: Firstly, as discussed above, during the critical period, orientation selectivity is optimized for binocular vision⁶⁴. Secondly, the distribution of preferred orientations in visual cortex is modified during development⁹³⁻⁹⁵ and finally matches visual scene statistics^{96, 97} such that cardinal orientations ([horizontal and vertical](#)) are over-represented. Finally, an increased number of neurons preferring a certain orientation correlates with a more precise discrimination in that orientation range^{98, 99}. Along this line, the over-representation of cardinal orientations in the visual cortex was suggested as the neuronal correlate of the so-called ‘oblique effect’¹⁰⁰, terming the better performance at cardinal compared to oblique orientations in a number of tasks, among them spatial acuity¹⁰¹, contrast sensitivity¹⁰², or orientation discrimination¹⁰³. Additional experience-dependent specialization has been shown to occur in humans: They can better discriminate angles which are present in italic letters compared to orthogonal orientations¹⁰⁴.

A potent paradigm for inducing experience-dependent plasticity of orientation preference in a defined and controllable experimental setting is stripe rearing. During stripe rearing, animals’ visual input is restricted to contours of only one single orientation, the experienced orientation. In the first experiments carried out in the early 70’s, cats were placed in large cylinders with a striped wall and a mirror floor¹⁰⁵. Other approaches involved goggles with striped screens⁹² or cylinder lenses¹⁰⁶. In cats, ferrets and more recently also rats, an over-representation of the experienced orientation in the visual cortex after stripe rearing was demonstrated using single unit recordings^{92, 107, 108} and intrinsic signal imaging^{108, 109}, a method based on changes in light reflectance of brain tissue during neuronal activation.

3.1.6 Permissive and instructive mechanisms in experience-dependent plasticity

Following the first stripe rearing studies, a controversy started on whether the visual environment induces plasticity instructively or permissively^{91, 110-112}. A permissive mechanism leads to the silencing of neurons which are not driven during the period of altered visual input. An example for a permissive change in cortical neurons is the rapid loss in responsiveness to deprived eye stimulation shortly after monocular deprivation in young mice⁷⁸. These changes are most likely caused by LTD due to the decorrelation of neuronal firing¹¹³. In addition, also pruning of synapses is observed¹¹⁴. In the context of stripe rearing, the permissive hypothesis predicts that neurons not preferring the experienced orientation loose responsiveness¹¹⁰ (Fig. 2). This would lead to a decrease in the fraction of responsive neurons

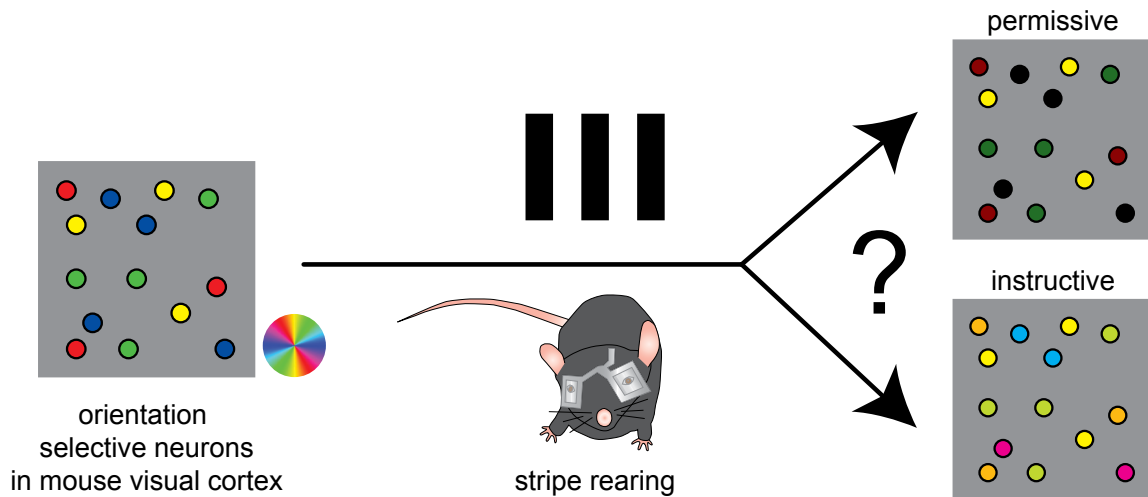


Figure 2: Permissive and instructive changes can explain the effects of stripe rearing. Permissive and instructive effects illustrated on the population level. *Colored dots* represent orientation-selective neurons as indicated by the *legend (colored wheel)*. In case of a permissive change, stripe rearing causes neurons not preferring the experienced orientation (*here: vertical/ yellow*) to cease responding (*black dots*), leading to a relative over-representation of the experienced orientation and an overall decrease in the fraction of responsive neurons. In case of an instructive change, many neurons change their preferred orientation towards the experienced one, again leading to a relative over-representation of the experienced orientation, but without a change in the fraction of responsive neurons.

after stripe rearing. Of the remaining neurons, a larger fraction would prefer the experienced orientation, leading to the observed over-representation.

In contrast, the instructive hypothesis predicts that, during stripe rearing, neurons in V1 are instructed by the visual input to actively change their orientation preference such that they match the experienced orientation¹⁰⁸ (Fig. 2). By pairing a specific visual stimulus, a grating of a certain orientation, with local cortical electrical stimulation, scientists have demonstrated that in principle neurons are capable of changing their orientation preference¹¹⁵⁻¹¹⁷. The change in preferred orientation could be achieved by a response potentiation of active inputs mediated through LTP in response to temporal correlation between inputs^{118, 119}. Alternatively, attention or reward could play a role. However, the latter mechanisms would require some form of top-down signaling which weights incoming visual signals¹²⁰.

3.1.7 Unraveling the role of the visual environment during experience-dependent plasticity

In order to address this issue, specifically, whether the visual environment has an instructive or permissive effect on primary visual cortex during experience-dependent plasticity, I developed a stripe rearing paradigm for mice. To this end and based on previous approaches in cats¹¹² and rats¹⁰⁹, I designed goggles for mice containing cylinder lenses. Using the synthetic calcium indicator Oregon Green BAPTA-1, AM (OGB1-AM), I measured orientation selectivity in V1 neurons with two-photon calcium imaging. Consistent with previous studies, I observed an over-representation of the experienced orientation after stripe rearing. By quantifying the fraction of responsive neurons and the fraction of neurons preferring the experienced orientation, both in stripe-reared and control mice, I observed a dominant role of instructive mechanisms during experience-dependent plasticity of orientation selectivity in layer 2/3 of mouse V1. In addition, the effect of stripe rearing on orientation selectivity and preference varied depending on depth within layer 2/3.

3.2 Interactions between V1 and higher visual areas in perception and learning

3.2.1 Investigating the role of V1 during learning

The first part of this thesis is concerned with the question of how the input statistics of oriented contours shape the representation of orientation selectivity in V1. In a given visual environment, these statistics remain, on a long term, stable. However, during ongoing learning, animals collect information about the behavioral relevance of visual features, for example in indicating food or threat. While the involvement of higher sensory and frontal areas in learning are evident, it remains controversial, whether and in which way such a learned assignment of behaviorally relevant information to a visual stimulus affects neuronal response properties in low sensory areas such as V1¹²⁰⁻¹²². Particularly, direct evidence demonstrating functional changes in individual V1 neurons during learning is lacking thus far. Therefore, I used repeated two-photon calcium imaging to quantify changes in orientation selectivity in individual neurons occurring during operant conditioning of mice on a visual orientation discrimination task. The data revealed potential roles of V1 in discrimination learning ranging from an orientation reference system over weighting of incoming information to facilitated categorization leading to feature separation in higher visual areas.

3.2.2 Higher visual areas

Orientation tuning can not only be changed by exposure to a specific stimulus as in stripe rearing, but has also been demonstrated to be plastic during learning¹²³⁻¹²⁵. In many forms of learning, the dopaminergic reward system, the attention system and higher sensory areas are involved¹²⁰. In primates and cat, V1 projects to several extrastriate visual areas, such as V4 and middle temporal area (MT)^{126, 127}, which further compute the visual input and receive their major input either directly or indirectly from V1. This central position of V1 is revealed by V1 lesions which lead to cortical blindness in humans¹²⁸. In primates, extrastriate visual areas have been assigned to two functional pathways. The dorsal pathway performs motion processing in several areas including MT and medial superior temporal area (MST).

The ventral pathway is specialized for detailed feature detection and comprises, amongst others, areas V4 and inferior temporal cortex (IT)¹²⁹.

Very recently, extrastriate visual areas in the mouse have been investigated in more detail. They are arranged around V1, all receiving direct input from V1¹⁵, other than primate extrastriate visual areas, of which only V2, V3, V4 and MT receive direct input from V1¹²⁶. In mice, many extrastriate areas display unique combinations of stimulus preferences, including orientation and direction, temporal and spatial frequency, and speed^{16, 24}. Analogous to primates (and to some degree, cats), a segregation into ventral and dorsal pathways was proposed also for the mouse visual system based on anatomical¹³⁰ and functional¹⁶ data. Areas AL, RL and AM were assigned to motion processing because of their strong direction selectivity and a preference for high temporal frequencies or high speeds. Areas LI and PM were assigned to feature detection because of their preference for high spatial frequencies and low speeds^{16, 24}.

Some extrastriate areas in primates, including V4 and MT, directly project to areas in the parietal and frontal lobes, which are involved in attention, visual working memory and motor planning¹³¹. The ventral pathway, together with some multimodal higher cortical areas, projects via TE in the ventral inferior temporal cortex to the perirhinal cortex in the medial temporal lobe¹³². Perirhinal cortex is involved in visual memory and most likely also in processing complex information about objects¹³². The hippocampus, another structure in the medial temporal lobe, is, beside memory formation, dedicated to spatial processing¹³². The traditional hierarchical view on sensory memory formation and retrieval attributes both to processes in the hippocampus or in “association” cortical areas, such as inferior temporal, posterior parietal, and prefrontal cortex¹³³. However, this view has been challenged by several fMRI studies in humans reporting on evidence for an involvement of lower visual areas in visual working memory¹³⁴ and memory retrieval¹³³. These findings support the hypothesis, that sensory information is stored within distributed networks spanning diverse cortical areas¹³³.

Visual areas are usually connected reciprocally, that is, both feedforward and feedback connections exist. V1 receives feedback from a number of areas to which it does not

project directly, such as MST, lateral intraparietal area (LIP) and frontal eye field (FEF)^{127, 135}. Taken together, this indicates a close interaction between V₁ and extrastriate areas during visual information processing. Hypotheses on the function of recurrent connections between extrastriate areas and V₁ range from feedback signaling, by which reliability of information is increased, over top-down modulations of V₁ activity to perceptual grouping or attentional selection¹³¹. Moreover, embedded in this recurrent network, V₁ neurons could represent an indexing system for perceptual binding¹³⁶ of disparate types of information that are analyzed in separate visual areas¹³¹.

3.2.3 Theories of visual awareness

While interactions between V₁ and higher visual areas are evident, the role of V₁ in higher-order visual computations involving cognitive processes, such as visual awareness, is controversially discussed. Hierarchical models and interactive models formulate two fundamentally different views. According to hierarchical models^{137, 138}, V₁ simply acts as a gateway for the information flow to higher cortical areas, where analysis of visual input is performed with increasing levels of complexity and specificity. As V₁ does not directly project to prefrontal cortex, hierarchical models assume that V₁ does not directly contribute to visual awareness. Rather, extrastriate areas including V₄, MT and IT are thought to represent conscious information about color, motion and object identity, respectively¹³⁹⁻¹⁴².

Conversely, interactive models¹⁴³⁻¹⁴⁵ suggest that V₁ forms dynamic recurrent circuits with extrastriate areas and thereby directly participates in visual awareness. Sustained activity between extrastriate areas and V₁ is proposed to be necessary for the maintenance of visual representation in awareness. V₁ is assumed to gate information flow to prefrontal cortex by supporting or not supporting information represented in extrastriate areas. Alternative theories consider consciousness as a product of a dynamic, global neuronal workspace¹⁴⁶ in which potentially any given brain region can participate in awareness by spreading its information.

3.2.4 Visual perceptual learning

Awareness and perception of visual information are substantially modulated by learning. Visual perceptual learning (VPL) is a continuous process occurring during day-

to-day visual experience thereby shaping our ability to detect ecologically relevant elements and features^{122, 147}. In a defined experimental setting, VPL leads to a long-term enhanced performance on a visual task¹²⁰. From a mechanistic viewpoint, VPL is conceptualized as a task-specific selective re-weighting of specific visual stimuli¹⁴⁸⁻¹⁵⁰. In this context, VPL is thought to induce task-specific changes in the strength of neural connections between the representational level in lower visual areas and higher cortical areas concerned with stimulus interpretation and decision making.

VPL has been shown to change neuronal response properties both in higher visual areas such as in V4, but also in V1. In primate V1, orientation discrimination learning affected orientation tuning. Tuning curve steepness increased such that neurons became better detectors for differences in the trained range of orientations¹²³. In a study conducted by Karni and Sagi, VPL was shown to be specific to the trained eye¹⁵¹. As monocular processing mainly occurs in V1 (or earlier), this study provides further indirect evidence for the involvement of V1 in VPL. In other cases, VPL transferred to untrained features¹⁵² or locations¹⁵³, indicating an involvement of higher visual areas. In line with this finding, V4 neurons in primates had increased response amplitudes, responded less variably and showed narrower orientation tuning after training on an orientation discrimination task^{124, 125, 154}. Changes were mainly found in those neurons which coded the most relevant information¹²⁴.

It is commonly assumed that VPL requires conscious effort^{155, 156}. The ‘reverse hierarchy theory of VPL’¹²² describes VPL as an increasing optimization in the use of task-relevant information which is guided by a sequence of top-down modifications. According to this theory, first high-level, then lower-level task-relevant information is amplified, while irrelevant information is suppressed¹⁴⁸. Along those lines, VPL could only be induced by a difficult task, after VPL on an easier task occurred¹⁵⁷. In fact, Pavlov was the first to describe the importance of beginning training with easy conditions (‘transfer along continuum’)¹²². Moreover, many studies provide evidence, that learning easy tasks mainly involves higher visual areas, while difficult conditions are rather learned at lower visual areas^{123, 125, 152, 157, 158}. However, there is evidence that also implicit processing without conscious effort happens both during and after training¹²⁰.

The memories, newly formed during learning, are subsequently stabilized. This so-called consolidation of memories takes place both immediately after training¹⁵⁹ and during subsequent sleep¹⁶⁰ (see also Frank and colleagues¹⁶¹). An initial phase of consolidation starts and is completed within one hour after training on a perceptual task¹⁵⁹. Further consolidation takes place both during rapid-eye-movement (REM) and non-REM sleep¹⁶²⁻¹⁶⁴ and involves highly localized low-level processing regions. For example, several functional magnetic resonance imaging (fMRI) studies observed sleep-induced VPL in V₁¹⁶⁵⁻¹⁶⁷.

3.2.5 Attention

While the effectiveness of the visual system can benefit from adaption to novel visual environments, the brain at the same time has to ensure sufficient functional stability for reliable information processing¹⁶⁸. In this context, attention restricts plasticity to relevant features^{123, 169}. Visual attention can be directed to a certain object, feature or area in the visual field¹³¹. Attention-controlling areas, such as the lateral prefrontal cortex (LPFC), enhance signals directed to a specific neuronal population in the brain, thereby increasing its functional weight^{170, 171}. These areas in addition actively suppress irrelevant features (attentional inhibition)^{170, 172}. Attentional modulations of neuronal activity are detectable in higher and lower visual areas. Initial electrophysiological studies mainly found effects in extrastriate visual areas, such as V₄¹⁷³. More recent studies reported attentional modulation also in V₁¹⁷⁴⁻¹⁷⁶. In addition, several fMRI studies confirmed strong attentional modulations in V₁ depending on visual task¹⁷⁷, spatial locus¹⁷⁸⁻¹⁸⁰ and feature¹⁸¹. V₁ activity was proposed to reflect the perceptual saliency of visual stimuli^{182, 183}. However, attentional effects in V₄ and IT precede attention-related signals in V₁, indicating that attentional modulation in V₁ arises from feedback signaling from higher visual areas¹⁸⁴. Consistent with this, attentional modulation in V₁ can occur during anticipation of a visual stimulus in the absence of visual stimulation¹⁸⁵.

3.2.6 Reward signaling

Other than attention, which affects specific neuronal populations, reward triggers spatially distributed signals which boost both relevant and irrelevant features of incoming sensory signals¹⁸⁶. The reward circuit (Fig. 3) includes frontal cortex, perirhinal cortex,

amygdala and striatum in the telencephalon, lateral hypothalamic area in the diencephalon, substantia nigra and ventral tegmental area in the mesencephalon (midbrain)^{187, 188} and is involved in reinforcement learning and goal-directed behavior¹⁸⁷.

Especially the involvement of midbrain dopaminergic neurons in reward computation has been described in great detail. In most midbrain dopaminergic neurons, an unpredicted reward elicits burst activity (phasic activation), while the omission of a predicted reward induces a depression of neuronal activity¹⁸⁹. A fully predicted reward elicits no response¹⁸⁹. Thus, these neurons compute the ‘reward prediction error’, which reflects the difference between predicted and obtained rewards and was proposed to be essential for reward-driven learning¹⁸⁹.

The reward circuit (Fig. 3) is connected to extrastriate areas via top-down signaling and indirectly to V1 through extrastriate-V1 feedback connections¹⁹⁰. Recently, another putative reward-related input to lower visual areas has been described. Komura and colleagues found thalamic neurons in lateral posterior nucleus and suprageniculate nucleus which transiently responded to reward-predicting stimuli¹⁹⁰. These thalamic nuclei receive input from perirhinal cortex and project to components of the reward circuit (amygdala, striatum and perirhinal cortex)^{191, 192} as well as to visual areas¹⁹⁰. Consistent with putative input of reward-related signals to V1, reward can affect cells in V1 of rats¹⁹³ and humans¹⁹⁴.

Experimentally, food, fluid or intracranial self-stimulation^{195, 196} is used as reward. In addition to that, successful task performance itself works as an internal reward¹⁹⁷. Reward has a beneficial effect on learning: VPL is facilitated by fake positive feedback on task performance, even if performance was actually bad¹⁹⁸.

3.2.7 Reinforcement learning

Reward, equally as punishment, strongly influences future decisions and behavior by driving reinforcement processes during learning. The strong impact of rewards is demonstrated by a recent study showing that an unconsciously perceived stimulus is learned, if it is paired with a reward¹⁹⁹. Generally spoken, reinforcement learning terms the process during which an animal (or an artificial model system) learns to predict the consequences of its

behavior and optimize its actions as measured by the action outcomes, that is, maximized reward and/ or minimized punishment^{121, 200}.

Reinforcement learning can be model-based or model-free^{121, 201}. Both rely on experience. However, during model-based reinforcement learning, a complex internal model of the environment and its possible states is established allowing for a flexible goal-directed behavior. Dorsomedial striatum²⁰² and orbitofrontal cortex²⁰³ are involved in the goal-directed system, as well as the associative cortico-basal-ganglia loop consisting of the basolateral amygdala, the mediodorsal thalamus and the dorsolateral prefrontal cortex²⁰⁴.

Model-free reinforcement learning can achieve the same optimal behavior by simple learning of one or two action values through a relatively slow process of trial-and-error. Other

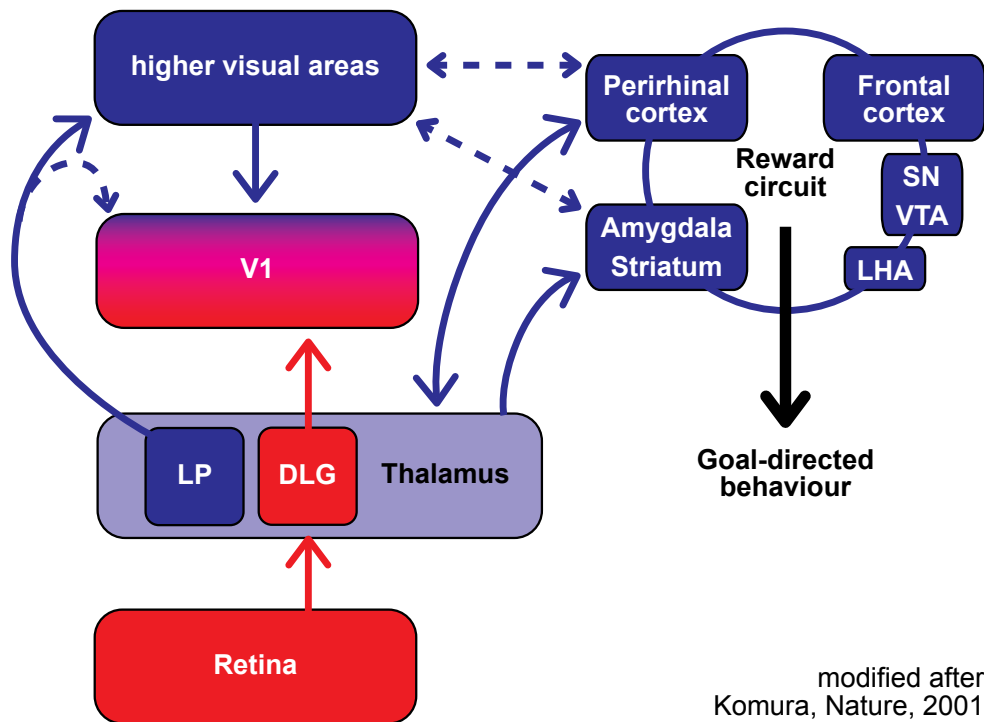


Figure 3: Potential pathways for top-down signaling to V1. Brain regions are indicated by squares, connections by arrows (dotted arrows: weak connections). Red: bottom-up pathway, blue: potential top-down pathways. V1: primary visual cortex, V2: secondary visual cortex, LP: lateral posterior nucleus, DLG: dorsal lateral geniculate nucleus, SN: substantia nigra, VTA: ventral tegmental area, LHA: lateral hypothalamic area.

than model-based reinforcement learning, model-free reinforcement learning cannot quickly adapt to changes in environmental states or in the value of the action outcome¹²¹. This type of learning involves the computation of prediction errors²⁰⁵ in midbrain dopaminergic neurons¹⁸⁷ and can form habits by assignment of a fixed value to an action, most likely involving infralimbic cortex²⁰⁶ and dopaminergic projections to dorsolateral striatum²⁰⁷.

3.2.8 Operant conditioning and functional plasticity

Classical conditioning is used to investigate how subjects learn to predict events without being able to influence them. In contrast, during operant (or *instrumental*) conditioning, animals learn to choose actions based on reinforcement¹²¹. In this thesis, I employed operant conditioning for training mice on an orientation discrimination task. Operant conditioning is often performed in an operant chamber^{208, 209}, an environment in which a restricted number of states (such as the presence or absence of a certain stimulus), actions (such as pressing a lever) and outcomes (such as obtaining food) can be defined and implemented. However, the value of the outcome can vary with motivational state¹²¹ and is influenced, for example, by satiation and wakefulness. Since the introduction of the operant chamber as a defined experimental environment, many studies have established that rodents can be trained to reliably repeat behavior and successfully learn complex tasks²¹⁰⁻²¹². Recently, researchers have pursued operant conditioning to investigate higher cognitive functions in rodents²¹³⁻²¹⁵.

Upon operant conditioning, changes in neuronal response properties were observed in lower sensory areas. In an auditory frequency discrimination task, rats moved around a chamber while a sound was presented with its frequency continuously changing depending on the location of the rat. The task was to identify the location which was paired with the highest frequency. After successful learning, high frequencies were more strongly represented in primary auditory cortex²¹¹. In another study, rats had to whisk in a certain direction in order to be returned to their home cage. This goal-directed whisking increased the phase-locking between vibrissa movement and electrical activity in primary sensory cortex²¹². Finally, after training rats on an operant odor discrimination task, neurons in piriform cortex showed substantial plasticity of intrinsic excitability^{216, 217}. Interestingly, these intrinsic changes in

neuronal firing behavior coincided with the ability of the rats to transfer the task to different odors (rule learning)²¹⁸. Based on this and similar findings in invertebrates^{219, 220} and vertebrates^{221, 222} after classical conditioning, plasticity of intrinsic excitability was proposed to play a role in memory formation, either indirectly by permitting it, by serving as a trigger for memory consolidation, or directly by contributing to the memory engram itself²²³.

3.3 Technical advances and impact of study

3.3.1 Benefits of two photon calcium imaging

A powerful method for measuring neuronal function in the intact brain *in vivo* is two-photon calcium imaging. Two-photon imaging^{224, 225} uses pulsed infrared laser light to excite fluorescent dyes. This has three beneficial effects. First, the red-shifted laser light excites the fluorescent dye in a much smaller volume compared to conventional confocal microscopy, because only in the very focus of the beam, photon density is sufficiently high to excite the dye. Second, the longer the wavelength of the excitation light, the deeper it can penetrate into tissue due to less scatter and reflection. This way, one can image deep in the cortex down to 450 μm or deeper. Third, pulsed laser light minimizes phototoxic effects and bleaching.

Combining two-photon imaging with calcium indicators allows imaging of neuronal activity^{226, 227}. Tightly coupled to neuronal firing, calcium influx leads to a rapid increase of the intracellular calcium concentration^{228, 229}. This modulates fluorescence intensity of the calcium indicator. As opposed to voltage-sensitive dyes, which provide a more direct readout of neuronal activity²³⁰, the fluorescence change of calcium indicators is typically much larger and therefore better suited for *in vivo* imaging^{226, 227}.

Two-photon calcium imaging provides major methodological advantages. While intrinsic signal imaging picks up population signals, but does not have cellular resolution, electrophysiology yields precise recordings, but only of small numbers of active neurons or putative single units. Calcium imaging allows simultaneous activity recording of large neuronal populations with single-cell spatial and nearly single-spike temporal resolution²³¹. However,

non-linearities in fluorescence change depending on neuronal activity^{227, 232} have to be considered and spike detection²³¹ is clearly less reliable compared to electrophysiology.

Importantly, two advantages of calcium imaging were key to this study. First, it allows identifying and re-finding individual neurons in subsequent imaging sessions over weeks and months^{233, 234}. Second, it permits to morphologically detect virtually every single neuron in a given optical section, also including non-responsive and silent neurons. This allowed a reliable determination of the fraction of neurons responsive to specific visual stimuli. In the first set of experiments, we used the synthetic calcium indicator OGB1-AM, an acetoxymethyl ester which is membrane-permeant. Inside cells, esterases cleave the ester bonds, rendering the dye membrane-impermeant and trapping it inside the cell. In the second part of this thesis, I aimed at repeatedly imaging the same neurons over up to 12 days, which is not possible with synthetic indicators. Also, this is very difficult using electrophysiology, with which very often activity of the identical neurons being recorded over subsequent sessions cannot be assured. I therefore resorted to the genetically encoded calcium sensor GCaMP3, which has been developed by the Looger lab²²⁷.

3.3.2 Aims of study

Investigating functional plasticity in the primary visual cortex was the goal of this study. Specifically, I have addressed two related questions. First, by inducing experience-dependent plasticity, I aimed to investigate the role of the visual environment, that is, whether instructive or permissive changes in the representation of orientations occur during stripe rearing. This question has been controversial for a long time and so far has not been answered conclusively because of methodological limitations.

Second, I studied which functional changes occur in individual V1 neurons during learning of a visual discrimination task under involvement of top-down signaling. While several studies point to an involvement of primary sensory areas in learning, only one study²³³ so far has attempted to describe functional changes in the same individual V1 neurons during learning. These functional changes are of particular interest, as the extent and nature of the involvement of lower sensory areas, such as V1, in learning and memory are highly

controversial. Even the extent of baseline variability and spontaneous functional changes in V1 neurons are not known. To resolve this issue, I employed repeated two-photon calcium imaging of individual neurons over almost two weeks. Thereby, I obtained a comprehensive dataset describing both baseline changes and changes during learning in individual neurons, which could be related to the performance of mice on the task.

Materials and Methods

4.1 Methods

All experimental procedures were carried out in compliance with institutional guidelines of the Max Planck Society and the local government ([Regierung von Oberbayern](#)). All experiments were performed using male C57/Bl6 mice in the age of between postnatal day (p) 25 and p51. Note that all materials used are referenced with a letter/ number superscript in the running text, and listed in a separate section below.

4.1.1 Surgical procedures

Depending on the experimental requirements, two types of approaches were performed. For assessing orientation selectivity in a single two-photon calcium imaging experiment, an “acute” cranial window was implanted ([section 4.1.1.1 ‘Acute window implantation’](#)). For repeated calcium imaging using the genetically encoded calcium indicator GCaMP3, a “chronic” preparation was carried out by implanting a permanent cranial window ([section 4.1.1.2 ‘Virus injection and chronic window implantation’](#)).

4.1.1.1 Acute window implantation

To measure the activity of neurons in primary visual cortex ([V1](#)), we used two-photon calcium imaging, employing the synthetic calcium indicator OGB1-AM. Mice (postnatal day (p) 45 – 51) were anesthetized using an intraperitoneal injection of a mixture of Fentanyl^{D.8} (0.05 mg/kg), Midazolam^{D.5} (5.0 mg/kg), and Medetomidin^{D.6} (0.5 mg/kg). Anesthesia was maintained by re-injecting one-fifth of the initial dose after two hours. A thin layer of cream^{D.11} was applied to the eyes to prevent dehydration during surgery. After attaching a

headplate^{T.11} to the skull, a trepanation was carried out to expose the cortical surface which was kept moist with artificial cerebrospinal fluid (ACSF; 125 mM NaCl, 5 mM KCl, 10 mM glucose, 10 mM HEPES, 2 mM MgSO₄, and 2 mM CaCl₂ [pH 7.4]). The calcium-sensitive dye Oregon Green 488 BAPTA-1, AM^{D.16} (OGB1-AM) was dissolved in 4 ml DMSO containing 20% pluronic acid^{D.17}, and further diluted (1/11) in dye buffer (150 mM NaCl, 2.5 mM KCl, and 10 mM HEPES [pH 7.4]) to a final concentration of about 0.9 mM. The astrocyte marker Sulforhodamine 101^{235, D.20} (SR101) was added, yielding a final concentration of 40 µM. The dye solution was delivered to the visual cortex by pressure injection at a depth of 200 – 300 µm using a micropipette^{T.1} (3 – 5 MΩ, 0.55 – 0.83 bar, 2 – 3 min). After the dye injection, the cortex was sealed with 2% agarose^{D.1} in saline^{D.13} and a coverslip^{T.3}. Immediately afterwards, two-photon calcium imaging was performed (see section 4.1.3 ‘two-photon calcium imaging’).

4.1.1.2 Virus injection and chronic window implantation

Surgery essentially followed the protocol described by Holtmaat and colleagues²³⁶, with several modifications: Mice at the age of p25 were anaesthetized with a mixture of Fentanyl^{D.8} (0.05 mg/kg), Midazolam^{D.5} (5.0 mg/kg), and Medetomidin^{D.6} (0.5 mg/kg). The analgesic Carprofen^{D.18} (4.0 mg/kg) and the immunosuppressant Dexamethasone^{D.9} (0.25 mg/kg) were injected intraperitoneally, dissolved in an infusion solution^{D.19}. The mouse head was then mounted in a stereotactic apparatus. The skin was locally anaesthetized with lidocaine^{D.22} and removed from the skull with scissors^{T.8}. Next, the skull was disinfected with iodine solution^{D.4}, cleared of hairs and roughened with a scalpel^{T.16, T.17}. Finally, the exposed bone was covered with Histoacryl^{C.2}. A round craniotomy, 5 mm in diameter, was made using a drill^{T.3, T.4}. After removing the bone lid, the brain was kept moist with ACSF (125 mM NaCl, 5 mM KCl, 10 mM glucose, 10 mM HEPES, 2 mM MgSO₄, and 2 mM CaCl₂ [pH 7.4]), and blood extruding from “meningeal vessels” was sucked up with Sugis^{T.19} until bleeding stopped.

Using a custom-made injector^{I.15} connected to a micropipette^{T.1} (5 – 8 MΩ) mounted to a micromanipulator^{I.9}, a total volume of about 1 µl of the virus solution (AAV2/1.hSyn-ap.GCaMP3.3.SV4^{OV.1}, titer: 9.9*10¹² GC/ml) was injected successively at a depth of about 350 µm below the cortical surface. Two to three injections were performed. After injecting the virus, the craniotomy was tightly sealed with a cover slip^{T.3}, which was held in place with

two-component dental cement^{C.3} hardened with an UV light curing unit^{T.20}. A custom-made metal headbar^{T.10} consisting of an oval plate with an 8 mm opening and two notches for fixing screws was mounted on the skull with cyanoacrylate glue^{C.6}, with the opening centered on the glass window. Finally, the exposed skull and the space between skull and headbar^{T.10} was covered with dental cement^{C.4}. A mixture of the opioid receptor antagonist Naloxone^{D.14} (1.2 mg/kg), the GABA_A receptor antagonist Flumazenil^{D.2} (0.5 mg/kg) and the $\alpha 2$ adrenergic receptor antagonist Atipamezole^{D.3} (2.5 mg/kg) was applied intraperitoneally. Mice were kept under a heat lamp^{T.12} for one hour and fed with water-soaked food pellets for one day.

4.1.2 Rearing and learning paradigms

4.1.2.1 Stripe Rearing

In order to stripe rear mice, three approaches were explored. First, male mice were grown in cages with striped walls (square-wave gratings, stripe width 5 mm) for three weeks starting from p25 (Fig. 4a). Second, male mice were placed once a day for three hours in an arena flanked by four monitors, which were continuously displaying moving gratings of a variety of spatial frequencies (Fig. 4b). Finally, I developed and designed metal goggles for mice with cylinder lenses^{106, 109, F.2}. The goggles were mounted on the skull (Fig. 5b & c) at postnatal day (p) 25 for 19 – 23 days. To this end, mice were anesthetized with a mixture of Fentanyl^{D.8} (0.05 mg/kg), Midazolam^{D.5} (5.0 mg/kg), and Medetomidin^{D.6} (0.5 mg/kg). A headbar^{T.9} with two threaded holes was implanted to the skull using dental cement^{C.3} after roughening the bone surface with a gel containing 35% phosphoric acid^{C.1} for 10 s. Custom-made goggles^{F.2} were individually adjusted to the mouse's head shape and screwed to a custom-made headbar^{T.9}. Blinkers restricted the mouse's field of view to the lenses. The goggles^{F.2} contained cylinder lenses made from acrylic^{F.1} with a refractive power of 167 diopters (dpt, refractive power of the orthogonal axis: 0 dpt) or, for control purposes, acrylic lenses with 0 dpt. Mice wearing goggles were kept in cages with striped walls, with the stripe pattern having the same orientation as the cylinder lenses. Cage walls of mice wearing control goggles displayed all orientations. Another control group not wearing goggles was kept under standard housing

conditions. For assessing orientation selectivity in V1, goggles were removed immediately before two-photon calcium imaging.

4.1.2.2 Environmental enrichment

For environmental enrichment, 14 male mice were born and raised in a special enrichment cage. Pregnant mice were placed in the cage about three weeks before giving birth. After weaning at p25, male mice were kept in the enrichment cage until the age of p43 – p51, and female mice including mothers were removed from the cage. The enrichment cage contained several levels (Fig. 15), stairs and tubes, creating spatial complexity in three dimensions. Running wheels and climbing devices permitted voluntary physical activity. Spatial dissemination of food trays, nesting material and shelters mimicked a natural mouse habitat to promote species-specific behavior. The large group of mice provided multiple social interactions. All items were re-arranged once per week.

4.1.2.3 Operant learning

4.1.2.3a Operant chamber

Mice were trained in a custom-made operant chamber^{0.4} comprised of a modular system^{0.6, 0.9 - 0.13} and a touch screen^{0.7} (Fig. 17) covered with a faceplate^{0.5} with two circular apertures (7 cm diameter at a height of 6.5 cm, measured from center of aperture). The training protocol was programmed in MED-PC IV^{S.8}, which controlled the operant chamber devices (food release, light, tone) and the placement, orientation, and on- and offset of the visual grating stimuli. Grating stimuli (square-wave grating, stripe width 1.2 cm) were generated and displayed on the touch screen using MATLAB^{S.7}. Selecting the target stimulus (a grating of one particular orientation, see below, section 4.1.2.3b ‘Training protocol’) triggered delivery of a food reward. A non-target stimulus (displaying a different grating orientation) was displayed simultaneously. After the mouse selected one of the gratings by a nose poke or using its forelimbs, the screens became black. On correct choices, a 20 mg food pellet^{0.8} was released into a food tray^{0.13} accompanied by a click sound. After a delay of 20 – 120 s (depending on training stage, see section 4.1.2.3b ‘Training protocol’), the next trial was initiated. Initiation of a trial by presentation of a target and a non-target grating was accompanied by a tone^{0.11} (0.5 s, 2900 Hz). Presses onto the touch screen within either of the two apertures

displaying the target and the non-target were tracked and assigned to 'left side' or 'right side' using LabVIEW^{S.6}. Onset of stimulus display, timepoints and side of presses as well as time when the mouse entered the food receptacle^{O.13} (measured with an infrared light barrier^{O.10}) were recorded by MED-PC IV^{S.8}. Training sessions were filmed with a webcam^{O.15}. Water was freely available throughout the training.

4.1.2.3b General training protocol

Generally, training was performed for at least 10 h every 24 hours, five days a week. Training was subdivided into different stages of increasing task complexity (Fig. 18). During stage A, no visual stimuli were presented. Mice freely explored the operant chamber for about 1 – 2 hours. About 3 pellets in the food tray indicated where food was to be found in later sessions. In stage B, mice had to press any of the two touch screens while both were displaying the target. During this stage, trials were spaced by one minute (starting from the first touch screen press after stimulus onset). In the following stages, training was sped up by successive shortening of the inter-trial interval. In stage C, only one screen displayed the target while the other screen remained black. In order to receive a reward, mice had to select the target grating. Trials were spaced by 50 s. In stage D, the target grating and a non-target with a differential orientation (dO) of 90° were displayed; trials were spaced by 40 s. In stage E, the target and one out of three non-target gratings with a -45°, 45° or 90° dO were displayed. Trials were spaced by 30 s. Finally, in stage F, the target and one out of seven non-target gratings with -67.5°, -45°, -22.5°, 22.5°, 45°, 67.5° or 90° dO were displayed. In stage F, trials were spaced by 20 s. During a subsequent, two week "food retrieval phase", with a similar design as in stage F, mice were placed in the operant chamber twice a day for 30 min in order to earn all of their food by solving the orientation discrimination task.

4.1.2.3c Long training regime for single cell assessment of learning-induced changes

Juvenile male mice were trained according to the above-described protocol starting from p25 onwards and, apart from training sessions, were kept under standard housing conditions. Access to water was unlimited; food was available exclusively in the operant chamber during training sessions of at least 10 h duration. Training was performed at night, when mice show elevated activity levels. Regular weighing assured that mice did not lose more than 10%

of their body weight during food deprivation between two training sessions. Following training stage F, mice entered the two-week food retrieval phase. Throughout training, all mice overall gained weight. Subsequently, orientation tuning was measured in acute two-photon calcium imaging experiments (see section 4.1.3 ‘Two-photon calcium imaging’).

4.1.2.3d Short training regime for repeated assessment of learning-induced changes in individual neurons

For studying learning-induced changes in individual neurons, p24 littermate mice were handled for a few minutes until they voluntarily sat on the experimenter’s hand. Subsequently, they were kept in groups of four in a large cage equipped with a running wheel^{F.4}, nesting material and a shelter^{F.3}. At p25, the GCaMP3 expression vector was injected and a chronic cranial window implanted (see section 4.1.1.2). After two weeks of GCaMP3 expression, orientation tuning was measured in four subsequent chronic two-photon imaging experiments (see section 4.1.3), spaced by four days each. Between sessions two and three, mice were trained in a short training protocol comprising training stages B, C and F. Stage F training was repeated twice. Mice were trained in 3 six-to-eight-hour sessions per 48 h. The last training was scheduled immediately before imaging session three.

4.1.3 Two-photon calcium imaging

4.1.3.1 Anesthesia

For anesthesia during two-photon calcium imaging using OGB1-AM, please refer to section 4.1.1.1. For repeated two-photon calcium imaging using GCaMP3, mice were briefly preanesthetized in a chamber with isoflourane^{D.12}. Mice were fixed under the microscope by mounting the headbar^{T.10} to two posts, ensuring a reproducible position between imaging sessions. For imaging, anesthesia was maintained with a mixture of 0.5 – 0.8% isoflourane^{D.12}, 50% N₂O and 50% O₂ delivered through a face mask. To support the anesthesia, the sedative Midazolam^{D.5} (5.0 mg/(kg*h)) was infused subcutaneously.

4.1.3.2 Imaging

During calcium imaging experiments using OGB1-AM, cells were imaged at nine depth levels with 20 µm intervals in random order, between 180 µm and 340 µm below the pial

surface in monocular V1. Using a custom built two-photon microscope equipped with a Spectra-Physics Mai Tai femtosecond laser^{M.15} and a 40x water immersion objective^{M.20} (0.8 NA), a 180 μm x 180 μm field of view was scanned at 2 Hz and 256 x 256 pixel resolution. Both, OGB1-AM and SR101 were excited at 830 nm. The emitted light was split by a 585 nm long-pass filter and detected through a 525/50 nm bandpass filter^{M.7} (OGB1-AM) and a 680 nm short pass filter^{M.10} (SR101). For repeated calcium imaging experiments using GCaMP3, neurons were imaged in several regions throughout layer 2/3 in monocular V1. A different custom built two-photon microscope was used which was equipped with a Mai Tai HP Deep See laser^{M.16} and a 40x water immersion objective^{M.20} (0.8 NA) and a resonant scanner^{M.24}. A 125 x 210 μm field of view as scanned at 20 Hz and 671 x 400 pixel resolution. GCaMP3 was excited at 930 nm. The emitted light was detected through a 535/50 nm bandpass filter^{M.8}.

4.1.3.3 Visual stimulation

In acute and chronic experiments, neurons were stimulated with moving gratings of 0.03 cycles per degree (cpd) spatial frequency and 1.5 Hz temporal frequency; 16 directions were displayed in a pseudo-randomized manner. In a separate calcium imaging (OGB1-AM) data set, we used spatial frequencies of 0.03 to 0.1 cpd and temporal frequencies of 1.5 to 3 Hz. The complete stimulus sequence was repeated four times. The correct placement of the monitor with respect to the receptive fields of the imaged neurons was confirmed in most experiments using a flickering retinotopy mapping stimulus. Location of the imaging site in monocular V1 was tested by stimulating the ipsilateral eye.

4.1.4 Data analysis

4.1.4.1 Analysis of two-photon calcium imaging data

4.1.4.1a Cell detection

Data were analyzed using MATLAB^{S.7} and ImageJ^{S.3}. Image sequences were full-frame corrected for tangential drift and small movements caused by heart beat and breathing. Recordings with significant brain movements or vertical drift were excluded from further analysis. In experiments with the synthetic indicator OGB1-AM, cell body detection was based on the OGB1-AM staining itself, derived from an average morphological image (8330 frames).

Astrocytes were identified by SR101-staining and removed from the dataset. For cell body detection in GCaMP3 data sets, maximum dF/F response maps were calculated based on aligned data from all four successive imaging experiments. This way, we limited our analysis to neurons which were responsive at least once in any of the four imaging experiments.

In both cases, neuronal cell bodies were detected semi-automatically as regions of interest using a set of morphological filters for cell intensity, size, and shape, and subsequently confirmed by visual inspection.

4.1.4.1b Orientation tuning

Baseline fluorescence was computed as the median dF/F. Cells were considered responsive if the response to any of the stimuli was significantly different from the baseline (ANOVA at $p < 0.001$). Cells were considered orientation selective if the response to at least one of the 16 directions was significantly different from the response to all other directions (ANOVA at $p < 0.001$). To determine orientation tuning, a Gaussian was fitted to the mean amplitudes of fluorescence changes evoked by gratings of eight equally spaced orientations moving in both directions. The preferred orientation was defined as the peak, and tuning width as the full width at half height (FWHH) of the Gaussian. In calcium imaging experiments using OGB1-AM, the median normalized residuals of the Gaussian fit were 0.0030 for control and 0.0023 for stripe reared mice ($p < 0.001$, Wilcoxon rank sum test). To ensure that the slightly better fits of tuning curves obtained from stripe reared mice did not influence the data analysis in a systematic fashion, we sub-sampled the data derived from control mice such that the distribution of normalized residuals was statistically indistinguishable from that in stripe-reared mice. The distribution of preferred orientations in control mice was not affected by this procedure, and further data analysis confirmed the presence of a significant stripe rearing effect compared to the sub-sampled control data.

4.1.4.1c Determining stripe rearing effect and horizontal bias in neurons measured with OGB1-AM

For display purposes and further statistical analysis, the distribution of orientation preferences was pooled into eight bins, each 22.5° wide, and centered on the eight orientations used as visual stimuli. The fraction of neurons preferring one of the eight orientations

was then normalized either to the total number of orientation selective neurons or to the total number of detected neurons. If not indicated otherwise, data are shown as mean \pm SEM. For quantification of the stripe rearing effect and analysis of the fraction of neurons tuned to horizontal and vertical orientations, the orientations of interest were pooled together with the two neighboring bins, spanning 67.5° in total. The stripe rearing effect was quantified as the “specific effect”, which is the increase in the experienced orientation plus the decrease in the orthogonal orientation relative to control mice. The “horizontal bias” was calculated as the difference between the fraction of neurons preferring horizontal and the fraction of neurons preferring vertical orientations. For statistical comparisons, a t test or a Wilcoxon rank sum test (for tuning width and amplitude) was performed unless indicated otherwise.

4.1.4.1d Determining response properties in repeatedly imaged neurons

In repeatedly imaged neurons, response properties of individual neurons were measured in four subsequent imaging sessions spaced by four days. To assess changes in amplitude and tuning width as a function of preferred orientation, neurons were binned according to their differential preferred orientation (dPO), i.e. the difference between the target stimulus orientation and the neuron’s preferred orientation; bin widths was 30° . Neurons gaining orientation selectivity during training were classified according to their dPO. Quantification of changes in orientation selectivity in single neurons was performed analogous to the established quantification of structural changes (e. g. spine dynamics²³⁷): For calculating the net gain in orientation selectivity, the number of neurons gaining orientation selectivity during training was normalized to the total number of orientation-selective neurons after training. Accordingly, the net loss in orientation selectivity was calculated as the number of neurons losing orientation selectivity during training, normalized to the number of neurons which were orientation-selective in the imaging session immediately before training. Further, turnover²³⁷ of orientation selectivity was determined as the sum of neurons losing or gaining orientation selectivity between two subsequent imaging sessions, divided by twice the number of orientation selective neurons in the first of the two imaging sessions.

For statistical comparisons, analysis of variance (ANOVA) or a Kruskal-Wallis test with *post hoc* Tukey-Kramer correction for multiple comparisons was performed as indicated.

4.1.4.2 Behavioral data

All scripts for data analysis were written in MATLAB^{S.7}.

4.1.4.2a Measures of task performance

For the long training regime (see section 4.1.2.3c), performance measures were averaged over the last two weeks of food retrieval. For the short training regime (see section 4.1.2.3d), performance was measured in a two-hour training session (stage F) immediately before imaging (see section 4.1.2.3d). Actions of the mouse on the touch screen were classified as follows: Any nose poke at any given time was termed a “press”. A “choice” was defined as the first press onto the touch screen following the onset of the target and non-target display. Overall performance was evaluated using the following parameters: “Efficiency” (EF) was calculated as the fraction of choices of the total number of presses. “Response delay” (RD) was defined as the delay between trial start (display of target and non-target) and choice. “Reward yield” (RY) is the fraction of rewards obtained of the maximally achievable number of rewards. Finally, “accuracy” (AC) is defined as the fraction of correct choices of the total number of choices. For most statistical analyses, t tests were used, with *post hoc* Tukey-Kramer correction, if necessary. Data are displayed as mean ± SEM. Response delay measurements are displayed as median and 90 percentiles; because of the strongly skewed distribution, a Wilcoxon rank sum test was used here for statistical testing.

For the short training regime (see section 4.1.2.3d), mice were assigned to either “good” or “bad” performers based on their accuracy (AC): We arbitrarily set a threshold at 62.5%, resulting in two groups of equal size (seven mice each).

4.1.4.2b Measures of orientation discrimination performance

In order to estimate the ability of mice to discriminate nearby orientations, task performance of all good performers was plotted as a function of the differential orientation (dO) between the target and non-target grating. The dO task performance was normalized to the performance at 90° dO. The orientation discrimination performance was then approximated by fitting a Weibull function^{238, 239, S.11}:

$$y = 1 - (1 - g)e^{-\left(\frac{kx}{t}\right)^b}$$

where

$$k = -\log \left(\frac{1-a}{1-g} \right)^{\frac{1}{b}}$$

In these equations, g is the performance at chance level ([here: 0.5](#)), t is the threshold (the y value at which the slope of the function is maximum), which is defined by the performance level a ([here: set to 0.51/3, for reference see S.11](#)). The variable b determines the slope of the function. For fitting, a maximum-likelihood criterion was used^{239, T.11}.

4.2 Materials

4.2.1 Cements, Glues & Gels

C.1.....GLUMA ® Etch 35 Gel, Heraeus Kulzer GmbH ([Hanau, Germany](#))

C.2.....Histoacryl ®, Aesculap AG ([Tuttlingen, Germany](#))

C.3.....iCEM ® self adhesive value pack, Heraeus Kulzer GmbH ([Hanau, Germany](#))

C.4.....Paladur ®, Heraeus Kulzer GmbH ([Hanau, Germany](#))

C.5.....Pattex ® BlitzKleber gel, Henkel CEE GmbH ([Wien, Austria](#))

C.6.....Pattex ® Classic Flüssig, Henkel CEE GmbH ([Wien, Austria](#))

4.2.2 Drugs, Chemicals & Solutions

D.1.....Agarose, Biomol GmbH ([Hamburg, Germany](#))

D.2.....Anexate ® ([Flumazenile](#)), Roche Pharma AG ([Grenzach-Wyhlen, Germany](#))

D.3.....Antisedan ® ([Atipamezole](#)), Pfizer Animal Health ([Madison, New Jersey, USA](#))

D.4.....Braunol ® 7.5 ([Iodine solution](#)), B. Braun Melsungen AG ([Melsungen, Germany](#))

D.5.....Dormicum ® V ([Midazolam](#)), Roche Pharma AG ([Grenzach-Wyhlen, Germany](#))

D.6.....Dormitor ® ([Methedomidine](#)), Janssen Animal Health ([Beerse, Belgium](#))

D.7.....Elfenbeinschwarz, Kremer Pigmente GmbH & Co. KG ([Aichstetten, Germany](#))

D.8.....Fentanyl, HEXAL AG ([Holzkirchen, Germany](#))

D.9.....Fortecortin ([Dexamethasone](#)), Merck KGaA ([Darmstadt, Germany](#))

Materials and Methods

- D.10.....HEPES, Carl Roth GmbH & Co. KG ([Karlsruhe, Germany](#))
- D.11Isopto-Max eye lubricant, Alcon Pharma GmbH ([Freiburg, Germany](#))
- D.12.....Isofluran Baxter, Baxter Deutschland GmbH ([Unterschleißheim, Germany](#))
- D.13.....Isotone Kochsalzlösung 0.9% Braun, B. Braun Melsungen AG ([Melsungen, Germany](#))
- D.14.....Naloxon-hameln ([Naloxone](#)), Hameln Pharmaceuticals GmbH ([Hameln, Germany](#))
- D.15.....Oculotect ® fluid sine 50 mg/ml PVD Augentropfen, Novartis Pharma GmbH ([Melsungen, Germany](#))
- D.16Oregon Green ® 488 BAPTA-1, AM, 50 µg, Life Technologies GmbH ([Darmstadt, Germany](#))
- D.17.....Pluronic ® F-127 20% solution in DMSO, Life Technologies GmbH ([Darmstadt, Germany](#))
- D.18.....Rimadyl ® ([Carprofen](#)), Pfizer Animal Health ([Madison, New Jersey, USA](#))
- D.19Stereofundin ® VG-5, B. Braun Melsungen AG ([Melsungen, Germany](#))
- D.20Sulforhodamine 101, Life Technologies GmbH ([Darmstadt, Germany](#))
- D.21.....T61, Intervet Deutschland GmbH ([Unterschleißheim, Germany](#))
- D.22Xylocain ® Pumpspray, AstraZebeca GmbH ([Wedel, Germany](#))

4.2.3 Further equipment

- F.1Acrylglas PMMA-Vollstab gs 6 mm, Findeis GmbH ([Kirchlengern, Germany](#))
- F.2.....Mouse goggles, Max Planck Institute Machine Shop ([Martinsried, Germany](#))
- F.3.....Mouse House, Tecniplast ([Buguggiate, Italy](#))
- F.4.....Running wheel 60821, Trixie Heimtierbedarf ([Tarp, Germany](#))

4.2.4 Instrumentation

- I.1.....AxoClamp 2B, Molecular Devices ([Sunnyvale, California, USA](#))
- I.2Digital storage oscilloscope Classic 5000, Gould Electronics GmbH ([Eichstetten, Germany](#))
- I.3Gas regulator N₂O 40 – 580 cm³, ABB Germany ([Mannheim, Germany](#))
- I.4Gas regulator N₂O 150 – 2150 cm³, ABB Germany ([Mannheim, Germany](#))
- I.5Gas regulator O₂ 40 – 580 cm³, ABB Germany ([Mannheim, Germany](#))

- I.6Gas regulator O₂ 150 – 2100 cm, ABB Germany ([Mannheim, Germany](#))
- I.7Homeothermic blanket with rectal probe, Harvard Apparatus ([Holliston, Massachusetts, USA](#))
- I.8Isofluorane vaporizer, Vapor 2000, Drägerwerk AG & Co. KGaA ([Lübeck, Germany](#))
- I.9Micromanipulator, Bachofer ([Reutlingen, Germany](#))
- I.10Micromanipulator MO-10, Narishige ([Tokyo, Japan](#))
- I.11Micromanipulator MP-285, Sutter Instruments ([Novato, California, USA](#))
- I.12Operationsmikroskop SOM-62, Karl Kaps GmbH ([Aßlar, Germany](#))
- I.13Patient monitor, UltraCare SLP, Spacelabs Healthcare ([Issaquah, Washington, USA](#))
- I.14Perfusor segura, B. Braun Melsungen AG ([Melsungen, Germany](#))
- I.15Pressure injector, custom-made, Max Planck Institute Machine Shop ([Martinsried, Germany](#))
- I.16Small animal respirator, KTR 5, Föhr Medical Instrumente GmbH ([Engelsbach, Germany](#))
- I.17Stimulator Master-8, A.M.P.I. ([Jerusalem, Israel](#))
- I.18TFT monitor L227WTP, LG Electronics Deutschland GmbH ([Ratingen, Germany](#))
- I.19TFT monitor 20", Dell GmbH ([Frankfurt am Main, Germany](#))
- I.20TooheySpritzer Pressure System Ile, Toohey Company ([Fairfield, New Jersey, USA](#))
- I.21Tripod Cullmann 40300, Cullmann Foto Audio Video GmbH ([Langenzenn, Germany](#))
- I.22Two-step vertical puller P-10, Narishige International Limited ([London, UK](#))

4.2.5 Microscope setup components

- M.1Autocorrelator, Carpe, APE ([Berlin, Germany](#))
- M.2CMOS monochrome camera, DMK 22BUC03, The Imaging Source Europe GmbH ([Bremen, Germany](#))
- M.3Controller for Pockels cell, model 302RM, Conoptics ([Danbury, Connecticut, USA](#))
- M.4Data acquisition card, NI 6008, National Instruments ([Austin, Texas, USA](#))
- M.5Data acquisition card, NI 6115, National Instruments ([Austin, Texas, USA](#))
- M.6Dichroic mirror, 670 nm, Chroma Technology ([Bellows Falls, Vermont, USA](#))
- M.7Emission filter 525/50 nm bandpass filter, AHF Analysetechnik ([Tübingen, Germany](#))

Materials and Methods

- M.8.....Emission filter 535/50 nm, Chroma Technology (Bellows Falls, Vermont, USA)
- M.9.....Emission filter 610/75 nm, Chroma Technology (Bellows Falls, Vermont, USA)
- M.10.....Emission filter 680 nm short pass filter, AHF Analysetechnik (Tübingen, Germany)
- M.11.....IR filter, type 092, 46 x 0.75, The Imaging Source Europe GmbH (Bremen, Germany)
- M.12....Linear stage and motor, LTA-HS and M-UMR8.51, Newport (Santa Clara, California, USA)
- M.13....Linear stage, M-VP-25-XA, Newport (Santa Clara, California, USA)
- M.14....Low-noise current amplifier, SR570, Stanford Research Systems (Sunnyvale, California, USA)
- M.15....MaiTai HP, SpectraPhysics/ Newport (Santa Clara, California, USA)
- M.16....MaiTai HP DeepSee, SpectraPhysics/ Newport (Santa Clara, California, USA)
- M.17....Mirrors, Eo3, Thorlabs GmbH (Dachau, Germany)
- M.18....Motion controller, ESP300, Newport (Santa Clara, California, USA)
- M.19....Mounting material, Thorlabs GmbH (Dachau, Germany)
- M.20...Objective LUMPlanFI/IR, 40x, 0.8 NA, water immersion, Olympus (Tokyo, Japan)
- M.21....Photomultiplier tube, R6357, Hamamatsu (Toyooka, Japan)
- M.22 ...Pockels cell, model 350-80, Conoptics (Danbury, Connecticut, USA)
- M.23 ...Power supply, NMC-100, Conrad Electronic SE (Hirschau, Germany)
- M.24 ...Resonant optical scanner, 4 KHz CRS, Cambridge Technology (Lexington, Massachusetts, USA)
- M.25 ...Scan lens, 50 mm, Leica Microsystems GmbH (Wetzlar, Germany)
- M.26 ...Tube lens, 300 mm, Thorlabs GmbH (Dachau, Germany)
- M.27 ...Yanus scanhead, TILL Photonics GmbH (Martinsried, Germany)

4.2.6 Operant chamber

- O.18 Input/16 Output SmartCtrl™ Package, Med Associates (St. Albans, Vermont, USA)
- O.2.....Data acquisition card NI USB-6009, National Instruments Germany GmbH (München, Germany)
- O.3.....Expanded PVC Sound Attenuating Cubicle, Med Associates (St. Albans, Vermont, USA)

- O.4.....Extra Wide Modular Test Chamber for Mouse, Med Associates ([St. Albans, Vermont, USA](#))
- O.5.....Faceplate with two apertures for touch monitor, custom-made, Max Planck Institute Machine Shop ([Martinsried, Germany](#))
- O.6.....House Light for Wide Mouse Chambers, Med Associates ([St. Albans, Vermont, USA](#))
- O.7.....Infrared touch monitor NEX104, iNEXIO ([Incheon, Korea](#))
- O.8.....MLab Rodent Tablet 20 MG, TestDiet ([Richmond, Indiana, USA](#))
- O.9Pedestal Mount Pellet Dispenser for Mouse, 20 mg, Med Associates ([St. Albans, Vermont, USA](#))
- O.10Pellet Receptacle Head Entry Detector for Wide Mouse Modular Chamber, Med Associates ([St. Albans, Vermont, USA](#))
- O.11Sonalert Module with Volume Control for Wide Mouse Chamber, 2900 Hz, Med Associates ([St. Albans, Vermont, USA](#))
- O.12.....Stainless Steel Grid Floor for Extra Wide Modular Test Chamber for Mouse, Med Associates ([St. Albans, Vermont, USA](#))
- O.13.....Switchable Dipper with Dual Pellet Receptacle for Classic Mouse modular Chamber, Med Associates ([St. Albans, Vermont, USA](#))
- O.14Voltage converter, custom-made, Max Planck Institute Machine Shop ([Martinsried, Germany](#))
- O.15.....Webcam SPZ5000, Philips Deutschland GmbH ([Hamburg, Germany](#))

4.2.7 Software

- S.1Colibri, a two-photon laser scanning microscope controlling software written in LabVIEW, LMU Biocenter and MPI of Neurobiology ([Martinsried, Germany](#))
- S.2.....FluoView™, Olympus ([Tokyo, Japan](#))
- S.3.....ImageJ, Wayne Rasband, National Health Institute (Bethesda, Maryland, USA, <http://rsbweb.nih.gov/ij>)
- S.4ImageJ Plugin “Register ROI”, Michael Abràmoff, Department of Ophthalmology and Visual Sciences, University of Iowa (Iowa City, Iowa, USA, <http://bij.isi.uu.nl>)
- S.5.....Java™, Oracle Corporation (Redwood Shores, California, USA, <http://www.java.com/de/download/>)
- S.6LabVIEW, National Instruments ([Austin, Texas, USA](#))

- S.7.....MATLAB, The MathWorks ([Natick, Massachusetts, USA](#))
- S.8MED-PC IV, Med Associates ([St. Albans, Vermont, USA](#))
- S.9Philips CamSuite, Philips Deutschland GmbH ([Hamburg, Germany](#))
- S.10Psychophysics Toolbox²⁴⁰, David H. Brainard, Department of Psychology, University of California (Santa Barbara, California, USA, <http://psychtoolbox.org>)
- S.11Scripts for fitting a Weibull function, Geoffrey Boynton, Department of Psychology, University of Washington (Seattle, Washington, USA, <http://courses.washington.edu/matlab2/library.html>)

4.2.8 Tools

- T.1Borosilicate glass capillaries GC150F-10, Harvard Apparatus ([Holliston, Massachusetts, USA](#))
- T.2.....Cotton tips, 15 cm, medical care & serve[®] ([Wurmlingen, Germany](#))
- T.3.....Deckgläser rund 5 mm, Menzel GmbH ([Braunschweig, Germany](#))
- T.4Dental drill SI-923, W&H Deutschland GmbH ([Laufen, Germany](#))
- T.5.....Drill bits HM-1005, Hager & Meisinger GmbH ([Neuss, Germany](#))
- T.6Dumont #5/45 Forceps, Fine Science Tools GmbH ([Heidelberg, Germany](#))
- T.7.....Dumont #7 Forceps, standard, Fine Science Tools GmbH ([Heidelberg, Germany](#))
- T.8Hardened Fine Iris Scissors, 8.5 cm, straight, Fine Science Tools GmbH ([Heidelberg, Germany](#))
- T.9Headbar ([bar type, 7 x 2 mm, resin-coated metal](#)), Max Planck Institute machine shop ([Martinsried, Germany](#))
- T.10Headbar ([chamber type, 24 x 10 mm, metal](#)), Max Planck Institute machine shop ([Martinsried, Germany](#))
- T.11Headplate ([chamber type, 46 x 14 mm, metal](#)), Max Planck Institute machine shop ([Martinsried, Germany](#))
- T.12Heatlamp, Glamox Luxo GmbH ([Bremen, Germany](#))
- T.13.....Injekt[®], B. Braun Melsungen AG ([Melsungen, Germany](#))
- T.14Introcan[®], B. Braun Melsungen AG ([Melsungen, Germany](#))
- T.15Omnican[®], B. Braun Melsungen AG ([Melsungen, Germany](#))
- T.16Scalpel blades #11, Fine Science Tools GmbH ([Heidelberg, Germany](#))

T.17Scalpel handle #7, Fine Science Tools GmbH ([Heidelberg, Germany](#))

T.18Sterican[®], B. Braun Melsungen AG ([Melsungen, Germany](#))

T.19Sugi[®], Kettenbach Medical ([Eschenburg, Germany](#))

T.20Translux[®] Power Blue[®] Light Curing Unit, Heraeus Kulzer GmbH ([Hanau, Germany](#))

4.2.9 Virus

V.1AAV2/1.hSynap.GCaMP3.3.SV40, University of Pennsylvania Vector Core Services ([Philadelphia, Pennsylvania, USA](#))

4.3 Solutions

All of the chemical compounds mentioned in the following were purchased from Sigma-Aldrich ([St. Louis, Missouri, USA](#)):

4.3.1 Cortex buffer (ACSF - artificial cerebral spinal fluid)

125 mM NaCl
5 mM KCl
10 mM Glucose*H₂O
10 mM HEPES
2 mM CaCl₂*2H₂O
2 mM MgSO₄*7H₂O

ASCF was adjusted to pH 7.4 with 1 N NaOH and sterile filtered.

4.3.2 Dye buffer

150 mM NaCl
2.5 mM KCl
10 mM HEPES

The buffer was adjusted to pH 7.4 using 1 N NaOH and sterile filtered.

Results

In this thesis, I investigated plasticity of orientation preference in two ways. First, I manipulated the visual input of mice to induce experience-dependent plasticity. Thereby, I focused on bottom-up signaling from retina to V₁, aiming to determine whether the visual environment acts instructively or permissively on receptive field properties in V₁ (Fig. 2, see *Introduction*). Second, I used an operant conditioning paradigm to train mice on an orientation discrimination task. By changing the behavioral relevance of a visual stimulus through reward association, I induced plasticity of orientation preference.

5.1 Experience-dependent plasticity of orientation preference in mouse V₁

5.1.1 Stripe rearing using standing and moving gratings

The simplest approach for stripe rearing mice is to keep them in cages with walls displaying gratings of a single orientation (Fig. 4a). In a preliminary experiment, I raised seven mice from p21 onwards for three weeks in cages enwrapped in transparency foils printed with vertical, horizontal or diagonal square-wave gratings (stripe width 5 – 7 mm). Subsequent measurement of orientation preference with two-photon calcium imaging using the synthetic calcium indicator OGB₁-AM did not reveal any over-representation of the experienced orientation in comparison to control mice kept in standard cages (data not shown). Because moving gratings might provide a stronger stimulus than standing gratings, the next approach was to stripe rear mice in an arena flanked by four monitors which were continuously displaying moving gratings of a variety of spatial frequencies (Fig. 4b). In preliminary experiments, I stripe reared four mice either for three hours immediately before imaging or for three hours

on three successive days with vertical or horizontal stripe patterns. I did not detect an over-representation of the experienced orientation with this method either (data not shown).

5.1.2 Stripe rearing using cylinder lens goggles

Switching to a more powerful stripe rearing approach, which allowed a more tight control of visual input over a longer period and independent of the mice's head position, I induced plasticity of orientation preference in mouse visual cortex using the spatial filtering effect of cylinder lenses

(Fig. 5a) with a refractive power of 167 diopters. Lenses were mounted on goggles (Fig. 5b) which were fixed to the mice's skulls¹⁰⁹ (Fig. 5c). The mice had normal visual experience from eye opening around p11 onwards until the goggle implantation at postnatal day (p) 25 (Fig. 5d). The subsequent three-week stripe rearing phase comprised the critical period for monocular deprivation which peaks around p30. Orientation tuning of individual layer 2/3 neurons in monocular primary visual cortex of stripe-reared and control mice was assessed with two-photon calcium

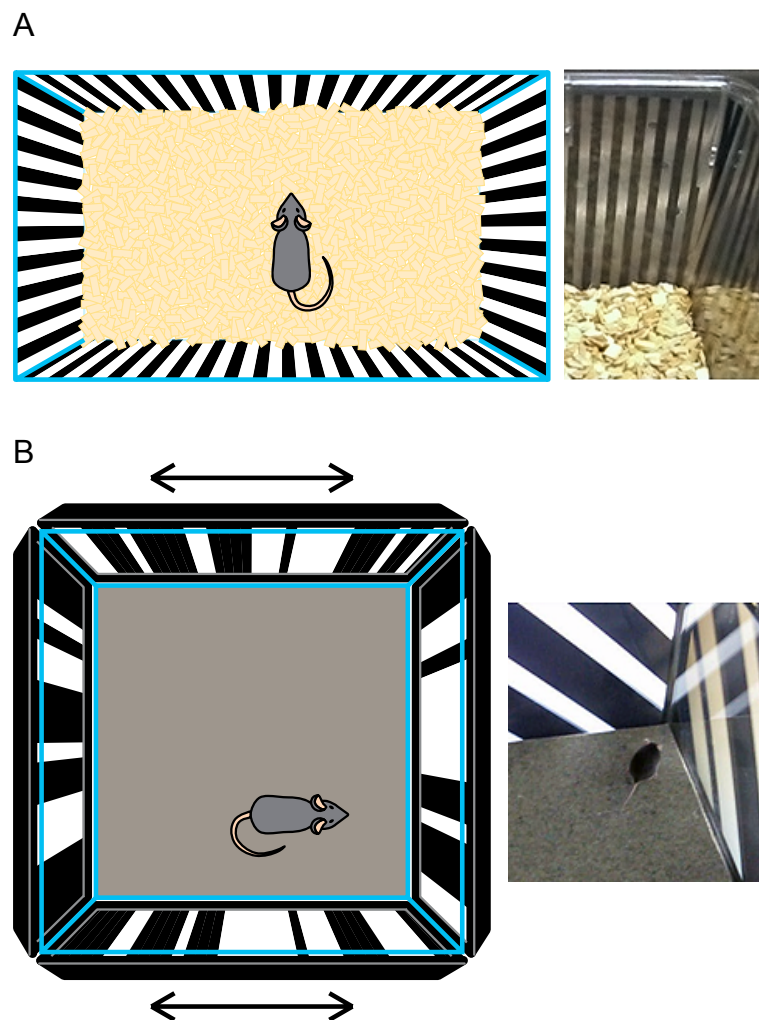


Figure 4: Stripe rearing using standing and moving gratings. (A) Mice are raised in a cage with walls covered with a square-wave grating. (B) Mice are placed daily in an arena flanked by four monitors displaying moving gratings of various spatial frequencies.

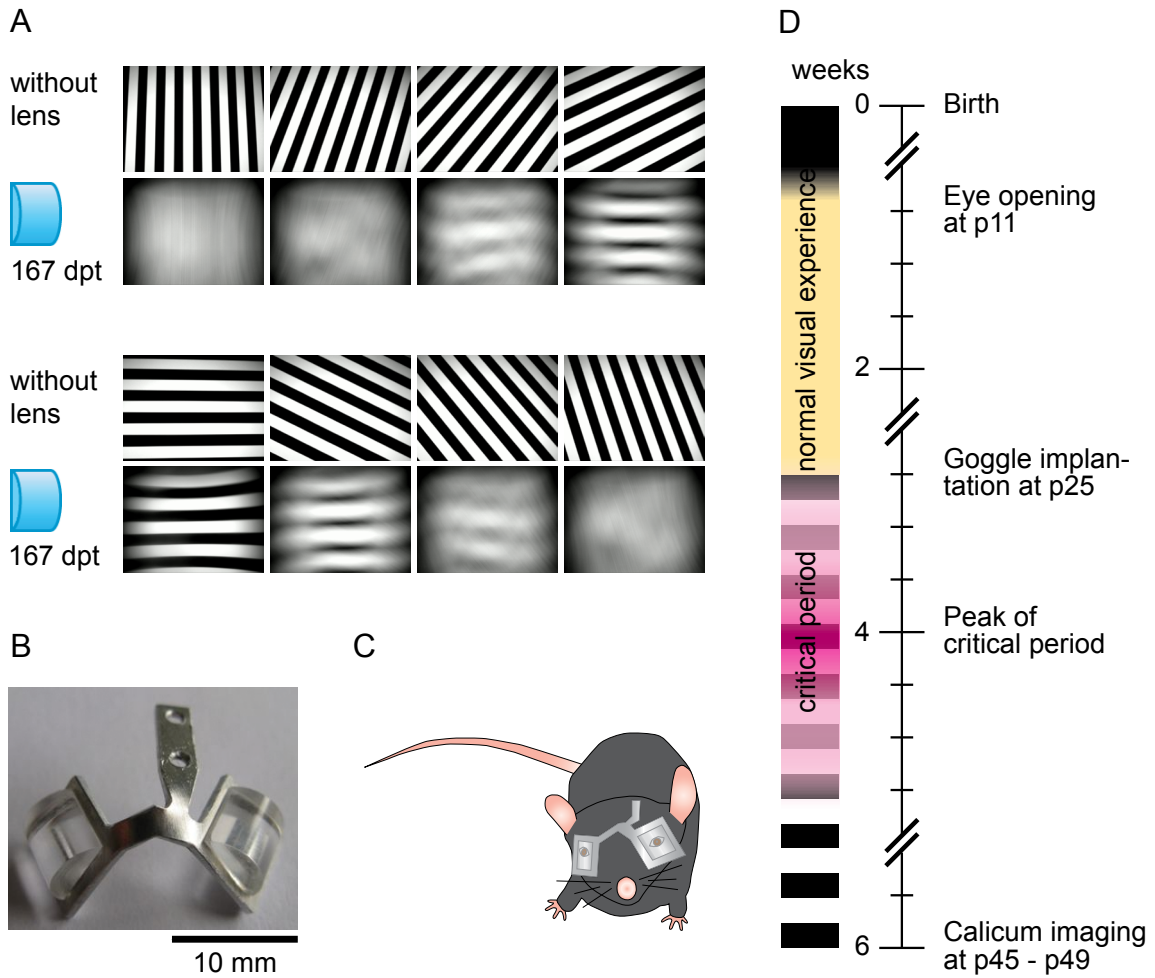


Figure 5: Stripe rearing using cylinder lens goggles. (A) Images of gratings of different orientations taken with and without 167 dpt cylinder lens oriented horizontally in front of the camera (Logitech QuickCam S 7500). Spatial frequency (0.1 cpd) is equivalent to a viewing distance of 5.7 cm from the mouse cage wall. (B) Goggles with 167 dpt cylinder lenses. (C) Mouse wearing cylinder lens goggles. (D) Timeline of the stripe rearing procedure.

imaging using OGB1-AM bolus loading²²⁶ (Fig. 6a – c). Astrocytes were identified by Sulforhodamine 101 staining²³⁵ (Fig. 6a) and were excluded from the dataset *post hoc*.

5.1.3 Stripe rearing shifts the distribution of orientation preference towards the experienced orientation

Mice were stripe reared using goggles from p25 onwards for about three weeks. To provide a high contrast visual input, the walls of the cages were covered with stripes. Control

Results

mice kept under standard housing conditions showed a modest over-representation of the cardinal orientations (0° and 90°) with a predominance of horizontally (0°) tuned neurons (Fig. 7a, fraction of neurons preferring horizontal and adjacent orientations [see *Materials and Methods*]: $14.6 \pm 0.9\%$, vertical: $10.7 \pm 1.0\%$, $p < 0.05$, t-test, $n = 8$ mice), similarly as has

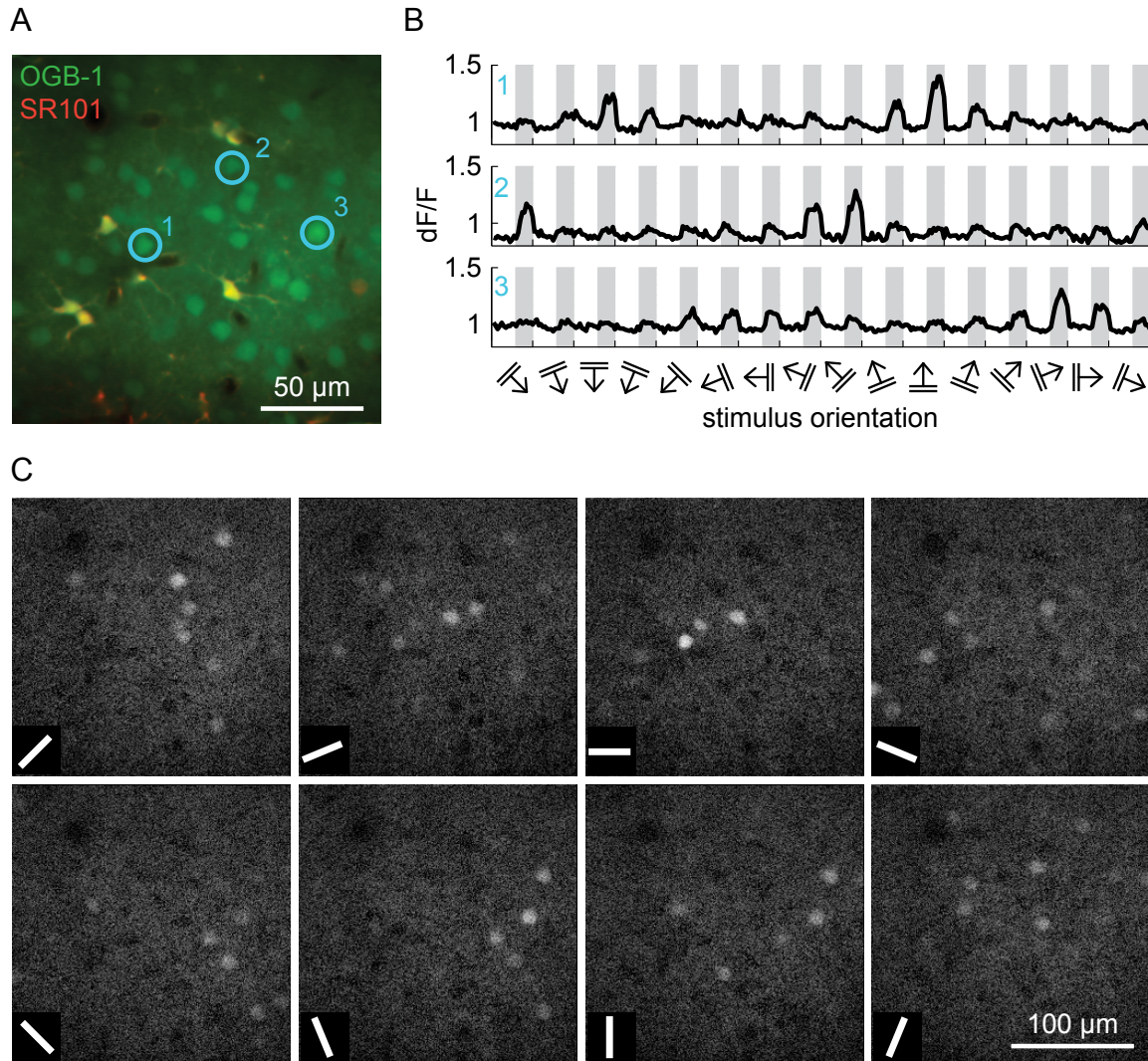


Figure 6: Two-photon calcium imaging of orientation selectivity. (A) Optical section at 280 μm depth stained with OGB1-AM (green) and astrocyte marker Sulforhodamine 101 (red). (B) Average dF/F time courses of three representative neurons during stimulus presentation. Stimulus orientation and direction are indicated by symbols below. (C) Response maps (dF/F) for eight stimulus orientations, indicated by white bars. All maps are scaled to the same maximum and minimum value.

been described in ferrets⁹⁴ and cats¹⁰⁰. On average, $69 \pm 6\%$ of the detected neurons were responsive (see *Materials and Methods*) to orientated gratings, of which $64 \pm 4\%$ were orientation-selective (see *Materials and Methods*). Tuning width was broadest in vertically and narrowest in horizontally tuned neurons (median $[0^\circ] = 31^\circ$, median $[90^\circ] = 47^\circ$, $p < 5 \times 10^{-19}$, Wilcoxon rank sum test, $n = 170$ horizontally and 140 vertically tuned neurons), again similar to findings in the cat¹⁰⁰. Response amplitudes of orientation-selective neurons (median dF/F: 18.7%) did not vary systematically with neurons' preferred orientation.

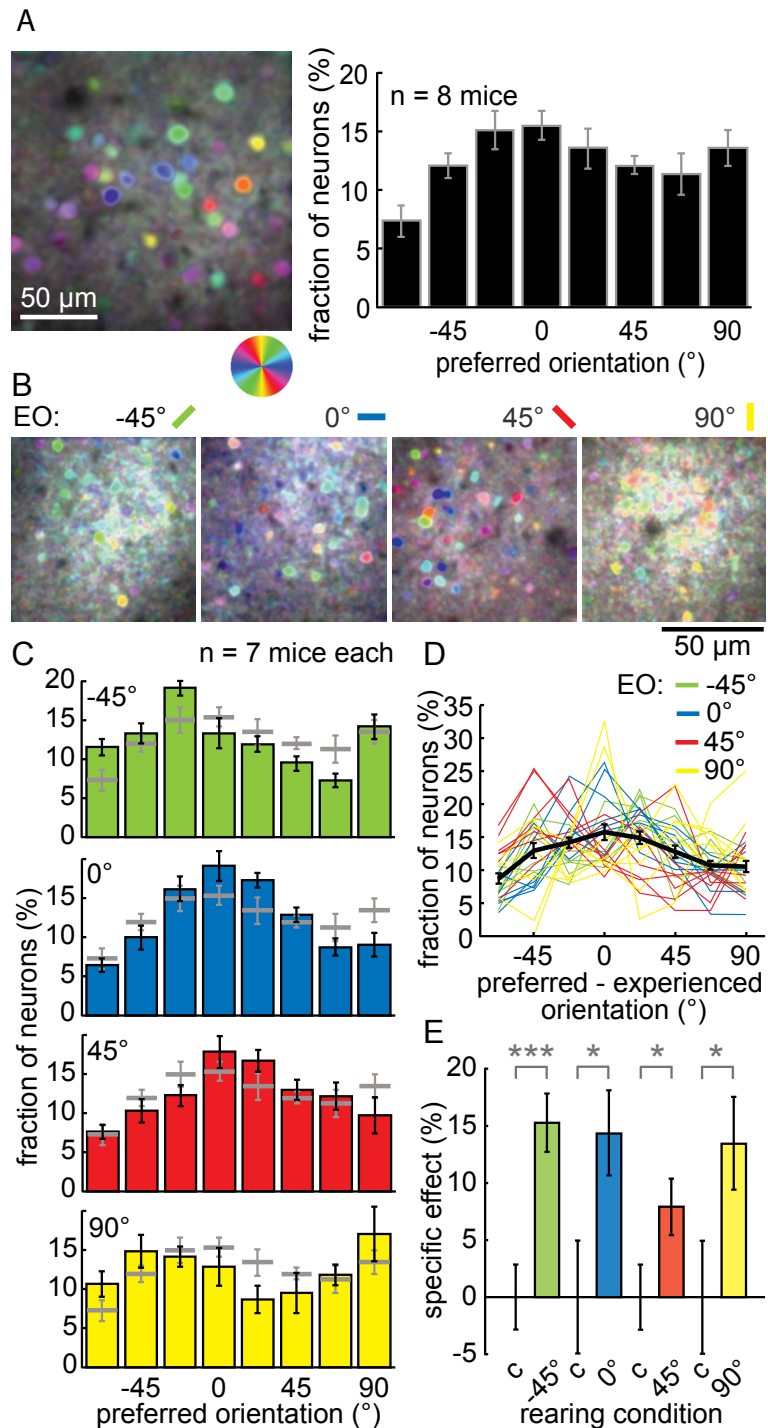
Stripe-reared mice showed an over-representation of the experienced orientation, on average by $64.6 \pm 14.8\%$, compared to the orthogonal orientation (Fig. 7b, c & d). This effect was of similar magnitude in the subpopulation of direction-selective neurons and was also reflected in the tuning of the neuropil (data not shown). To quantify the specific effect, I added the increase in the fraction of neurons preferring the experienced orientation to the decrease in preference for the orthogonal orientation (see *Materials and Methods*). As shown in Fig. 7e, the specific effect of stripe rearing was pronounced after stripe rearing with -45° ($17.9 \pm 2.9\%$, $p < 0.001$), 0° ($16.7 \pm 4.4\%$, $p < 0.05$) and 90° ($15.7 \pm 4.8\%$, $p < 0.05$), but weaker after stripe rearing with 45° ($9.3 \pm 2.9\%$, $p < 0.05$, all one-sided two-sample t-tests, $n = 7$ stripe-reared mice each, $n = 8$ control mice). I did not observe any significant effect of stripe rearing on the median of response amplitudes and tuning widths (data not shown). Notably, the fraction of non-orientation-selective neurons decreased only after rearing with 45° ($-9.3 \pm 0.8\%$ compared to control group, $p < 0.05$, one-sided t-test, $n = 7$ stripe-reared and 8 control mice).

In order to test whether experimentally determining orientation preference interferes with the bias induced by stripe rearing^{66, 118}, I imaged one test optical section at the beginning and again at the end of most experiments. The average duration of an imaging experiment was 2 hours, during which the anesthetized mouse was almost continuously exposed to standing and moving gratings of all orientations. Of a total of 741 neurons detected at the beginning of 25 imaging experiments, I was able to re-identify 78.4% at the end. For the population of neurons significantly tuned at the start and the end of an experiment I found no net changes in preferred orientation ($0.0 \pm 0.9^\circ$, n.s., one-sample t-test) for both control and stripe-reared animals. Thus, orientation preference is not altered by measuring it.

5.1.4 Shifts in orientation preference of orthogonal rearing conditions are complementary

Next, I analyzed whether the functional changes induced by different experienced orientations relate to each other in a systematic fashion. Specifically, I asked whether two experienced orientations,

which are perpendicular, would cause complementary modifications of the distribution of preferred orientation or rather lead to common changes. To this end, I calculated the average distribution of preferred orientations of all four stripe rearing conditions. The resulting distribution was very similar to that of the control group (data not shown). The same was true when averaging the distributions of preferred orientations of both orthogonal stripe rearing conditions separately (Fig. 8). This suggests that the shift in the distribution caused by one experienced orientation is complementary to the one



that occurs in mice exposed to the orthogonal experienced orientation. The average distributions (Fig. 8) also show that the horizontal bias is preserved in stripe-reared mice, which explains the asymmetric shift of the distributions of preferred orientations; they are biased towards the horizontal orientation as is best visible in mice with oblique experienced orientations (Fig. 7c).

5.1.5 Fraction of responsive neurons is slightly decreased after stripe rearing

The results demonstrate a clear effect of stripe rearing in layer 2/3 of mouse visual cortex. A long-standing question has been whether the observed over-representation of the experienced orientation can be explained by permissive changes, i.e. changes in responsiveness (rather than orientation preference) of certain neuronal populations^{108, 241}. To address this question, I compared the fraction of responsive neurons in control and stripe-reared mice. As the goggle frames occlude part of the visual field, I first tested whether wearing goggles with planar lenses (0 diopters) would result in any kind of visual deprivation effect. Mice with such goggles did not display any difference in the fraction of responsive neurons ($70 \pm 3\%$, $n = 7$ mice) as compared to control mice ($69 \pm 6\%$, $n = 8$ mice). The distribution of preferred

Figure 7: Orientation preference in the primary visual cortex of control and stripe-reared mice. (A) Orientation preference in control mice raised under standard housing conditions. *Left*: pixel-based orientation map with coding for preferred orientation (*hue*), response amplitude (*lightness*) and tuning width (*saturation*). *Right*: distribution of preferred orientations (mean \pm SEM, $n = 8$). (B) – (E): Orientation preference in stripe-reared mice. (B) Pixel-based orientation maps after stripe rearing with cylinder lenses of 167 dpt for three weeks, experienced orientations (*EO*) are indicated by values and *colored bars* above maps. (C) Histograms of preferred orientations (mean \pm SEM, $n = 7$ for each rearing condition), experienced orientations are indicated above the graphs, *light gray data points*: distribution in control mice. (D) Distribution of preferred orientations normalized to the experienced orientation (*EO*, as indicated by the color code in the *legend*, set to 0°) for 28 stripe-reared mice, *black*: average distribution (mean \pm SEM). (E) Average specific effect calculated as the sum of the increase in the fraction of neurons preferring the experienced orientation and the decrease in the fraction of neurons preferring the orthogonal orientation (see *Materials and Methods*) of all four rearing conditions (mean \pm SEM, $n = 7$ each) compared to four respective data subsets derived from control (*c*) mice ($n = 8$). *One asterisk*: $p < 0.05$, one-sided t test, *three asterisks*: $p < 0.001$, one-sided t test.

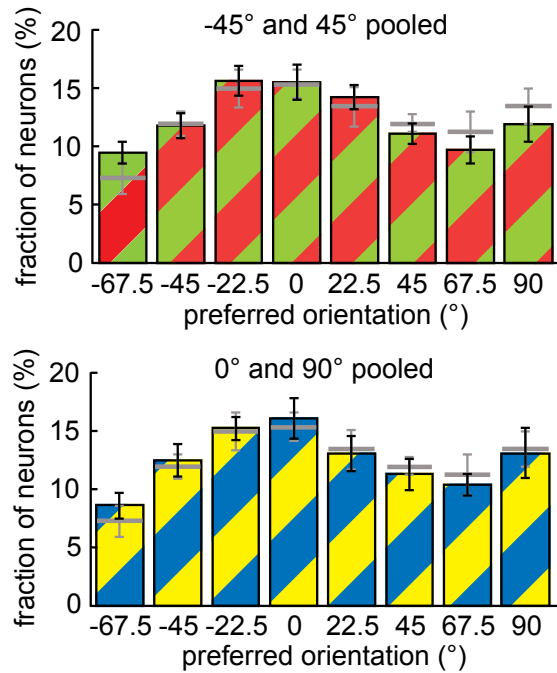


Figure 8: Shifts in distribution of preferred orientations after stripe rearing are complementary. Pooled distribution of preferred orientations of mice reared with orthogonal orientations. *Top*: -45° and 45°, *bottom*: 0° and 90°. *Light gray data points*: distribution in control mice.

orientations was slightly flatter than in the control group, but this effect was not significant (two-sample Kolmogorov-Smirnov test, $p = 0.52$).

While there was no difference between control mice and mice wearing goggles with 0 diopter lenses, stripe-reared mice showed a small drop in the overall fraction of responsive neurons ($-11 \pm 4\%$, $-6 \pm 6\%$, $-15 \pm 7\%$ and $-4 \pm 5\%$ for rearing with -45°, 0°, 45° and 90° orientation, respectively, $n = 7$ mice each, Fig. 9). This difference was not statistically significant for each individual stripe rearing condition. However, pooling all stripe-reared mice yielded a significant drop in responsiveness ($p = 0.0475$, one-sided t test, $n = 8$ control mice and 28 stripe-reared mice). Overall, the weak tendency towards reduced responsiveness suggests that the stripe rearing procedure may also result in some permissive changes.

5.1.6 Stripe rearing effect varies with depth in layer 2/3 and is caused by instructive changes in lower layer 2/3

Closer inspection of the distribution of preferred orientations in control mice revealed that the over-representation of horizontally tuned neurons (Fig. 7a, right panel) was mainly derived from the upper parts of layer 2/3 and decreased with cortical depth (180 – 220 μm depth: horizontally tuned: $16.7 \pm 0.9\%$, vertically tuned: $9.7 \pm 1.1\%$, $p < 0.0005$; 240 – 280 μm : horizontal: $14.9 \pm 1.6\%$, vertical: $10.3 \pm 1.2\%$, $p < 0.05$; 300 – 340 μm : horizontal: $13.2 \pm 0.8\%$, vertical: $11.7 \pm 1.3\%$, n.s., t -test, $n = 8$ control mice each, Fig. 10a). Together with previously re-

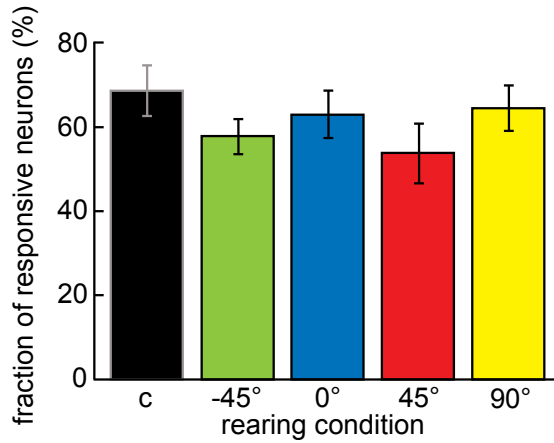


Figure 9: Effect of stripe rearing on the fraction of responsive neurons. Fraction of responsive neurons in control (c) mice and after stripe rearing with different orientations.

ported differences in the degree and developmental time course of plasticity between cortical layers^{113, 242, 243}, this prompted us to test whether the stripe rearing effect also

changed with depth in cortical layer 2/3. I found this to be the case: the magnitude of the shift increased with cortical depth. In the uppermost tier (180 – 220 μm below the cortical surface) the specific effect was small ($8.6 \pm 6.1\%$, n.s., t test). It increased at the next depth level (240 – 280 μm ; $15.5 \pm 2.6\%$, $p < 0.001$, t test), and was largest among the bottom cells in layer 2/3 (300 – 340 μm ; $18.2 \pm 3.1\%$, $p < 0.00005$, t test, $n = 28$ stripe-reared and 8 control mice in each case).

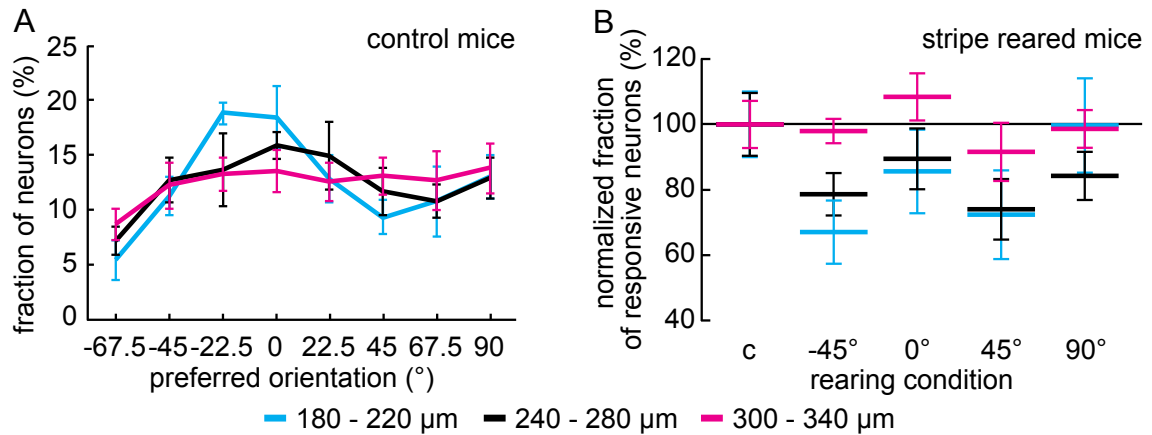


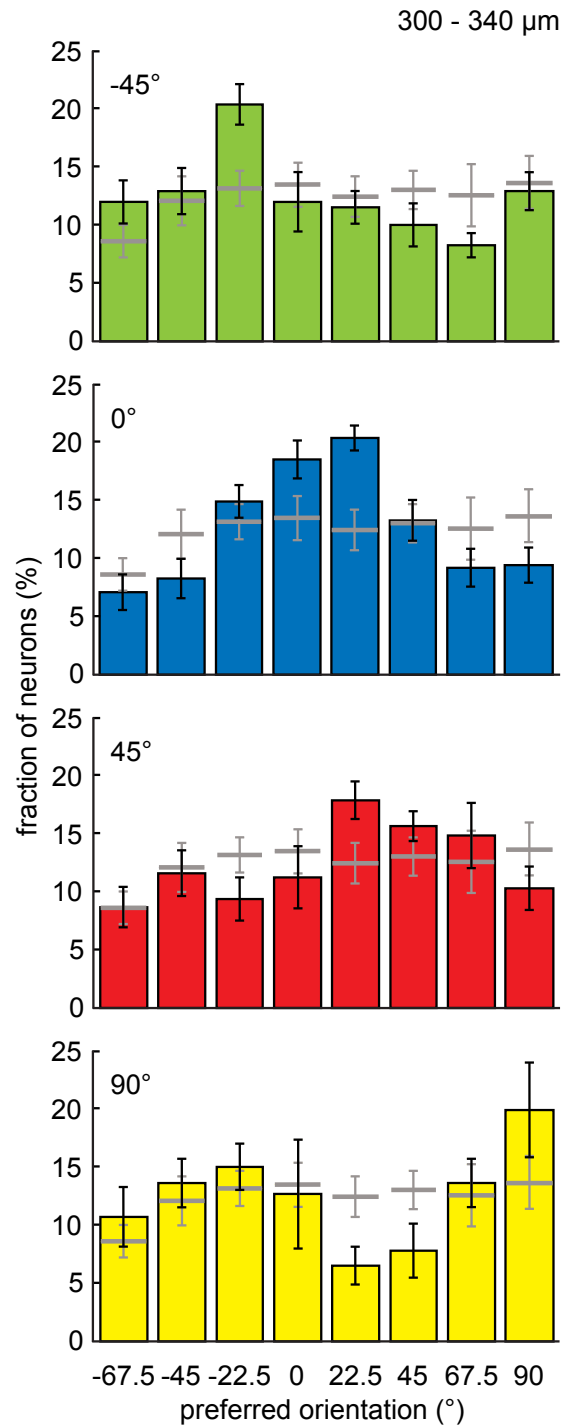
Figure 10: Horizontal bias and permissive effect depend on depth in layer 2/3. (A) Distribution of preferred orientations with increasing depth in layer 2/3 (mean \pm SEM, $n = 8$), cortical depth is coded in color as indicated at the *bottom*. (B) Fraction of responsive neurons with increasing depth in layer 2/3. Note that responsiveness in lower layer 2/3 (*magenta*) of stripe-reared mice does not change relative to controls.

Similarly, the changes in responsiveness following stripe rearing depended on cortical depth (Fig. 10b). The fraction of responsive neurons dropped only in the upper ($-18.5 \pm 6.5\%$, $p = 0.1605$) and middle tier ($-18.4 \pm 4.0\%$, $p < 0.05$) of layer 2/3, which is compatible with a permissive mechanism. In lower layer 2/3, in contrast, the fraction of responsive neurons did not change ($-0.8 \pm 3.3\%$, $p = 0.8935$, t-test, all relative to the fraction of responsive neurons in control mice, $n = 28$ stripe-reared and 8 control mice each). This suggests that the comparatively strong stripe rearing effect I observed among neurons in lower layer 2/3 (Fig. 11) is not caused by permissive changes but can be fully accounted for by an instructive mechanism, i.e. a change in the orientation tuning or response amplitude of individual neurons.

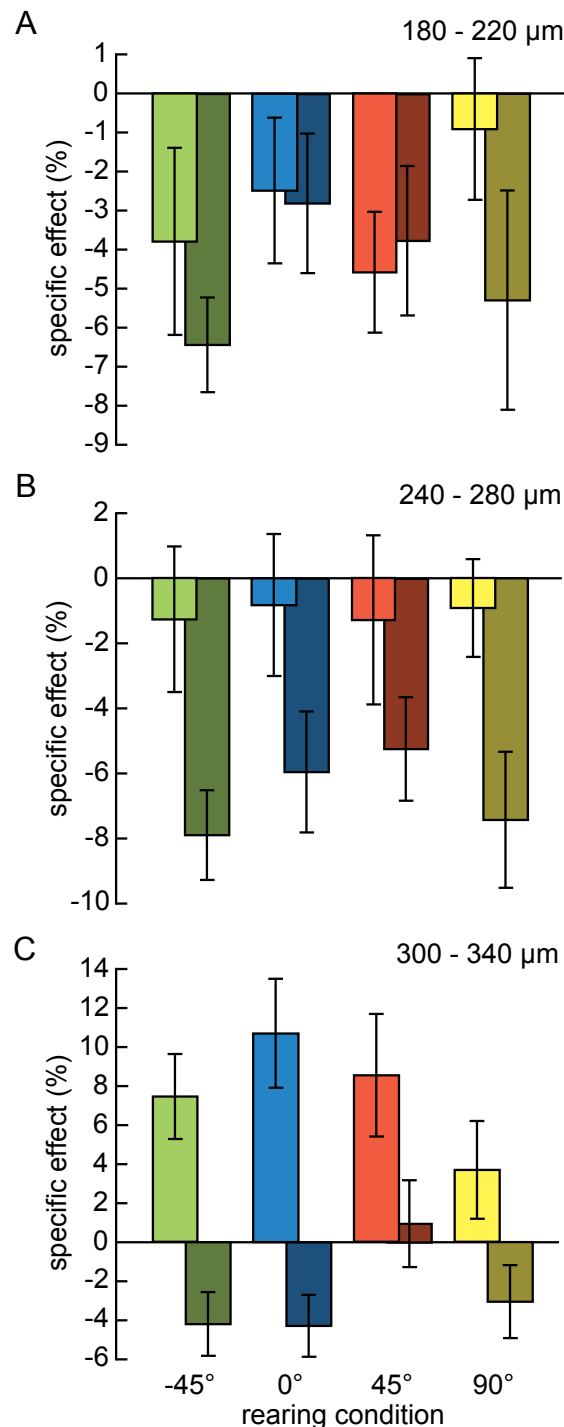
5.1.7 Absolute number of neurons tuned to the experienced orientation increases in lower layer 2/3

In order to test the latter conjecture in a more direct fashion I computed the number of neurons tuned to a particu-

Figure 11: Stripe rearing has a stronger effect on neurons in lower layer 2/3. Distribution of preferred orientations at a depth of 300 – 340 μm (lower layer 2/3) from stripe-reared mice with experienced orientations of -45° , 0° , 45° and 90° as indicated. *Light gray data points*: distribution in control mice.



lar orientation as a fraction of the total number of neurons detected. Thereby, I made use of a technical advantage of two-photon calcium imaging, which, unlike electrophysiological recordings, permits the detection of all neurons within a field of view, including the non-responsive and the non-orientation-selective ones. While the fractions of neurons preferring



the experienced or the orthogonal orientation were both strongly decreased in upper layer 2/3 (180 – 220 μm : experienced orientation: $-3.0 \pm 1.0\%$, orthogonal orientation: $-4.6 \pm 1.1\%$, Fig. 12a), only the fraction of neurons preferring the orthogonal orientation was decreased in the middle tier of layer 2/3 (240 – 280 μm : experienced orientation: $-1.1 \pm 1.1\%$, orthogonal orientation: $-6.7 \pm 0.9\%$, Fig. 12b). In lower layer 2/3 (300 – 340 μm), the fraction of neurons preferring the orthogonal orientation did not

Figure 12: Global specific effect of stripe rearing at different depths of layer 2/3. Global specific effect calculated as percentage of all morphologically detected neurons (see *Materials and Methods*) derived from the population of orientation selective neurons normalized to the total number of detected neurons in each animal at (A) 180 – 220 μm , (B) 240 – 280 μm and (C) 300 – 340 μm . *Bright bars*: experienced orientation, *shaded bars*: orthogonal orientation. Note that the fraction of neurons preferring the experienced orientation is increased in lower layer 2/3, while in upper layer 2/3, both the fraction of neurons preferring the experienced and the orthogonal orientation are decreased.

change much ($-2.7 \pm 1.0\%$, Fig. 12c), whereas the fraction of neurons preferring the experienced orientation strongly increased by $7.6 \pm 1.5\%$ ($n = 28$ stripe-reared and 8 control mice each, Fig. 12c), corresponding to an increase by $40.2 \pm 7.7\%$ when normalized to the fraction of neurons preferring the experienced orientation in control mice. The effects in middle layer 2/3 are somewhat intermediate to those in upper and lower layer 2/3, which might be explained by either a specific drop in the fraction of responsive neurons implying permissive changes, or by a combination of an unspecific drop in responsiveness as found in upper layer 2/3 and a specific increase in the fraction of neurons preferring the experienced orientation as observed in lower layer 2/3. Together, this analysis demonstrates that the changes caused by stripe rearing are diverse and depend on a neuron's vertical position in the cortex: In upper layer 2/3, we find small effects of stripe rearing; rather, the fraction of orientation-selective neurons is reduced regardless of orientation preference. In lower layer 2/3, there is a clear stripe rearing effect with changes largely due to an instructive mechanism, which leads to shifts in the tuning curves of a large number of neurons.

5.1.8 Can the drop in responsiveness explain the specific effect?

Those neurons which loose responsiveness in stripe-reared mice are mainly located in upper and middle layer 2/3 (Fig. 10b). Are neurons, which prefer the orientation orthogonal to the experienced one, selectively affected by this drop in responsiveness, or does it occur independently of orientation preference? If the first was true, we would expect that stripe-

reared mice with a comparatively strong decrease in the fraction of responsive neurons

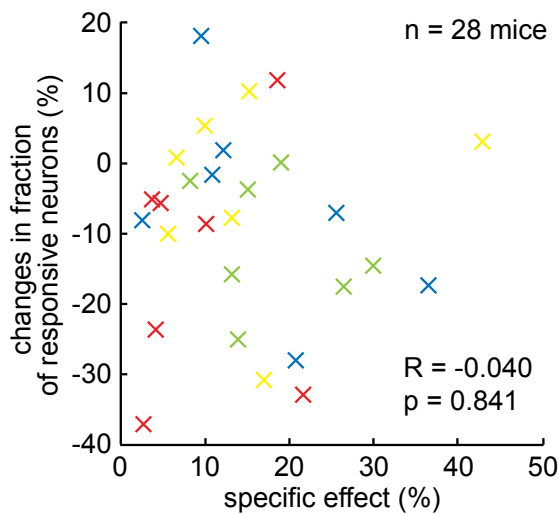


Figure 13: No correlation between change in responsiveness and specific stripe rearing effect. Change in the fraction of responsive neurons after stripe rearing as a function of the specific effect for 28 individual mice with experienced orientations as indicated by colors: *green* (-45°), *blue* (0°), *red* (45°) and *yellow* (90°).

should show an equally stronger over-representation of the experienced orientation, quantified as the specific effect. Therefore, I plotted the change in responsiveness as a function of the specific effect for each stripe-reared mouse (Fig. 13). The two parameters were not correlated ($R = -0.04$, n.s., $n = 28$ stripe-reared mice). This was also true when I analyzed data obtained at different cortical depths separately. These results indicate that changes in responsiveness occur, but they are rather unlikely to account for the over-representation of the experienced orientation caused by stripe rearing.

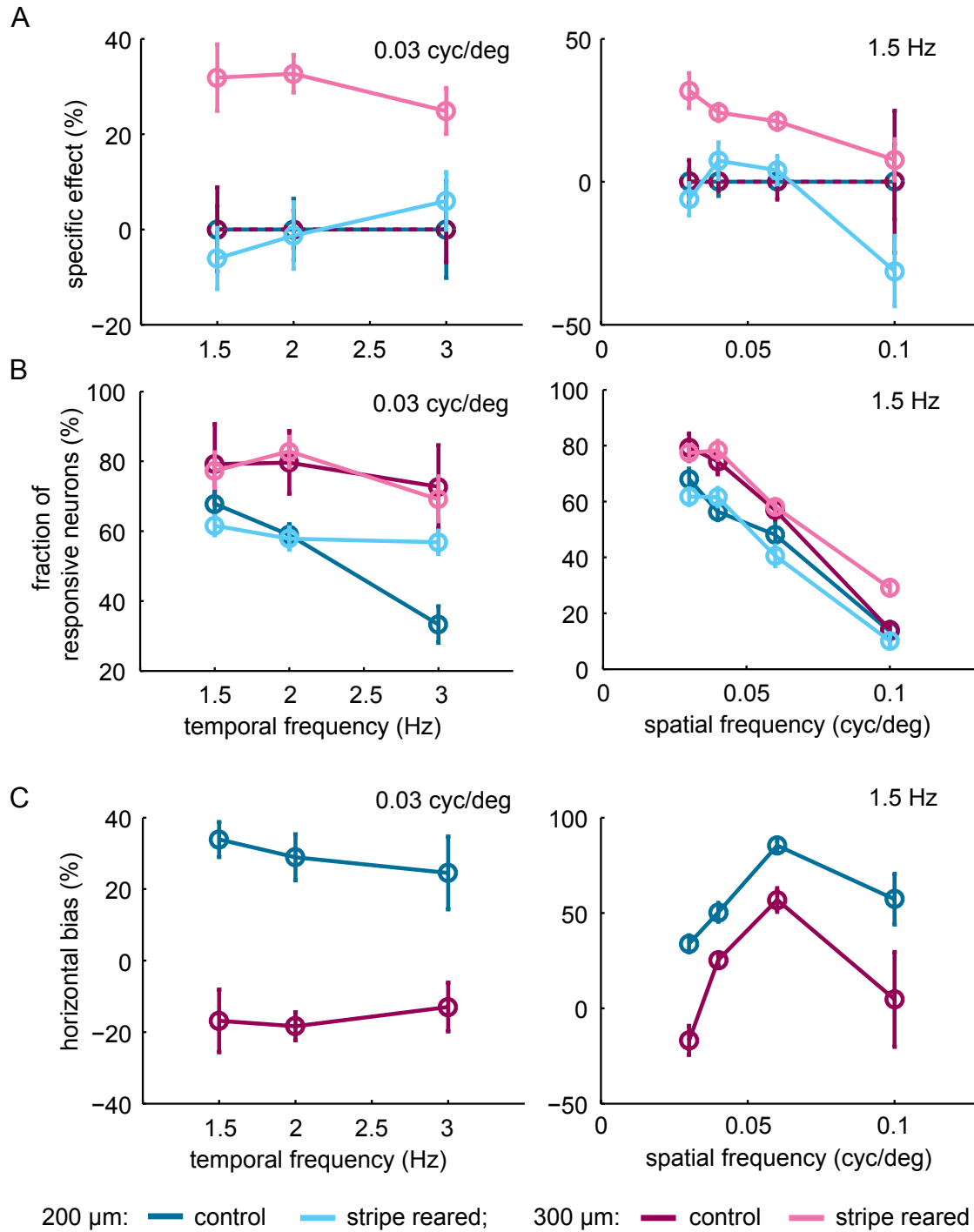
5.1.9 Stripe rearing effect is stable over a range of temporal and spatial frequencies

In addition to removing certain contour orientations, the cylinder lenses likely also change the spatial and temporal frequency composition of visual input in stripe-reared mice, which might in turn alter neurons' tuning for these features and render our standard visual stimulus (0.03 cpd and 1.5 Hz) non-optimal. Therefore, we determined orientation preference using a variety of spatial (0.03, 0.04, 0.06 and 0.1 cpd) and temporal (1.5, 2 and 3 Hz) frequencies in an additional set of experiments, consisting of four control and eight stripe-reared mice (four with 0° and four with -45° as experienced orientation) at cortical depths of 200 μm and 300 μm .

In stripe-reared mice, I reproduced my previous findings: First, the specific effect was large at 300 μm and absent at 200 μm cortical depth (Fig. 14a). Second, there was no significant drop in the fraction of responsive neurons, neither at 200 μm nor at 300 μm depth (Fig. 14b). At the same time, there was also no increase in the fraction of responsive neurons in stripe-reared animals at any of the tested stimulus parameters (Fig. 14b), indicating that the stripe rearing procedure did not shift neuronal response properties towards higher spatial or temporal frequencies on a population level. Importantly, both, specific effect and fraction of responsive neurons were largely independent of temporal and spatial frequency (Fig. 14a & b). An exception is the highest spatial frequency tested (0.1 cpd), where the specific effect appeared to decline, however, only in the rather small fraction of neurons still responsive to this spatial frequency (Fig. 14b). Taken together, these data support the results from

Results

the larger data sample reported above, pointing to an instructive nature of the stripe rearing effect in lower layer 2/3, which does not depend much on the spatial and temporal frequency of the stimulus.



5.1.10 Horizontal bias changes with spatial frequency

Likewise, I confirmed in control mice that the horizontal bias is larger at 200 μm ($33.8 \pm 8.5\%$ at 0.03 cpd and 1.5 Hz) than at 300 μm ($-16.9 \pm 15.2\%$, both at 0.03 cpd and 1.5 Hz) depth ($p < 0.05$, two-sample t test, $n = 4$ mice, Fig. 14c). Changing the temporal frequency did not affect the magnitude of the horizontal bias. However, it strongly increased with increasing the spatial frequency up to 0.06 cpd, but decreased again at 0.1 cpd (Fig. 14c). Closer inspection of the changes in response properties of individual neurons depending on the combination of stimulus parameters revealed two components underlying this effect: Partially, the overall increase in horizontal bias was caused by the recruitment of neurons preferring higher spatial frequencies (7.4 % of the neurons responding at 0.04 cpd were newly recruited compared to 0.03 cpd and 14.6 % of the neurons responding at 0.06 cpd were newly recruited compared to 0.04 cpd). Most of these were tuned to horizontal orientations (52.6 % at 0.04 cpd and 78.1 %

Figure 14: Response properties in stripe-reared and control mice characterized with gratings of different spatial and temporal frequencies. (A) Specific effect and (B) fraction of responsive neurons at different temporal (*left panels*) and spatial frequencies (*right panels*). Data were assessed at 200 μm (*cyan*) and 300 μm (*magenta*) in a separate dataset of control (*dark*) and stripe-reared mice (*bright*). (C) Horizontal bias calculated as the difference between the fraction of neurons preferring horizontal (0°) and the fraction of neurons preferring vertical (90°) orientations (see *Materials and Methods*) as a function of temporal (*left panel*) and spatial frequency (*right panel*) at cortical depths of 200 μm (*dark cyan*) and 300 μm (*dark magenta*). Data are presented as mean \pm SEM (control mice: $n = 4$, stripe-reared mice: $n = 8$ in total, 4 each with 0° and -45° experienced orientation, respectively).

at 0.06 cpd). Partially, the effect can be attributed to shifts in preferred orientation when changing the spatial frequency of the stimulus: Of all neurons responsive at 0.04 cpd, 65.9% changed their preferred orientation towards horizontal by on average $19.4 \pm 1.6^\circ$ and 26.7% changed their preferred orientation towards vertical by on average $17.8 \pm 3.0^\circ$ as compared to 0.03 cpd. Likewise, of all neurons responsive at 0.06 cpd, 71.8% changed their preferred orientation towards horizontal by on average $17.8 \pm 1.5^\circ$ and 13.6% changed their preferred orientation towards vertical by on average $14.3 \pm 4.0^\circ$ as compared to 0.04 cpd. This seems to be at odds with studies in cat visual cortex, which report-

ed preferred orientation to be independent from stimulus spatial frequency^{244, 245}. However, large shifts in orientation preference ($> 10^\circ$) occurred in about 70 % of cases in neurons with low response amplitudes ($< 11\% \text{ dF/F}$), in which the determination of preferred orientation is more error-prone.

5.1.11 Depth-dependent horizontal bias in layer 2/3 is also present in an enriched environment

Visual input significantly influences the maturation of the visual system during development^{59, 246, 247}. The horizontal bias in upper and middle layer 2/3 of V1, which I observed in mice raised under standard housing conditions, could thus potentially be caused by an improper maturation of the visual system caused by the relatively poor visual input the mice receive through their development in a standard cage. Other parameters, such as responsiveness, selectivity, tuning width or response amplitude could be affected, too. To test



Figure 15: Enriched environment. Mice were born and raised in a cage equipped with several levels, running wheels, climbing devices, food trays, nesting material and shelters.

whether a richer visual input would impact orientation selectivity and preference in V1, I raised mice in an enriched environment providing more diverse and high-contrast contours and allowing for frequent and intense self-generated visual input during exercise such as climbing or running. Fourteen male mice were born and raised together in one large cage (Fig. 15) equipped with various elevated levels, running wheels, climbing and balancing devices, nesting materials, food trays and shelters. Mice showed extensive use of all equipment and materials, especially running wheels and climb-

ing devices. Usually they slept in a shelter on an elevated level. Mice socialized and showed very low aggression levels, such that all 14 male littermates could well be kept in one cage.

Between p43 and p51, calcium imaging in V1 using OGB1-AM was performed to measure orientation preference. Neuronal response properties were very similar in mice raised in an enriched environment and in mice raised under standard housing conditions. In enriched mice, on average $79 \pm 2\%$ of the detected neurons were responsive (*see Materials and Methods*) to orientated gratings, of which $66 \pm 3\%$ were orientation-selective (*see Materials and Methods*). Even though responsiveness was higher in enriched mice than in standard-housed mice by trend, responsiveness ($69 \pm 6\%$) and selectivity ($64 \pm 4\%$) in standard-housed mice were not significantly different ($p = 0.10$ and $p = 0.77$, respectively, *t* test). Tuning width in enriched mice was narrower than in standard-housed mice (medians: 37.1° [$n = 319$ neurons] and 40.0° [$n = 2416$ neurons], $p < 0.05$, Wilcoxon rank sum test) and was, as observed in standard-housed mice (*see above*), broadest in vertically and narrowest in horizontally tuned neurons (median [0°] = 31° , median [90°] = 47° , $p < 0.001$, Kruskal-Wallis test with *post hoc* Tukey-Kramer correction for multiple comparisons, $n = 264$ horizontally and 158 vertically tuned neurons). Response amplitudes of orientation-selective neurons in enriched mice

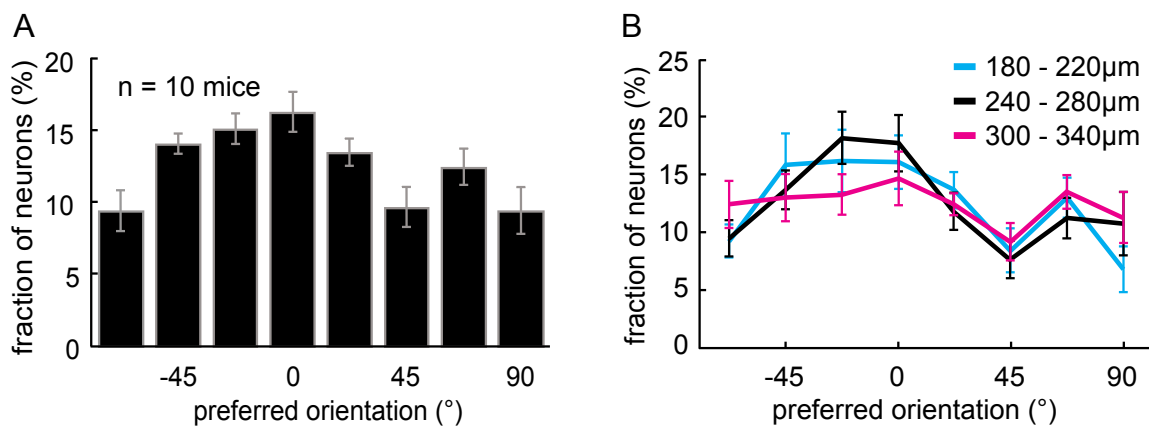


Figure 16: Distribution of preferred orientations of mice raised in an enriched environment. (A) Distribution of preferred orientations (mean \pm SEM, $n = 10$). (B) Distribution of preferred orientations with increasing depth in layer 2/3 (mean \pm SEM, $n = 10$), cortical depth is coded in color as indicated at the *upper right* of the graph. For comparison with mice raised in standard cages, see Fig. 7a and Fig. 10a.

were smaller than those in standard-housed mice (medians dF/F: 16.3% and 18.7%, $p < 0.05$, Wilcoxon rank sum test) and did not vary systematically with neurons' preferred orientation in both groups.

Like standard-housed mice, enriched mice showed a modest over-representation of the cardinal orientations (0° and 90°) with a predominance of horizontally (0°) tuned neurons (fraction of neurons preferring horizontal and adjacent orientations [see *Materials and Methods*]: 46.3 \pm 3.1%, vertical: 30.7 \pm 3.5%, $p < 0.01$, t test, $n = 10$ mice, Fig. 16a). Similarly, the over-representation of horizontally tuned neurons was mainly detected in the upper and middle parts of layer 2/3 and was decreased in lower layer 2/3 (180 – 220 μm depth: horizontally tuned: 16.9 \pm 2.1%, vertically tuned: 5.7 \pm 1.2%, $p < 0.001$; 240 – 280 μm : horizontal: 17.9 \pm 1.6%, vertical: 9.0 \pm 2.3%, $p < 0.01$; 300 – 340 μm : horizontal: 15.6 \pm 1.9%, vertical: 10.8 \pm 1.7%, n. s., t-test, $n = 10$ mice each, Fig. 16b). Overall, standard housing conditions seem to have only a very modest effect on the maturation of the visual system in mice. While median tuning widths and response amplitudes are slightly decreased in mice raised in an enriched environment, characteristic changes in tuning width with preferred orientation and in horizontal bias with depth in layer 2/3 are not affected, and are therefore most likely not attributable to degenerate visual input.

5.1.12 Synopsis – experience-dependent plasticity of orientation preference

In summary, stripe rearing mice with cylinder lens goggles induces an over-representation of the experienced orientation in the visual cortex. The effect of stripe rearing on responsiveness varied with depth in layer 2/3, such that the number of responsive neurons decreased slightly in upper and middle layer 2/3, but not in lower layer 2/3. Yet, I found a prominent stripe rearing effect in lower layer 2/3. Importantly, in lower layer 2/3 I observed an absolute increase in the number of neurons preferring the experienced orientation. Before discussing why these data suggest that instructive changes play a key role for experience dependent plasticity of orientation selectivity in mouse visual cortex, I will present the results of a different set of experiments, measuring changes in orientation tuning during learning.

5.2 Plasticity of orientation tuning in mouse V1 induced by operant conditioning

In order to investigate plasticity of orientation preference in a behaviorally relevant context, we employed operant conditioning, a procedure during which the brain establishes an optimized behavioral pattern based on sensory input. More specifically, the aims of this study were, first, to induce an association between a food reward and a grating of a particular orientation by training on an orientation discrimination task, and second, to quantify and describe functional changes in V1 induced by this learning paradigm on the level of individual neurons.

5.2.1 An orientation discrimination task designed for mice

We trained juvenile mice in an operant chamber (Fig. 17, view from top) to choose a grating with a certain orientation (**target**) over a grating with an alternative orientation (**non-target**), the two of which were simultaneously displayed on touch screens. The presentation of the target (**either on the left or the right touch screen**) was pseudo-randomized. After indicating its choice by pressing the corresponding touch screen with its forelimbs or nose, the

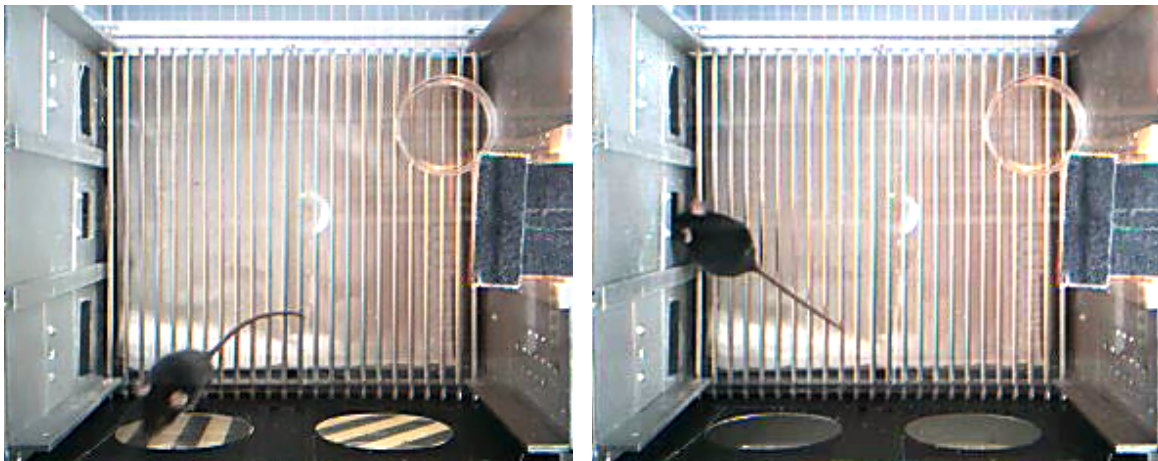


Figure 17: Mouse solving a visual task in the operant chamber. Out of two displayed gratings, the mouse has to identify the vertical one by pressing the respective touch screen (*left image*) to receive a food pellet at the reward site (*right image*).

Results

mouse either received a reward for a correct choice or no reward for a wrong choice. The next trial started with a constant delay in both cases.

Mice were trained from the age of p25 onwards (Fig. 18a) for at least 10 hours per session overnight as mice are nocturnal animals. Between training sessions, mice were kept in a cage under standard housing conditions. Water was freely available *ad libitum* both in the operant chamber and the cage. Outside the operant chamber, mice did not receive any food except on Saturdays. On average, mice gained 11.0 ± 0.5 % of their body weight during a training or food retrieval session in the operant chamber and lost 8.3 ± 0.4 % of their body weight between training or food retrieval sessions. The training consisted of six different stages (A – F, Fig. 18b) with increasing levels of difficulty. For a detailed description please see *Materials and Methods*.

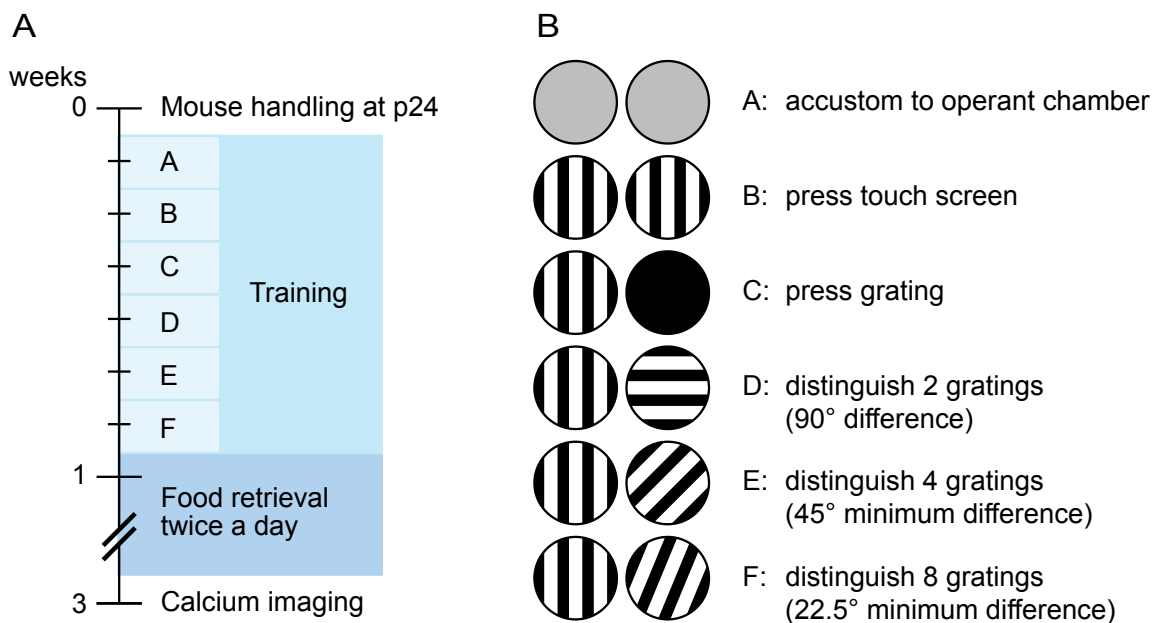


Figure 18: Mouse training protocol for the visual task. (A) Timeline of training (*bright blue*) and subsequent food retrieval phase (*middle blue*) during which the trained mouse earns its food by solving tasks twice a day for 30 min. (B) Different stages of training with increasing complexity. *Patterned circles*: schematized touch screens displaying example target and non-target stimuli at the respective training stage. Training included stages A: exploring operant chamber, B: pressing target grating displayed on both screens, C: choosing target over black screen, D: choosing target over non-target with 90° differential orientation (*dO*), E: choosing target over three non-targets with minimum 45° *dO*, and F: choosing target over seven non-targets with minimum 22.5° *dO*.

In the following, the rewarded orientation will be termed “target”. Alternative orientations which are displayed simultaneously are referred to as “non-target”. Actions of the mice were classified into three categories: “Presses” are touch screen pokes at any time during the training session. “Choices” are presses onto a displayed stimulus, either target or non-target. Retrieving food from the food receptacle is termed “food retrieval”. To assess mouse performance, I quantified several behavioral parameters: “Accuracy” measures the percentage of correct choices, “efficiency” corresponds to the percentage of choices out of all presses, “reward yield” is the percentage of obtained rewards out of the maximally possible number of rewards. In addition, the temporal delays between stimulus display and choice ([response delay](#)) and between choice and food retrieval ([food retrieval delay](#)) were calculated.

5.2.2 Mice improve in task performance during a single 10-hour training session

At the start of each training session, mice were naive with regard to the specific task to be solved. During a session of about 10 hours duration, mice improved substantially on the task.

During the second training session ([training B](#)), mice had to press either of the two screens in order to receive a food reward. The reward was only given, if the monitors were displaying the target during pressing, but not, if they were black. Over time, pressing frequency increased and at the same time, response delay decreased ([Fig. 19a & b](#), [Table 1](#)). Apparently,

time span (h)	0 – 2	2 – 4	4 – 6	6 – 8	8 – 10
presses (/min)	0.1 ± 0.0	0.4 ± 0.1	0.5 ± 0.1	0.4 ± 0.1	0.6 ± 0.1
efficiency (%)	61.8 ± 7.9	45.5 ± 5.2	32.5 ± 5.9	32.4 ± 4.9	19.5 ± 6.7
response delay (min)	3.6	4.0	1.2	0.6	0.7

Table 1: Average performance assessed every two hours during training B in 10 mice. *White shading:* significant increase, *dark gray shading:* significant decrease, *light gray shading:* not significantly different from the first datapoint ($p < 0.05$, one-way ANOVA (presses and success rate) or Kruskal-Wallis test (response delay) with *post hoc* Tukey-Kramer correction for multiple comparisons). Mean ± SEM (presses and success rate) or median (response delay).

Results

the mice increasingly associated pressing the screen with the reward. On the other hand, they showed a decreasing preference of pressing the target pattern, as the efficiency, quantifying the percentage of cases in which the mice pressed the target as opposed to the black

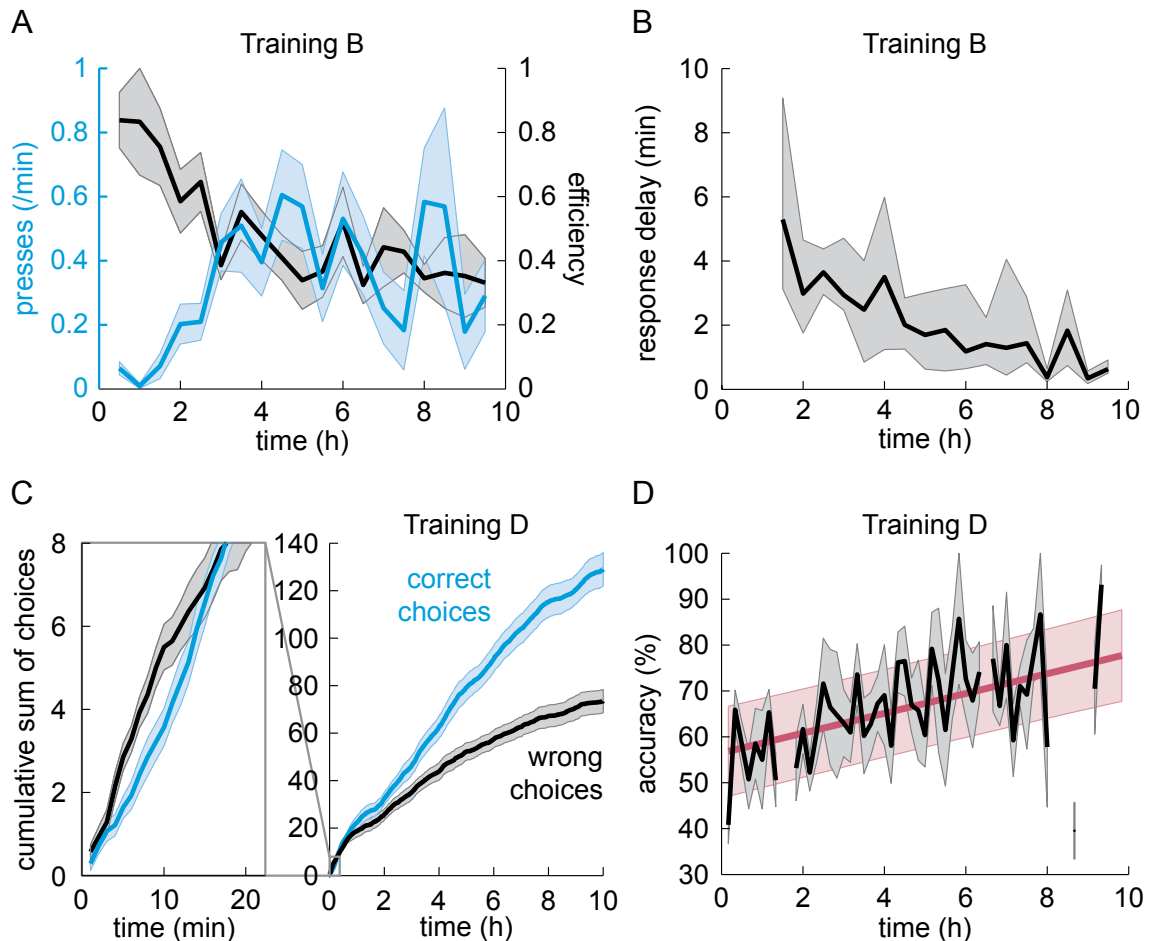


Figure 19: Improvement within single training sessions. (A and B) Average ($n = 10$ mice) performance during training B (reward for pressing either of two touch screens both displaying the target grating): (A) touch screen presses per minute (*blue*) and efficiency (*black*, fraction of presses while the gratings were presented as opposed to black screens), both mean \pm SEM, data binned every 30 min. (B) Response delay (interval between grating display and mouse touching the screen), median and 25/75 percentiles, data binned every 30 min. (C and D) Average performance ($n = 14$ mice) during training D (reward for choosing the target grating over an orthogonal non-target grating): (C) cumulative sum of correct (*blue*) and wrong (*black*) responses over time. *Left inset*: initial 22 min of the training session. (D) Accuracy quantified as percentage of correct responses (*black*, mean \pm SEM, data binned every 10 min) and linear fit with 95% confidence intervals (*dark red*)

time span (min)	target choices (/min)	non-target choices (/min)	significance level (t test)
0 – 5	0.33 ± 0.01	0.57 ± 0.02	p < 0.01
5 – 10	0.39 ± 0.02	0.53 ± 0.02	n. s.
10 – 15	0.60 ± 0.02	0.29 ± 0.02	p < 0.01
15 – 20	0.57 ± 0.02	0.34 ± 0.02	p < 0.05

Table 2: Average frequency of target and non-target responses assessed every five minutes during the first 20 minutes of training D in 14 mice. Frequency of non-target choices was significantly higher (*white shading*) than frequency of target choices in the first five minutes, not significantly different (*light gray shading*) during minutes 5 – 10, and significantly lower (*dark gray shading*) during minutes 10 – 20; mean ± SEM.

screen, decreased (Fig. 19a, Table 1). At this point their main strategy for receiving food pellets seemed to be a more frequent pressing of a touch screen, independently of what it displays.

In the next training session (training C), mice had to learn to choose the target grating over a black screen in order to receive a food reward. In training D, a grating with a differential orientation (dO) of 90° to the target was shown as a non-target for the first time.

This led to an initial preference of the non-target over the target (Fig. 19c, Table 2), an effect known from delayed matching-to-sample experiments²⁴⁸. The preference is significant during the first five minutes and reverses after 10 minutes in favor of the target.

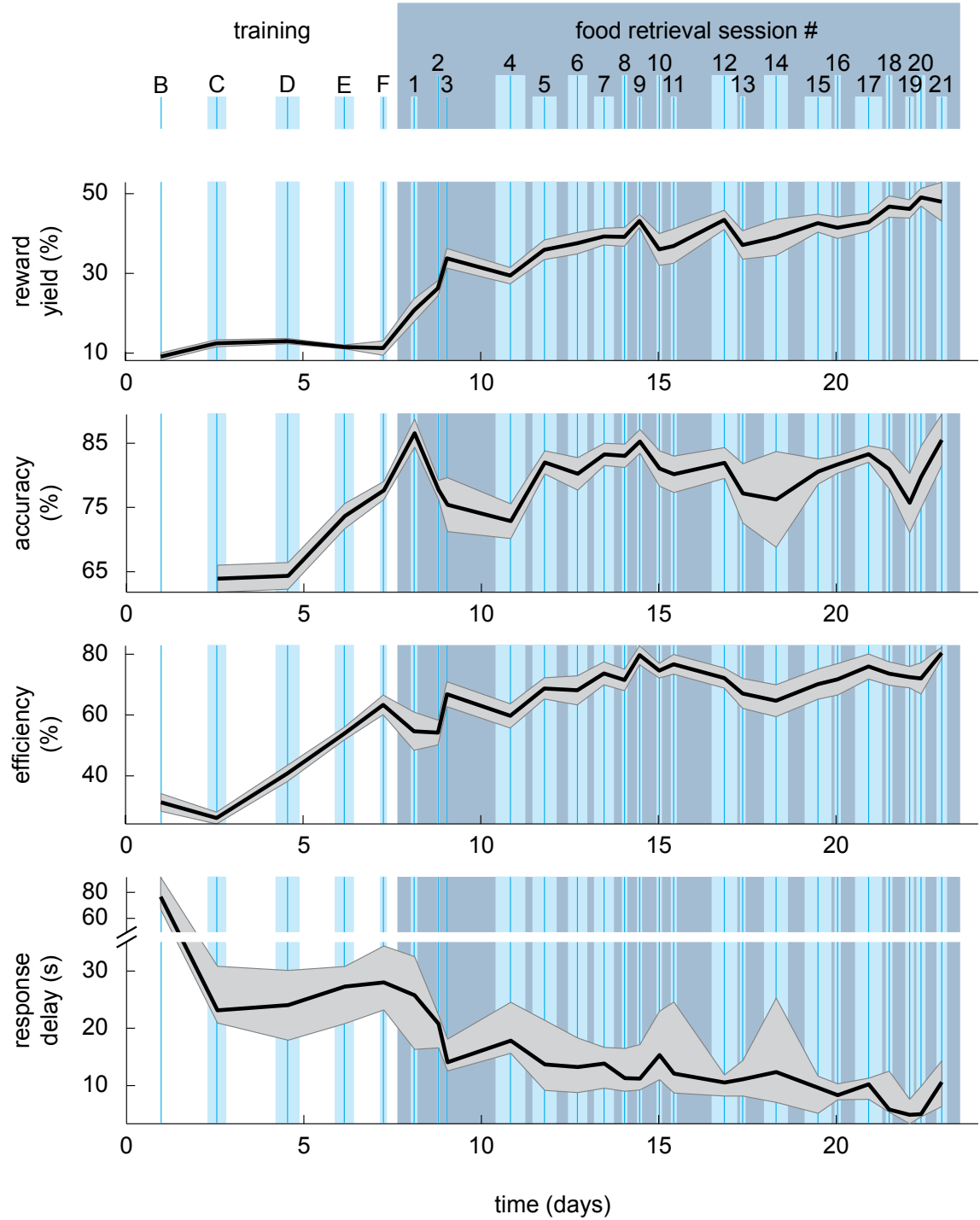
During the following 10 h of training D, mice further increased the fraction of correct responses (Fig. 19d, Table 3). Unlike during training B, the frequency of presses was highest

time span (h)	0 – 2	2 – 4	4 – 6	6 – 8	8 – 10
presses (/min)	1.5 ± 0.2	1.1 ± 0.2	0.8 ± 0.1	0.7 ± 0.1	0.8 ± 0.2
accuracy (%)	56.0 ± 2.8	62.3 ± 3.0	67.0 ± 2.7	73.7 ± 4.0	70.6 ± 2.4

Table 3: Average performance assessed every two hours during training D in 14 mice. *White shading*: significant increase, *dark gray shading*: significant decrease, *light gray shading*: not significantly different from the first datapoint; p < 0.05, one-way ANOVA with *post hoc* Tukey-Kramer correction for multiple comparisons; mean ± SEM.

Results

initially in training D and decreased over time, likely due to satiation or tiredness and as a consequence of a stronger goal-directed behavior.



5.2.3 Mice increase accuracy during training and efficiency after introducing time pressure

After a little more than a week of training, mice solved the task with a significantly higher accuracy and higher efficiency, an indicator for a stronger goal-directed behavior

Figure 20: Improvement over sessions.

Changes in performance of 12 mice over five training and 21 food retrieval sessions. From *top to bottom*: reward yield (the fraction of possible rewards earned, mean \pm SEM), accuracy (percentage of correct responses, mean \pm SEM), efficiency (the percentage of presses onto a grating as opposed to a black screen, mean \pm SEM), response delay (median and 25/75 percentiles). *Vertical thin blue lines* indicate average timepoints of session, *width of bright blue bars* shows SEM. The food retrieval phase is marked by a *gray box*.

(Fig. 20, Table 4). The response delay decreased only initially by trend, but not significantly. Simultaneously, the reward yield, which is the fraction of potential rewards the mice received, barely increased (Fig. 20, Table 4). Both can be explained by the lack of time pressure during the training sessions, which led to a virtually unrestricted availability of food once the mice had learned the task.

Subsequent to the six-session training phase, the mice entered the food retrieval phase during which they had to

solve the task twice a day for 30 min over a period of on average two and a half weeks (Fig. 18a). By the introduction of temporal restriction, mice were forced to increase the reward yield. They did so by decreasing the response delay significantly (Table 4), initially at the expense of accuracy, quantified as the fraction of correct responses (Fig. 20, see food retrieval sessions #1 – 4). In subsequent sessions, reward yield further increased significantly compared to the start of the food retrieval phase, mainly through a significant increase in efficiency (Fig. 20, Table 4). In addition, the response delay decreased further by trend while accuracy, after recovery from the brief drop, remained mostly stable on a high level (Fig. 20, Table 4).

5.2.4 Performance is limited by mice's orientation discrimination threshold

Few data have been published on the physiological orientation discrimination limit of mice. The non-target gratings we used had differential orientations (dO) between 22.5°

Results

time (d)	0 – 2.5	2.5 – 5	5 – 7.5	7.5 – 10	10 – 12.5	12.5 – 15	15 – 17.5	17.5 – 20	20 – 22.5
RY (%)	9.1 ± 1.0	12.7 ± 0.7	11.4 ± 1.0	26.9 ± 1.7	32.7 ± 1.9	39.8 ± 1.9	38.3 ± 2.8	40.9 ± 3.2	45.1 ± 1.5
AC (%)	-	64.1 ± 1.7	75.7 ± 1.5	80.3 ± 1.6	77.4 ± 1.6	82.9 ± 1.0	80.1 ± 2.1	78.0 ± 3.5	80.7 ± 0.7
EF (%)	31.3 ± 2.9	33.5 ± 1.8	58.6 ± 2.0	58.2 ± 3.7	64.2 ± 2.9	73.2 ± 2.6	72.6 ± 2.3	66.4 ± 3.4	73.2 ± 2.0
RD (min)	76.6	25.0	28.8	20	17.5	11.3	12.4	10.9	7.6

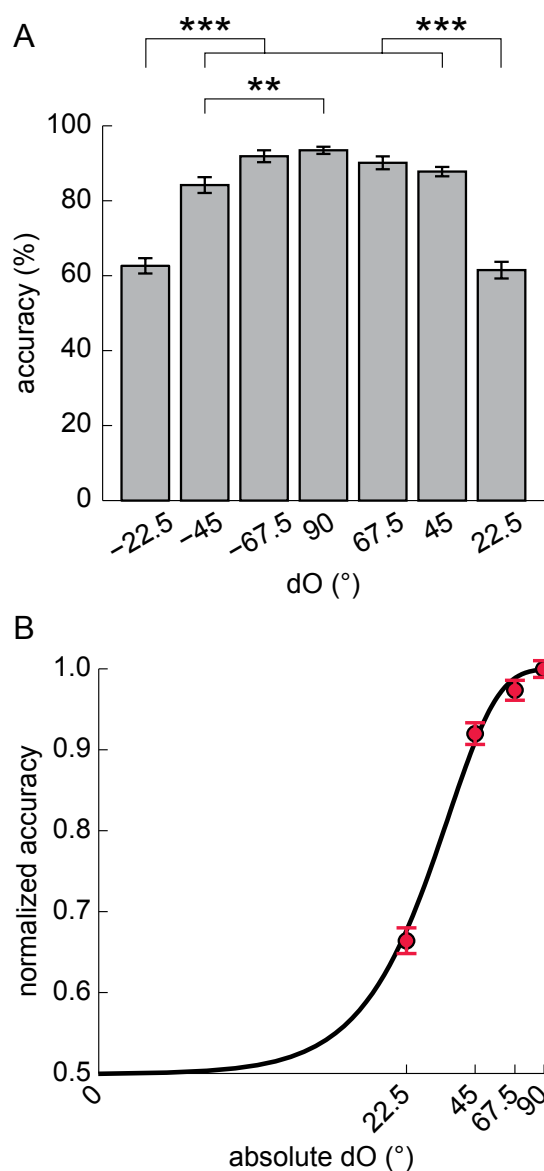
Table 4: Average performance during training and food retrieval phase assessed every 2.5 days in 14 mice. RY: reward yield (fraction of potential rewards received), AC: accuracy (fraction of correct responses), EF: efficiency (fraction of targeted responses), RD: response delay. *Red line*: start of food retrieval phase. *White shading*: significant increase, *dark gray shading*: significant decrease, *light gray shading*: not significantly different from the first training session. Significant changes in performance starting from the introduction of time pressure during the first food retrieval session is indicated by *red shading* (significantly higher than first food retrieval session, $p < 0.05$, one-way ANOVA (RY, AC and EF) or Kruskal-Wallis test (RD) with *post hoc* Tukey-Kramer correction for multiple comparisons); mean \pm SEM (RY, AC and EF) or median (RD).

and 90° compared to the target grating. To estimate how close a differential orientation of 22.5° is to the orientation discrimination limit and whether, in the range of differential orientations used, smaller differential orientations increase task difficulty, we quantified the accuracy for each type of non-target. For this analysis, we considered food retrieval sessions starting from session #5, where a stable level of accuracy was reached (Fig. 20), to session #21. Mice performed significantly worse both at 22.5° dO ($61.5 \pm 2.2\%$) and -22.5° dO non-targets ($62.6 \pm 2.0\%$) compared to $\pm 45^\circ$ dO ($87.8 \pm 1.2\%$ and $84.2 \pm 2.1\%$), $\pm 67.5^\circ$ dO ($90.1 \pm 1.7\%$ and $91.9 \pm 1.6\%$) or 90° dO non-targets ($93.4 \pm 1.0\%$, all mean \pm SEM, $p < 0.001$, one-way ANOVA with *post hoc* Kruskal-Wallis correction for multiple comparisons, Fig. 21a). For a comparison of accuracy between small and large dO trials, $\pm 22.5^\circ$ and $\pm 67.5^\circ$ dO non-targets are best suited, because both these non-target orientations were introduced in training F and displayed with the same frequency. Moreover, accuracy for $\pm 67.5^\circ$ dO non-targets is not different from accuracy for 90° dO non-targets. On average, mice performed much better in large

Figure 21: Performance depends on the difference between target and non-target orientation.

(A) Accuracy as a function of differential orientation (dO) between target and non-target (mean \pm SEM, $n = 12$ mice). Two asterisks: $p < 0.01$, three asterisks: $p < 0.001$ (one-way ANOVA with Tukey-Kramer *post hoc* correction for multiple comparisons). (B) Accuracy (normalized to value at 90° dO) of all mice ($n = 12$, gray symbols) was fitted by a Weibull function using a maximum-likelihood fitting criterion²³⁹ (black line, t : 32.21° , b : 1.97, log likelihood: 1553.8); red symbols: mean \pm SEM accuracy across mice.

dO trials and achieved only $62.0 \pm 1.7\%$ of their $\pm 67.5^\circ$ dO non-target accuracy when a $\pm 22.5^\circ$ dO non-target was displayed. Fitting orientation discrimination accuracy with a Weibull function^{238, 239} reveals that 22.5° differential orientations are below the sensory threshold of 32° (corresponding to approximately 80% normalized accuracy [see *Materials and Methods*], Fig. 21b).



5.2.5 Training-induced changes in cortical orientation tuning

During the food retrieval phase of on average two and a half weeks duration, all mice were rewarded for pressing the vertical grating. Subsequently, two-photon calcium imaging using the synthetic calcium indicator OGB1-AM was performed to measure orientation selectivity in the visual cortex. While the average distribution of preferred orientations differed slightly from the characteristic smooth distribution observed in control mice (Fig. 22a), no significant differences could be detected. Specifically, the (rewarded) vertical orientation (that is, 90°) was not over-represented. Rather, some trained mice showed a strong vertical

Results

bias, which was rarely seen in control mice. In contrast, other mice showed a pronounced horizontal bias, which was, unlike in control mice, restricted to a very narrow range around 0° (for examples, see Fig. 22b). Neither the magnitude of deviation from the control distribution, nor the ratio of neurons preferring vertical or horizontal orientations correlated with mouse performance in the learning task (data not shown).

The median tuning width of neurons in mice trained in an operant chamber (43.5°) was broader than in mice raised under standard housing conditions (40.0°) and in an enriched environment (37.1° , $p < 0.05$, Kruskal-Wallis test with *post hoc* Tukey-Kramer correction for multiple comparisons). While the tuning width of neurons preferring the target orientation (vertical/ 90°) was not different among all three groups, neurons with a horizontal preference were tuned significantly broader (Fig. 23a) in trained mice. The median response amplitude was lower in trained mice compared to standard-housed mice or enriched mice (Fig. 23b). Neither tuning width nor response amplitude was correlated with performance in trained mice (data not shown).

Taken together, I found only minor changes in neuronal response properties in these

experiments. However, these changes did not correlate well with mouse performance, partially because all mice were performing on a high level at this stage of the training. The main problem, however, was that in these experiments, we could only compare

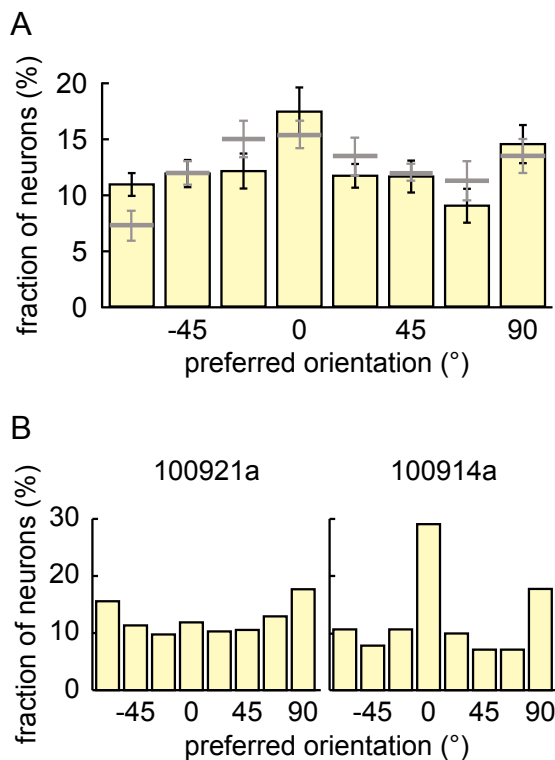


Figure 22: Distribution of preferred orientations after training with a vertical target. (A) Average distribution of preferred orientations in mice trained in an operant chamber on a vertical (90°) target (bright yellow bars) and mice raised under standard housing conditions (light gray lines), mean \pm SEM, $n = 7$ mice each. (B) Two example distributions of preferred orientations of individual mice trained on a vertical target.

trained with non-trained groups at the population level, and both groups were very heterogeneous with regard to orientation preference. In an ideal experiment, one would like to observe the changes in orientation tuning occurring in individual neurons over time during an earlier phase of training. To this end, we employed repeated two-photon imaging using a genetically encoded calcium indicator, GCaMP3, which allows repeated imaging from the same neurons over time.

5.2.6 Adapted orientation discrimination task for combination with repeated calcium imaging

The synthetic calcium indicator OGB1-AM is not well suited for repeated calcium imaging. Instead, we used GCaMP3, which we expressed with an AAV vector yielding sufficient expression two weeks after injection²²⁷. In order to allow for a stable cranial window, we worked with young adult mice which show less synaptic plasticity^{77, 249} and also perform

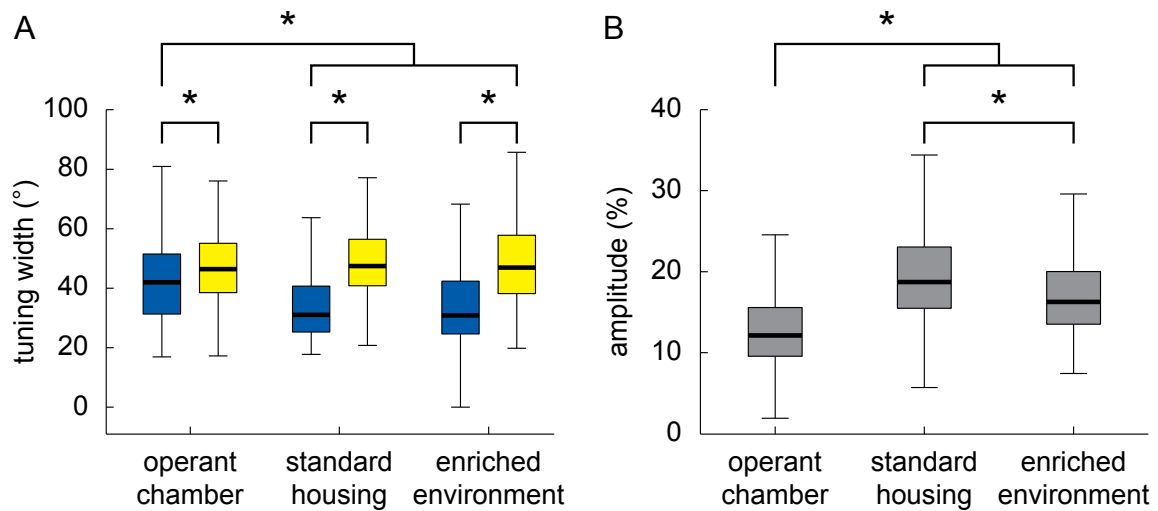


Figure 23: Tuning width and response amplitude after training on a vertical target. Box-plots (black lines: median, colored boxes: 25/75 percentiles, errorbars: 10/90 percentiles) of (A) tuning width of neurons preferring vertical (90°, yellow) or horizontal (0°, blue) orientations. (B) Response amplitude of all orientation selective neurons in mice trained on a vertical target in an operant chamber, in mice raised under standard housing conditions, and mice raised in an enriched environment. Asterisk: significant difference ($p < 0.05$, Wilcoxon rank sum test with Tukey-Kramer *post hoc* correction for multiple comparisons).

worse in learning paradigms compared to juvenile mice^{86, 90}. This drawback can be overcome partially by specific rearing conditions: mice regularly running in wheels as well as mice housed in an enriched environment show enhanced synaptic plasticity⁸⁸ and perform better in learning tasks^{86, 89}. Thus, in order to increase the success rate in our training paradigm, male mice, which perform better than females in some forms of, among them reward-based, learning^{250, 251}, were kept from p24 onwards (Fig. 24a) in groups of four in a large cage containing a running wheel, a shelter and nesting material. In addition, they were kept in a room with a shifted light-cycle, in order to match training phases with phases of highest activity of the mice (and the PhD student).

Based on my own (see below) and other lab-members' experience, GCaMP3 expression levels, and therefore GCaMP3 baseline fluorescence intensity, are largely constant over 12 days. Thus, calcium imaging data acquired over this time period can be considered to be comparable. Within 12 days, we performed four imaging experiments in total, each spaced by four days (Fig. 24a). Two imaging experiments were conducted before training, in order to measure baseline variability in orientation preference. The third imaging experiment was performed within one hour after the last training session of an intense 3.5-day training period to assess learning-induced changes in orientation tuning. After four more days without training, we assessed orientation tuning in a final imaging experiment to quantify delayed changes induced by training (Fig. 24a). In order to match training to the four-day-spaced imaging sessions, I shortened training to stages B (pressing either of two screens, both displaying the target), D (choosing the target over a simultaneously displayed non-target with a differential orientation [dO] of 90°) and F (choosing the target over one out of seven non-targets with minimum 22.5° dO) by leaving out stages A, C and E (for a detailed description of the stages, please refer to *Materials and Methods*, see also Fig. 18b). Training took place for at least 10 h over night. The mice did not undergo any food retrieval phase, instead training F was repeated (Fig. 18b and Fig. 24a). This training regime did not only accommodate our imaging experiments, but also allowed us to assess training-induced plasticity at a much earlier stage of learning compared to the extended training protocol (Fig. 18a). Moreover, we used the advantage of a broader distribution of performance levels mice achieved during the short

training, ranging from chance level up to an accuracy of 83%. This opened the opportunity of correlating performance with functional changes in individual neurons occurring during training.

Despite the rather short training period and the age of the mice, about half of the mice learned the task very well, making more than 62.5% correct choices in the final training ses-

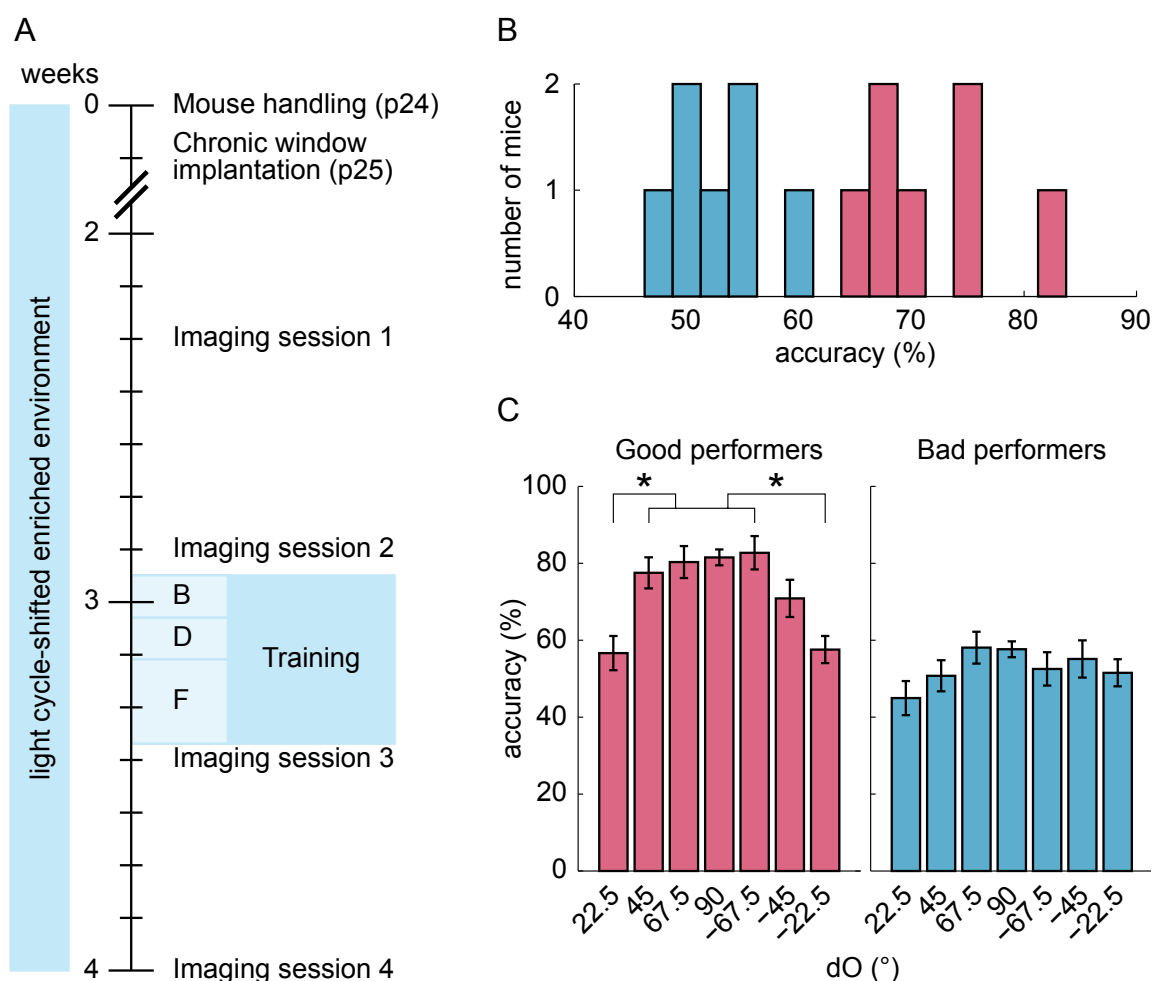


Figure 24: Modified training protocol compatible with chronic calcium imaging. (A) Time-line of modified training protocol and calcium imaging sessions. (B) Accuracy (percentage of correct responses) of 14 mice in their last session. *Magenta*: mice classified as good performers, *blue*: mice classified as bad performers. (C) Accuracy of good (*left panel*) and bad (*right panel*) performers depending on the differential orientation between target and non-target (dO, mean \pm SEM, n = 7 mice each). *Asterisk*: significant difference (p < 0.05, one-way ANOVA with Tukey-Kramer *post hoc* correction for multiple comparisons).

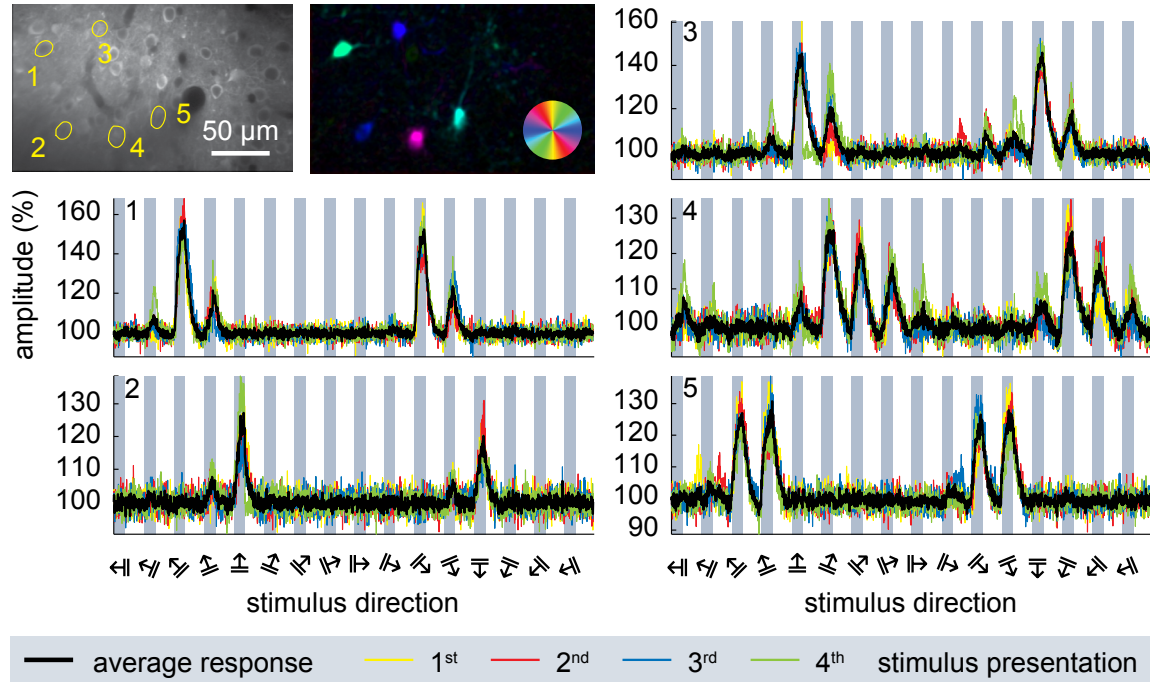
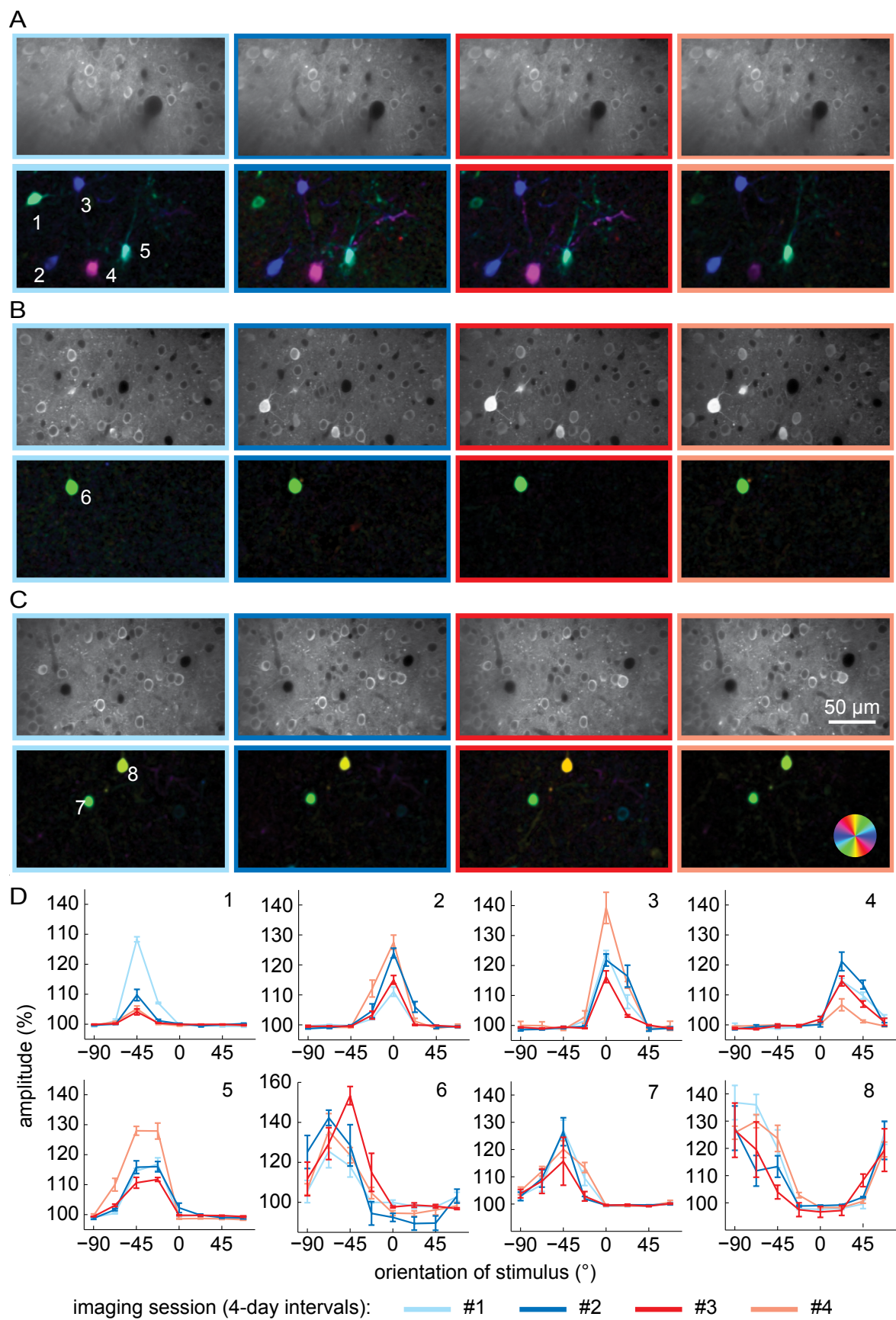


Figure 25: Imaging orientation preference with the genetically encoded calcium indicator GCaMP3. *Top left image:* average fluorescence image (left, 8330 frames) with regions of interest (ROIs) marked in yellow. *Right image:* corresponding pixel-based orientation map (HLS map) with coding for preferred orientation (*hue*), response amplitude (*lightness*) and tuning width (*saturation*). *Graphs:* average dF/F (black) signal of corresponding ROIs and dF/F signals to four repetitions (yellow, red, blue and green) of moving grating presentation (gray shading).

sion (Fig. 24b). These mice were classified as good performers ($n = 7$), while an equally large group of mice which made less than 62.5% correct choices in the final training session were classified as bad performers ($n = 7$). Good adult performers achieved an accuracy of $72.4 \pm 2.4\%$ correct choices after three training sessions, while the bad adult performers performed with only $53.1 \pm 1.5\%$ accuracy on average ($p > 0.01$, t test).

Like in juvenile mice, the accuracy of the good performers among the young adult mice depended on the differ-

Figure 26: Repeated two-photon calcium imaging in mouse V1. The same cortical regions were imaged every 4 days (light blue: timepoint 1, blue: timepoint 2, red: timepoint 3, light red: timepoint 4). (A – C) Average fluorescence images (upper rows, 8330 frames) and HLS maps (lower rows) of four successive imaging sessions. (D) Responses to moving gratings of neurons marked by white numbers in the upper panels in four successive imaging experiments.



ential orientation (dO) between target and non-target (Fig. 24c). They achieved on average $70.7 \pm 4.7\%$ accuracy during trials with 22.5° dO non-targets compared to 67.5% dO non-targets ($p < 0.05$, one-way ANOVA with *post hoc* Tukey-Kramer correction). In contrast, there was no significant difference in bad performers. The likelihood of food retrieval site entry, that is, the mouse entering its head into the food receptacle, before the onset of the next trial depended on the accuracy in the respective trial. If the choice was correct, mice entered the food retrieval site in $94.5 \pm 3.5\%$ of cases (good performers only: $97.7 \pm 0.6\%$), if the choice was wrong, only in $52.5 \pm 5.1\%$ of cases ($p < 0.001$, t test).

5.2.7 Repeated orientation preference measurements in individual neurons using GCaMP₃

Using the genetically encoded calcium indicator GCaMP₃, we measured reliable orientation-selective responses in V1 of anesthetized mice (Fig. 25). We re-found and re-imaged each region (112 regions in 14 mice) in layer 2/3 every four days over a total duration of 12 days (Fig. 26). Only a minority of neurons showed a strong increase in baseline fluorescence (such as in Fig. 26b), with elevated GCaMP₃ expression in the nucleus. Such neurons often show only weak fluorescence changes with unusually slow kinetics upon activation, and are considered to be potentially damaged. In general, however, expression levels were largely stable in the vast majority of neurons throughout the 12 day imaging period.

Of all 777 neurons which were classified as orientation-selective in at least one of the four imaging experiments, a majority was only orientation-selective during either one (16.1 %), two (21.4 %) or three (31.3 %) experiments, most of them actually classified as non-responsive in the remaining experiments. Only 31.3 % were orientation-selective in all four imaging sessions. In the following, I describe the functional changes observed in this population of neurons. It should be kept in mind that these data are, as demonstrated above, based on a small population of neurons within visual cortex.

5.2.8 Good performers show increased plasticity in orientation preference before training

Learning an orientation discrimination task may influence the representation of orientation preference in V1 neurons. Monitoring orientation preference over time (Fig. 27a), we found that baseline changes in preferred orientation were relatively small. The median magnitude of changes during the first four days was by trend larger in good (8.0° , $n = 49$ neurons) than in bad (6.3° , $n = 68$ neurons) performers ($p = 0.07$, Wilcoxon rank sum test, Fig. 27b). Notably, in good performers, median changes in preferred orientation were reduced during

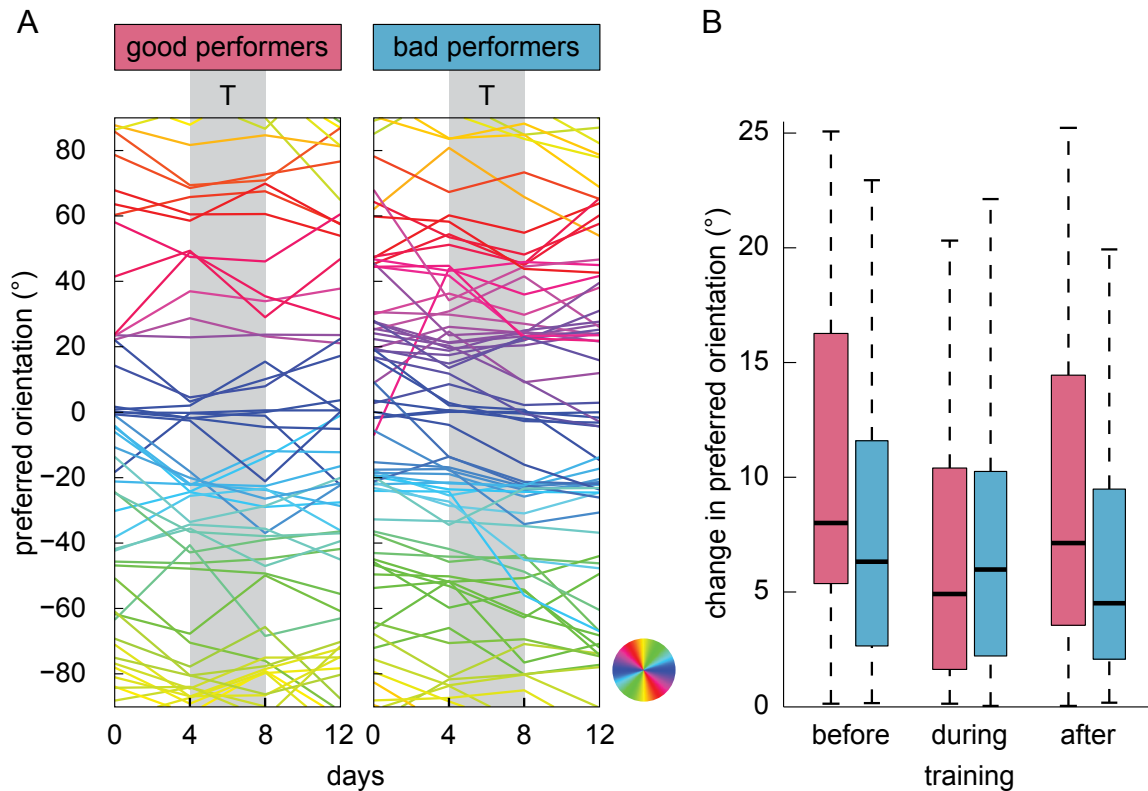
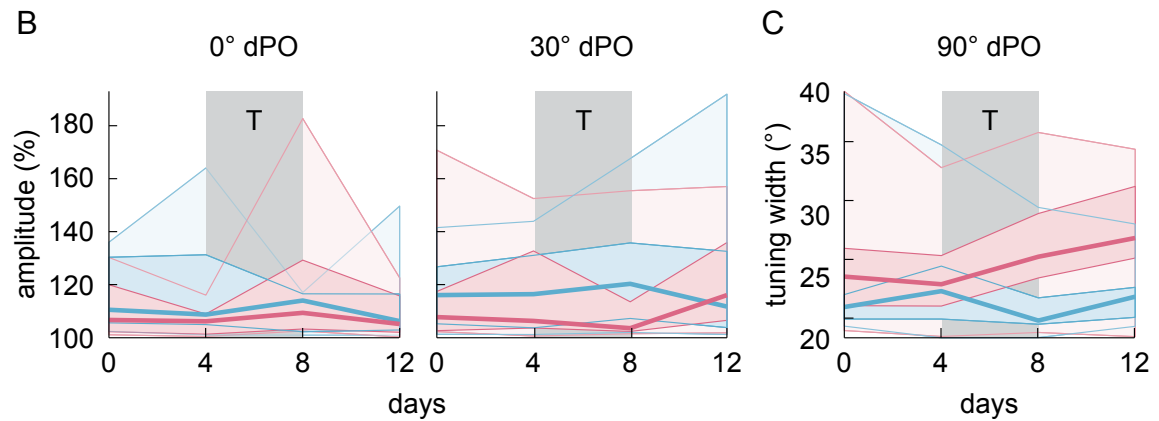
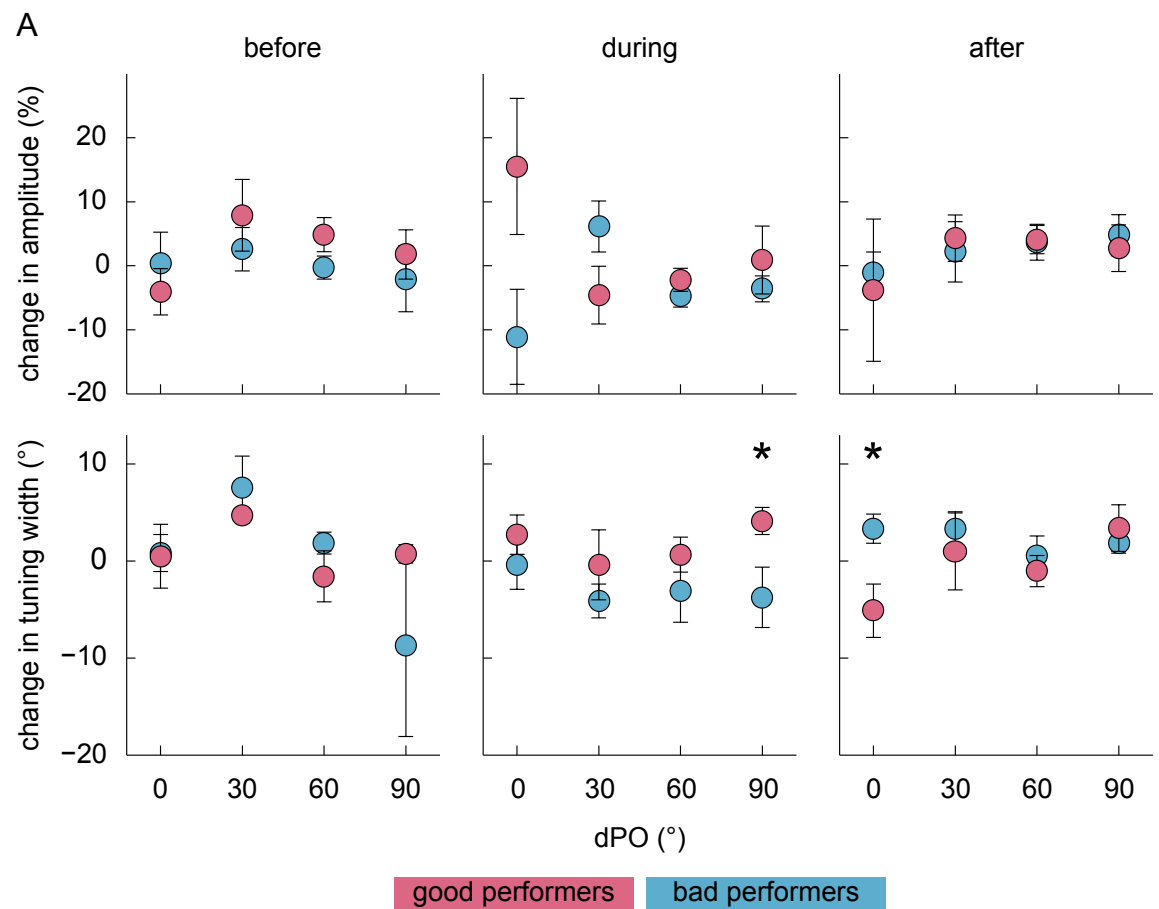


Figure 27: Changes in orientation preference of individual neurons over time in good and bad performers. (A) Preferred orientation of individual neurons measured in four successive imaging experiments. *Hue* of traces indicates, according to *legend*, preferred orientation on day 4 during the second imaging session immediately before training (*T*, gray shading). (B) Changes in preferred orientation before, during and after training (median, 25 and 75 percentiles, 10 and 90 percentiles), *magenta*: good performers ($n = 49$ neurons), *blue*: bad performers ($n = 68$ neurons). Note that changes are reduced by trend during training in good performers.

Results

the four-day training period (4.9°) compared to the four-day periods before training (8.0°) in good performers ($p = 0.061$, Kruskal-Wallis test with *post hoc* Tukey-Kramer correction, Fig. 27b). However, no systematic shifts in orientation preference, for example towards the target orientation, were observed during training.



5.2.9 Modulations in response amplitude and tuning width correlate with performance

Next, we analyzed, whether orientation tuning in individual V₁ neurons, particularly response amplitude and tuning width, was affected by reward-based learning of an orientation discrimination task. Indeed, individual neurons showed characteristic changes in their response properties during training. Some of these changes were even correlated with mouse performance.

Changes in response amplitude and tuning width did not occur in all neurons, but showed a clear dependence on the angle between a neuron's preferred orientation and the orientation of the target stimulus (differential preferred orientation – dPO). There were no systematic changes in response amplitude before or after training (Fig. 28a). During training, neurons preferring the target orientation (0° dPO) by trend showed an increase in amplitude in good ($15.5 \pm 10.6\%$, $n = 7$ neurons) and a decrease in amplitude in bad performers

($-11.1 \pm 7.4\%$, $n = 9$ neurons, $p = 0.052$, t test, Fig. 28a). At the same time, neurons with 30° dPO showed an inverse trend, namely a decrease in amplitude in good ($-4.6 \pm 4.5\%$, $n = 13$ neurons) and an increase in bad performers ($6.1 \pm 4.0\%$, $n = 18$ neurons, $p = 0.086$, t test, Fig. 28a).

We also detected systematic changes in tuning width between good and bad performers (Fig. 28a). During training, neurons with 90° dPO increased tuning width in good ($4.1 \pm 1.4^\circ$, $n = 13$ neurons) and decreased tuning width in bad performers ($-3.7 \pm 3.1^\circ$, $n = 12$ neurons, $p < 0.05$, t test). After the offset of training, neurons with 0° dPO showed a decrease in tuning

Figure 28: Changes in neuronal response properties before, during and after learning in good and bad performers. (A) Changes in amplitude (*top*) and tuning width (*bottom*) of individual neurons between imaging sessions as a function of differential preferred orientation (dPO). *Left graphs*: baseline changes before training, *middle graphs*: changes during training, *right graphs*: changes after training. (B) Distribution of response amplitudes of individual neurons with 0° dPO (*left*) and 30° dPO (*middle*). (C) Distribution of tuning widths of individual neurons with 90° dPO. *Bold lines*: median, *colored area flanked by lines*: 25 and 75 percentiles, *faintly colored area flanked by light lines*: 5 and 95 percentiles. *Magenta*: good performers, *blue*: bad performers, all mean \pm SEM. *Asterisk*: significant difference ($p < 0.05$, t test).

Results

width in good ($-5.1 \pm 2.8^\circ$, $n = 8$ neurons) and an increase in tuning width in bad performers ($3.3 \pm 1.5^\circ$, $n = 9$ neurons, $p < 0.05$, t test). Over time (Fig. 28c), median tuning widths of

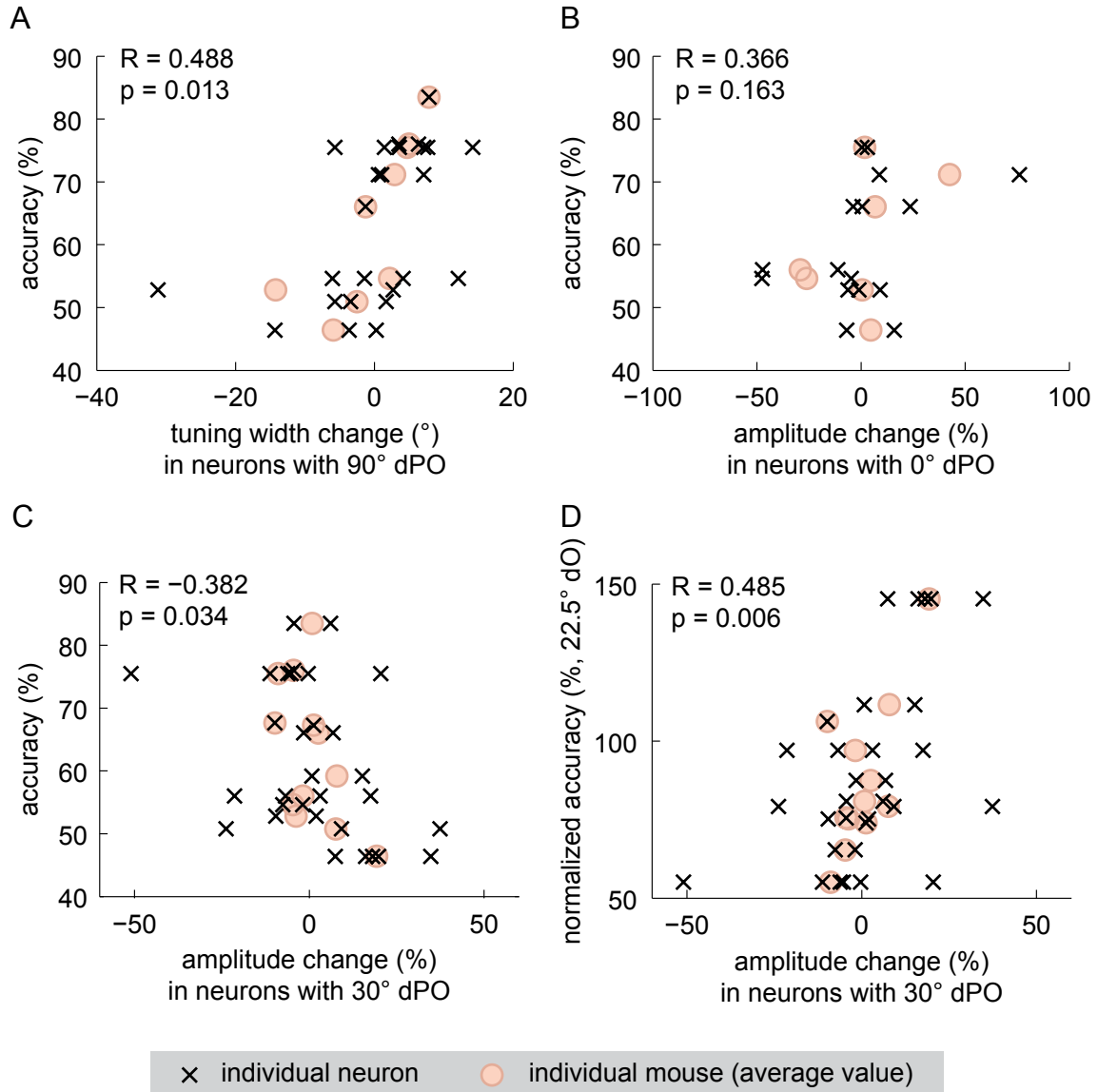
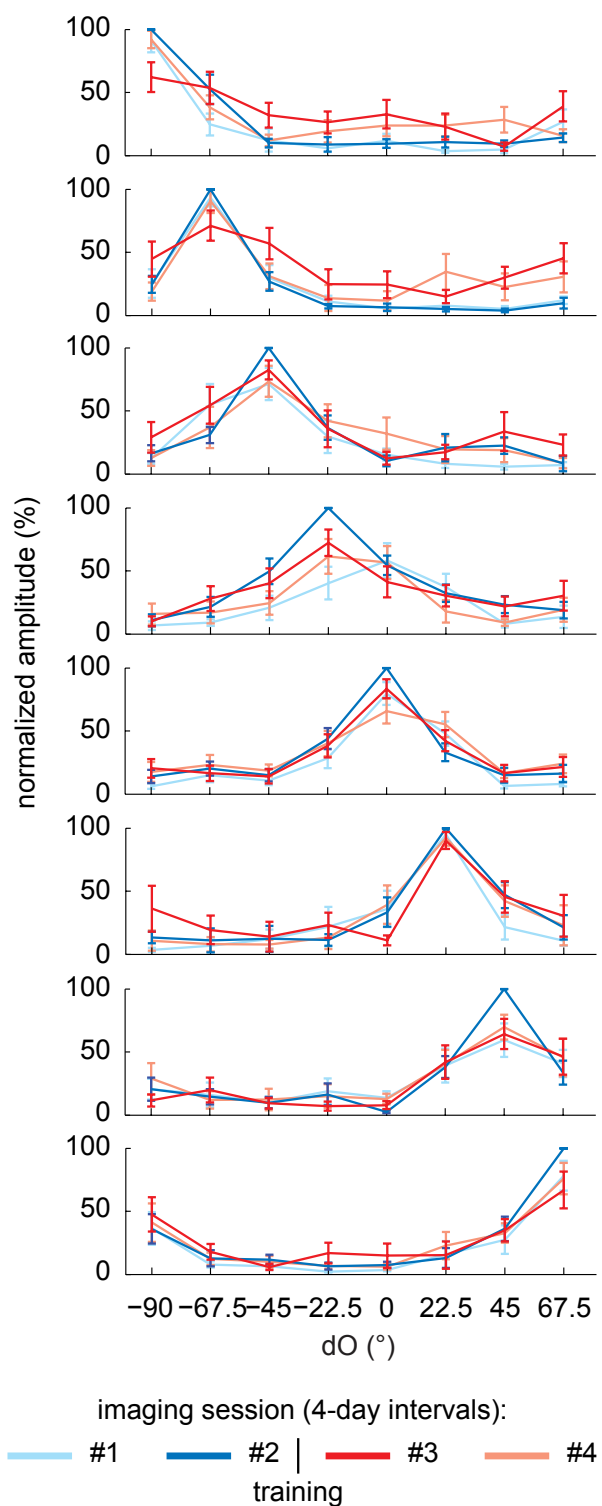


Figure 29: Correlations between performance and learning-induced changes in neuronal response properties. Correlations between accuracy and (A) tuning width changes in neurons with 90° differential preferred orientation (dPO), (B) amplitude changes in neurons with 0° dPO and (C) in neurons with 30° dPO. (D) Correlation of the normalized performance during presentation of a 22.5° differentially oriented (dO) non-target and amplitude changes in neurons with 30° dPO. *Black symbols:* individual neurons, *light red circles:* average values for individual mice. *R:* correlation coefficient, *p:* p value, calculated based on single neurons.

neurons with 90° dPO are in the same range before training in good and bad performers and permanently diverge after training so that neurons are more broadly tuned in good (30.5° and 33.6°) than in bad performers (19.6°, $p < 0.05$, Wilcoxon rank sum test, and 23.6°, $p < 0.01$, Wilcoxon rank sum test).

Thus far, assigning mice to two groups according to their task performance allowed detecting systematic changes in response properties during training. However, in order to directly relate these changes to learning, I correlated the task performance in each individual mouse with the magnitude of functional changes detected in their V1 neurons (Fig. 29). Tuning width changes in neurons with 90° dPO were positively correlated with performance, such that the better the mouse performed, the broader the tuning became during training ($n = 25$ neurons, Fig. 29a). While amplitude changes in neurons with 0° dPO were not signifi-

Figure 30: Changes in orientation tuning curves before, during and after training. Average normalized tuning curves of neurons grouped according to differential preferred orientation (dPO) in imaging session 2 (immediately before training). *Light blue*: imaging session 1, *blue*: imaging session 2, *red*: imaging session 3, *light red*: imaging session 4.



cantly correlated with performance ($n = 16$ neurons, Fig. 29b), amplitude changes in neurons with 30° dPO correlated negatively with performance: The better the mouse performed, the higher was the decrease in amplitude ($n = 31$ neurons, Fig. 29c). As neurons with 30° dPO should be relevant for task solving when target/non-target-pairs with small differential orientations are displayed, we also quantified the near-limit orientation discrimination performance by normalizing the fraction of correct responses during display of a 22.5° dO (differential orientation) non-target to the fraction of correct responses during display of a 45° dO non-target in the last operant chamber session. Interestingly, the near-limit orientation discrimination performance was positively correlated with amplitude changes in 30° dPO neurons ($n = 31$ neurons, Fig. 29d). Thus, mice with higher amplitude increases in 30° dPO neurons performed better at discriminating gratings of nearby orientations.

5.2.10 Specific changes of average tuning curves

The overall changes in functional properties that occurred during training were also reflected in the average tuning curves (Fig. 30). Neurons with peak responses at a large dO (differential orientation) tend to be more broadly tuned on average after training. Neurons with peak responses at 22.5° dO tend to respond more weakly to 0° dO gratings after training (Fig. 30), resulting in a steeper slope of the tuning curve similar to observations made by Schoups and colleagues after orientation discrimination training in monkey V1¹²³.

5.2.11 Good performers gain more orientation-selective neurons during training

So far, I described functional changes in neurons which were orientation-selective throughout all four imaging experiments. However, neurons gaining or loosing orientation responsiveness and selectivity, especially during training, may also be relevant for learning. Therefore, I quantified and functionally characterized neurons gaining or losing orientation selectivity during training. Specifically, neurons non-selective before (first two imaging experiments) and orientation-selective after training (third imaging experiment, compare Fig. 24a) were classified as gain. Neurons which were selective before and non-selective after training were classified as loss. As only 4% of responsive neurons were non-selective, neurons

in most of the cases actually gained or lost also responsiveness. In bad performers, the numbers of neurons gaining and losing orientation selectivity during training were of similar magnitude (44 and 55 neurons, respectively). On the contrary, in good performers clearly more neurons gained than lost selectivity during training (75 and 31 neurons, respectively, Fig. 31a).

In order to compare the gain and loss in the number of selective neurons between mice, I calculated the net gain and the net loss, which were normalized to the total number of orientation-selective neurons in individual mice (for details, see *Materials and Methods*). In accordance with the above presented data, the net gain was higher in good ($58.0 \pm 13.6\%$)

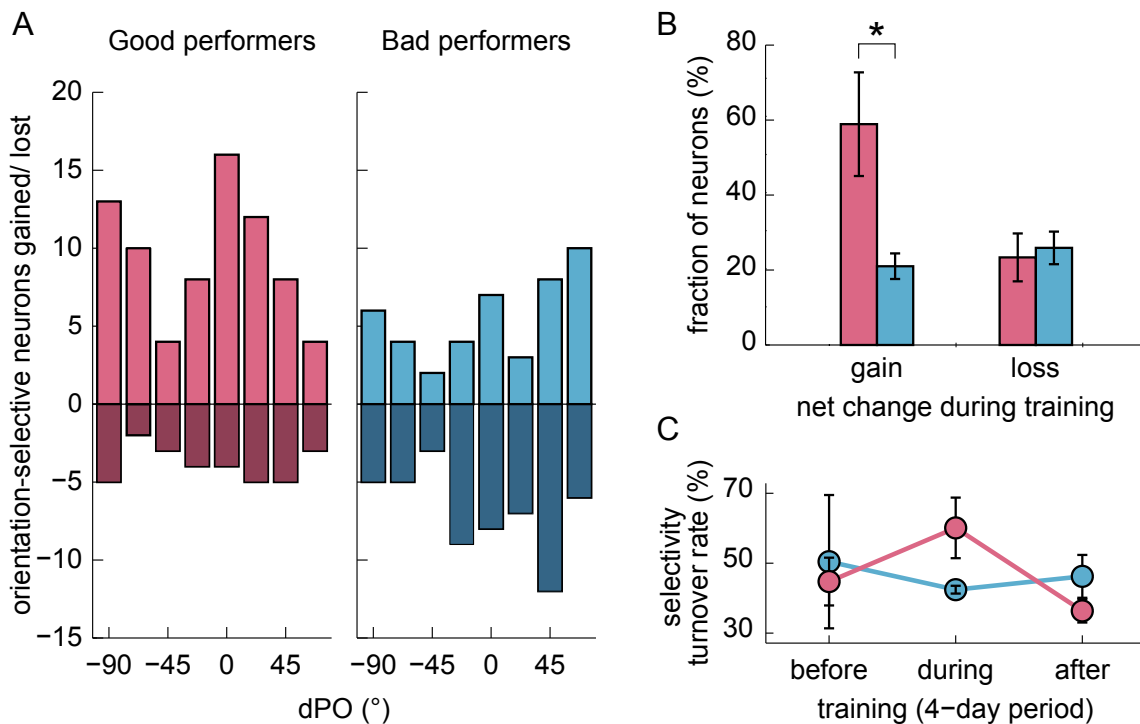


Figure 31: Learning induced changes in selectivity in individual neurons. (A) Number of neurons losing (*dark*) and gaining (*bright*) orientation selectivity during training as a function of differential preferred orientation (*dPO*). (B) Net gain and loss (see *Materials and Methods*) in orientation selectivity during training in individual neurons. (C) Selectivity turnover rate before, during and after training. *Magenta*: good performers, *blue*: bad performers. *Asterisk*: significant difference ($p < 0.05$, *t* test). Note that only 4% of responsive neurons were non-selective. Thus, most neurons gaining or losing selectivity also gained or lost also responsiveness.

Results

than in bad performers ($20.7 \pm 3.4\%$, $p < 0.05$, t test, Fig. 31b). In contrast, there was no difference in the net loss of selective neurons ($23.0 \pm 6.3\%$ and $25.5 \pm 4.3\%$, respectively, Fig. 31b). Likewise, the selectivity turnover rate, the summed gain and loss normalized to the initial number of orientation-selective neurons (see *Materials and Methods*), was increased during training in good performers by trend compared to the bad performers ($p = 0.066$, t test, Fig. 31c).

Next, I investigated, whether the neurons gaining selectivity during training (*newly selective*) were functionally distinct from neurons, which were orientation-selective starting from the first imaging experiment (*stably selective*). Remarkably, newly selective neurons in good performers (Fig. 31a) differed from stably selective neurons (Fig. 27a) in orientation preference: Most newly selective neurons in good performers were tuned to either the target orientation (0° dPO), or to the orientation orthogonal to the target orientation (90° dPO, Fig. 31a), corresponding to vertical (90°) or horizontal (0°). Such a bimodal distribution with over-represented cardinal orientations could arise from the horizontal bias inherent to the representation of orientation preference in mouse V1^{22, 118}. Therefore, I analyzed orientation preference of neurons gaining orientation selectivity during training in individual mice. Ranging on a scale from 1 (*only neurons tuned to 0° dPO*) to -1 (*only neurons tuned to 90° dPO*), both 0° and 90° dPOs were almost equally strongly represented, with a small tendency towards more neurons preferring 0° dPO (0.29 ± 0.21). On the other hand, horizontally and vertically tuned neurons were equally represented (0.07 ± 0.24 , index ranging from 1 [*only horizontally tuned neurons*] to -1 [*only vertically tuned neurons*]) in individual mice. Therefore, the orientation preference of neurons gaining orientation selectivity seems to depend mainly on the target orientation during training. In addition, newly selective neurons showed lower median response amplitudes (3.86%) compared to stably selective neurons (5.65%, $p < 0.005$, Wilcoxon rank sum test). There was no difference in median tuning width (23.7° and 24.6° , respectively, $p = 0.59$, Wilcoxon rank sum test). Moreover, newly selective neurons were more likely to lose selectivity compared to neurons, which were stably selective in imaging sessions 1 – 3: A higher fraction newly selective neurons (66.4%) lost orientation selectivity between imaging sessions 3 and 4 compared to stably selective neurons (18.7%).

5.2.12 Synopsis – plasticity of orientation tuning induced by operant conditioning

In summary, I successfully trained mice on an orientation discrimination task using operant conditioning. During operant conditioning, reward-based learning elicited moderate effects in individual V1 neurons. The representation of orientation preference did not change systematically, but rather showed a reduced variability. Systematic learning-induced changes in response amplitude and tuning width occurred in neurons with certain differential preferred orientations (dPOs) in relation to the target orientation. In individual mice, a better performance on the task was correlated with an increased tuning width in neurons with 90° dPO, and a decreased response amplitude in neurons with 30° dPO. In addition, good performers displayed a higher gain in the number of orientation-selective neurons, most of which were tuned to the target (0° dPO) or the orthogonal (90° dPO) orientation. The functional implications of these learning-induced changes, such as facilitated categorization of visual stimuli, will be discussed below.

Discussion

Exposed to constantly changing environments, animals are forced to keep exploring new strategies to survive. Particularly, learning to identify predictors for food and threats is essential. Such learning is reflected in functional changes in neurons throughout the brain. Specifically, both altered sensory input and sensory learning do change neuronal response properties in sensory cortices as often demonstrated on the population level^[62, 111, 123, 211]. It remains, however, largely elusive, how such changes are reflected at the level of individual neurons (with a few exceptions, e. g. hippocampal place fields²⁵²⁻²⁵⁴). The mammalian visual cortex lends itself to the study of such questions, since neuronal response properties and neuronal plasticity, especially during the critical period, have been characterized extensively. In the first part of this thesis, I investigated how primary visual cortex adapts to modified visual input statistics. To this end, I used stripe rearing, a well established method for inducing experience-dependent plasticity in cats^{92, 105, 108} and rats¹⁰⁹. I found a clear stripe rearing effect, which varied with neurons' vertical location in layer 2/3: on the one hand, there was an increase in the fraction of neurons preferring the experienced orientation in lower layer 2/3, and, on the other hand, I observed a decreased number of both neurons preferring the experienced and neurons preferring the orthogonal orientation in upper layer 2/3. In the second part of this thesis, I developed a visual learning paradigm and tested, if assigning a behavioral relevance to specific visual features alters neuronal responses in the primary visual cortex. I observed an increased gain in the number of orientation-selective neurons in mice that performed well on the task. In addition, single neurons underwent changes in response amplitude and tuning width, depending on both their orientation preference and the orien-

tation of the rewarded target grating. Importantly, these changes correlated with how well individual mice learned to solve the visual task.

6.1 Experience-dependent plasticity in single V₁ neurons

In the first part of my thesis, I investigated how stripe rearing affects the response properties of single neurons in mouse visual cortex. Limiting visual experience to contours of a single orientation for three weeks caused a modest over-representation of the experienced orientation. Instructive modifications as well as a small drop in responsiveness were observed. The stripe rearing effect had a clear instructive component in lower layer 2/3 as indicated by an increase in the absolute number of neurons tuned to the experienced orientation. Thus, for this subpopulation of neurons in mouse visual cortex, the visual environment acts as an instructive signal, which changes the response properties of single neurons in an adaptive fashion. These changes could either reflect a shift in orientation preference towards the experienced orientation, or an increased response amplitude in neurons, which are tuned to the experienced orientation, but were previously only weakly responsive to moving gratings.

6.1.1 Orientation selectivity in layer 2/3 of mouse V₁

I performed all experiments in mouse primary visual cortex, where neurons show selective responses to a variety of visual stimulus parameters like visual field position, spatial and temporal frequency, and direction of motion^{22, 25}. Importantly, many neurons are orientation-selective, and their tuning widths are comparable to those of neurons in higher mammals such as cats and ferrets²⁵. Orientation preference in rodents is not organized into a continuous map, but rather forms a “salt-and-pepper” arrangement^{22, 34, 35}. This organization might help assessing the potential effects of stripe rearing since it is less prone to sampling biases than the clustered layout for orientation preference observed in monkeys, cats, ferrets, and other species^{30, 255, 256}. While mouse visual cortex lacks an orientation preference map, I observed several similarities in single neuron response properties between the mouse on the one hand, and ferret⁹⁴ and cat¹⁰⁰ on the other hand. For example, I found that the tuning width of neurons depended on their preferred orientation, with horizontally tuned neurons showing a narrower tuning than those with a vertical orientation preference. In addition,

and consistent with previous reports in mouse V1^{22, 118}, I observed an over-representation of horizontal orientations in normally reared mice, similar to what has been described in cats and ferrets^{94, 95}. Surprisingly, the horizontal bias found here was not uniformly distributed throughout layer 2/3. Rather, the distribution of preferred orientations changed markedly within only a few hundred micrometers: In upper layer 2/3, I observed a strong overrepresentation of horizontally tuned neurons, while the distribution of preferred orientations was nearly flat in lower layer 2/3 using standard stimulus parameters.

While in general neuronal response properties are known to vary systematically with cortical depth in mouse²⁵ and cat V1^{50, 257}, variations within a single cortical layer are less well documented and anisotropies in orientation preference have not been described. In principle, the horizontal bias and its depth dependency within layer 2/3 could be an artifact caused by incomplete maturation of the visual system under standard housing conditions, which provide only sparse sensory input and restrict motor behavior. In an enriched environment⁷⁹ where animals receive a complex inanimate and social stimulation and have ample opportunity for voluntary motor activity, the development of the visual system and especially acuity have been shown to be strongly enhanced in mice^{84, 86}. However, I found here that mice born and raised in an enriched environment do not show any difference in orientation tuning in layer 2/3 of V1. In particular, I also observed the depth dependency of the horizontal bias in layer 2/3 in these mice. This suggests that the horizontal bias observed in middle and upper layer 2/3 is probably not attributable to degenerate visual input. Rather, it might be caused by layer specific termination of input from specific subsets of retinal ganglion cells relayed via the lateral geniculate nucleus²⁵⁸⁻²⁶⁰.

6.1.2 Design and effect of stripe rearing paradigm

Unlike most previous stripe rearing studies, we did not interfere with the early development of response properties in visual cortex, but rather induced plasticity of orientation preference at a slightly later stage. Therefore, instead of being dark-reared, mice had normal visual experience until postnatal day (p) 25, at which time orientation selectivity is well established, though not completely mature⁶⁴. On the one hand, this might limit the extent of plas-

tivity¹¹², on the other hand, it allows dissociating functional impairment by abnormal visual cortex development from plasticity effects^{246, 261, 262}. Stripe rearing was performed for about three weeks, thus including the peak of the critical period for ocular dominance plasticity around p30, at which time also orientation selectivity has been shown to be highly plastic⁶⁴.

In our experiments in mouse visual cortex, the experienced orientation was over-represented after stripe rearing, similar to results previously obtained in kittens^{92, 105, 107, 108, 110, 263} and rats¹⁰⁹. The specific effect, i.e. the sum of the increase in the experienced and the decrease in the orthogonal orientation, was on average 15%. The magnitude of the effect is thus similar to that found in kittens¹⁰⁸, showing that mice display a considerable degree of orientation plasticity⁶⁴, even after previous normal visual experience. The specific effect was of similar size under three stripe rearing conditions (-45° , 0° , 90°), but smaller after rearing with 45° . Considering that the distribution of preferred orientations is initially not equal, this finding may not be surprising. However, when we pooled data from animals reared with -45° or 45° as well as from those reared with 0° or 90° , the result was statistically indifferent from the control distribution. This indicates that the shift in the distributions of preferred orientations after stripe rearing may actually be convolved with the horizontal bias. In this context, shifts induced by two orthogonal experienced orientations cancel out each other.

6.1.3 Instructive and permissive environmental effects can be assessed with two-photon calcium imaging

The ability to image all neurons, including the non-responsive ones, allowed us to test two ideas that have been put forward to underlie the stripe rearing effect, instructive and permissive ones. While the permissive hypothesis describes experience-dependent plasticity as a passive process, mainly caused by input loss similar to deprivation, the instructive hypothesis assumes remodeling of circuitry, thereby causing a change in response properties of single neurons. These two mechanisms are not mutually exclusive, but could occur in combination¹⁰⁶. The importance of permissive changes for the stripe rearing effect has been under debate for decades^{106, 108, 110}, but its exact contribution has been hard to quantify, due to the

lack of adequate sampling methods. With two-photon microscopy we were able to quantify, in an unbiased fashion, the fraction of responsive neurons.

6.1.4 Drop in responsiveness and its significance during experience-dependent plasticity

Stripe rearing did cause a slight drop in responsiveness, but the magnitude of this effect was unevenly distributed across the depth of layer 2/3. While a loss of about 19% in responsiveness occurred in upper and middle layer 2/3, respectively, it was absent in lower layer 2/3 (Fig. 10b). It has been shown previously that orientation preference plasticity as well as other types of plasticity in the visual cortex vary in their time course and extent between layers^{113, 242, 243, 264-266} or even sublayers²⁶⁷. Still, this variability within one layer is remarkable. Previous results indicated that the effect of stripe rearing depends on neuronal subtype and is especially weak in neurons with small receptive fields²⁶⁸. However, what functionally distinguishes neurons located in upper or lower layer 2/3 in mouse visual cortex remains to be determined.

The weak decrease in responsiveness upon stripe rearing, in the order of 10% on average, would in principle be compatible with a permissive mechanism. However, in upper layer 2/3, changes in both responsiveness and selectivity affected neurons regardless of their preferred orientation, largely independent of the experienced orientation (Fig. 12). Thus, while stripe rearing reduces overall cortical responsiveness to some degree, its contribution to the shift in orientation preference seems rather small. This is further strengthened by the observation that there is no correlation between the change in responsiveness and the stripe rearing effect. Instead of enhancing the over-representation of the experienced orientation, a decreased responsiveness might serve other functions, like maintaining network balance. In this context, it will be interesting to investigate the effect of stripe rearing on specific neuronal subpopulations, such as inhibitory neurons. Upon monocular deprivation, they show the same degree of plasticity as excitatory neurons during the critical period²⁶⁹, but only after a temporal delay²⁷⁰. In the stripe rearing paradigm, they might undergo different types of plasticity, for example silencing. As inhibitory neurons constitute about 20% of the neuronal

population in visual cortex, they would provide the capacity for the observed 10% decrease in responsiveness. Since most inhibitory neurons are very broadly tuned^{35, 44, 47, 49} (but see also Runyan and colleagues⁵¹), silencing would by and large not affect the distribution of preferred orientations, which is what we actually found.

6.1.5 Instructive changes during experience-dependent plasticity

In contrast to permissive mechanisms, instructive changes were critical for the stripe rearing effect, at least in the cortical layers we observed. This was most obvious in lower layer 2/3, where permissive effects were absent and the total number of neurons preferring the experienced orientation increased strongly. Thus, the stripe rearing effect in this population of neurons is entirely explained by an instructive mechanism. In other populations of neurons, this effect was less pronounced. Using temporally precise pairing between an oriented visual stimulus and electrical stimulation in the visual cortex^{115, 116}, it was shown that neurons can in principle undergo instructive changes of preferred orientation when activated appropriately. Under more physiological conditions, presentation of moving gratings immediately after eye opening⁶⁶, repeated presentation of a single orientation to awake mice¹¹⁸ and learning an orientation discrimination task¹²³ instructively changed neuronal response properties in primary visual cortex. Proving that neurons change their preferred orientation during stripe rearing, our data demonstrate that instructive mechanisms also contribute to experience-dependent orientation plasticity. A substantial amount of synaptic^{77, 237}, and most likely also structural, plasticity can be expected to underlie the strong increase which we observed in the fraction of lower layer 2/3 neurons preferring the experienced orientation. In fact, dendritic tree morphology changed after stripe rearing in cat visual cortex^{265, 271}.

In summary, visual experience is capable of modifying orientation selectivity in an instructive manner. A priori both, instructive and permissive changes could have caused the well-known effects of stripe rearing. We demonstrate that instructive changes play the main role in layer 2/3, obviously not precluding that this could be different in deeper layers that we have not imaged. Still, for the upper layers, this indicates that neurons not driven by stimuli present in the sensory environment are not simply silenced; rather, their response

properties actively adapt to the specific input - in view of optimally using resources and optimizing performance certainly an advantageous strategy. This assumption is underlined by the following three arguments: Firstly, the response properties of neurons are fine-tuned during development⁹³⁻⁹⁵, until their distribution matches natural scene statistics with its bias of cardinal⁹⁶, and in particular horizontal orientations⁹⁷. Secondly, an increased number of neurons preferring a certain orientation seems to facilitate more precise discrimination in the over-represented orientation range^{98, 99}. This relationship becomes most obvious in the so-called “oblique effect”, which terms the better performance at cardinal compared to oblique orientations in a number of measurements, such as spatial acuity, contrast sensitivity, or orientation discrimination. Li and colleagues¹⁰⁰ described the over-representation of cardinal orientations in cat visual cortex as its neural basis. Finally, an optimal representation of orientations in the brain should help facilitating the rapid detection of relevant at the expense of less important features. Such functional specialization can also be observed in humans, for example as facilitated reading of italic letters¹⁰⁴. All these phenomena point to an instructive, experience-dependent process, continuously shaping the sensory brain paths with the benefit of improved perception that allows for a proper reaction to challenges in an altering environment.

6.2 Plasticity of orientation tuning in individual V1 neurons induced by learning

In the first part of my thesis I have shown that manipulating the visual input can reveal how the brain adapts to an altered visual environment. However, in the long run and in a given environment, visual input statistics do change less frequently than the potential behavioral relevance of moment by moment information delivered via the visual input. In this context, visual perceptual learning¹²⁰ is an important process in which an animal learns to detect and extract information from visual input. This situation can be relatively easily implemented by an operant conditioning paradigm, in which a mouse learns to solve a visual discrimination task. Therefore, in the second part of my thesis, I developed and implemented

a visual perceptual learning paradigm for mice, with the aim of investigating plasticity of orientation tuning in individual V1 neurons induced by learning.

6.2.1 Visual discrimination learning in mice

While visual perceptual learning is classically studied in humans^{186, 272} and monkeys^{123, 125}, also mice are actually well able to learn odor²⁷³, tactile²⁷⁴, auditory²¹¹ and visual²³³ discrimination tasks. Interestingly, performance in operant conditioning tasks depends strongly on the genetic background²⁷⁵. C57/Bl6 mice perform reasonably well compared to other mouse strains²⁷⁵, as has also been observed in other learning tasks²⁷⁶. Learning during operant conditioning and object recognition also depends on the sex, with male mice performing better in reward-based operant learning and object recognition^{250, 251}. We therefore used male C57/Bl6 mice, which were trained to visually discriminate a target from a non-target grating which differed in orientation. To induce visual perceptual learning, we performed reward-based operant conditioning²⁷⁷, a process in which several higher cortical areas are involved¹²¹.

To solve the orientation discrimination task, mice had to choose the target over a simultaneously displayed non-target. While identifying the proper strategy for optimizing behavior in a complex task requires the formation of an internal model of the environment during learning, a simple simultaneous discrimination task can be solved without an internal model¹²¹. Model-free reinforcement learning entrains so-called habitual actions²⁰¹. Dorsolateral striatum and the amygdala are believed to play a key role in habit formation^{204, 206}. The neuronal basis of positive reinforcement (or reward-based) learning has been assigned to midbrain dopaminergic neurons which work as reward predictors and error detectors and receive crucial input from habenula^{189, 278}.

6.2.2 Design of an effective learning paradigm for mice using operant conditioning

Only few reports have been published on an optimal learning paradigm and task design for mice. In an extended training regime starting with a very simple task and increasing complexity over six training stages, we reached a high performance level of about 80% correct

responses with little variation between individual (juvenile) mice (Fig. 20). First, mice were allowed to explore the operant chamber²⁷⁹ to decrease distraction by the novel environment during the following training sessions. This is important, because memory formation depends on attention²⁸⁰. Moreover, a high load of working memory, such as during learning to solve a very complex task, has been shown to impair feature-selective attention²⁸¹. Therefore, we started with a very simple task design. In the following two training sessions, mice had to detect the target grating displayed first on both (training session B) and in the subsequent training session C only on one of the two touch screens. For rodents, this type of discrete trial discrimination task²⁸² is easier to solve than a simultaneous discrimination task²⁸³. However, while the mice showed a clear increase in the frequency of pressing the touch screen during training session B, efficiency, i. e. the frequency of pressing an actual stimulus rather than a black screen, deteriorated. This finding points to an increased association between reward and touching the screen in general, rather than specifically selecting the visual stimulus. Starting with training session D, in which the simultaneous discrimination task was introduced, association between the target grating orientation and the reward increased as indicated by a 70% preference of this grating over the non-target gratings after eight hours of training (Fig. 19d). Initially, in the first 5 minutes of exposition to the novel non-target grating in session D, mice preferred the novel stimulus over the familiar one (Fig. 19c). Rodents expose a delay-dependent tendency to explore novel objects and stimuli, as shown in a number of one-trial object recognition experiments^{248, 284, 285}, a variant of delayed matching-to-sample experiments²⁸⁶. This kind of delayed object recognition memory is, among other brain structures²⁸⁵, dependent on the hippocampus^{287, 288} and especially on the perirhinal cortex²⁸⁹, which receives input from the ventral visual pathway. The initial, short-lasting preference for the novel, unrewarded grating indicates that the mice have developed a long-lasting reference memory in the previous training session 24 hours ago. Consistent with this, performance further increased, compared to the respective previous training session, during training sessions E and F (Fig. 20), in which more and more non-target stimuli with smaller difference angles to the target grating were added. This implies a transfer of learned content between the tasks.

In the first food retrieval session, which was identical to the previous training session F except that the total duration was reduced from at least 10 hours to 30 min, mice showed already a high level of about 86% accuracy, but only intermediate levels of efficiency and response delay. By introducing a strong temporal restriction of food availability, mice were forced to maximize their reward yield. They did so by first reducing the response delay, then increasing efficiency both at the transient expense of accuracy, leading in two steps (Fig. 20) to a continuously increasing reward yield over the following two weeks. This demonstrates that accuracy does not only depend on learning, but can be substantially influenced by the task design.

6.2.3 Additional factors affecting task performance and learning

An overall trend towards decreased accuracy at the end of long training sessions underlines the effect of motivation¹²¹, which is modulated by satiation and curiosity. Therefore, the true memory performance is probably masked by lack of attention on the one hand and curiosity on the other hand. Not least, maintenance of curiosity should increase overall success in operant learning as it allows for exploring new, potentially more successful strategies. In addition, performance clearly depended on task difficulty. With smaller angles (differential orientations, dO) between target and non-target grating, performance decreased. Mice achieved an average performance of only 62% in trials with a 22.5° dO non-target compared to trials with a 67.5° dO non-target.

In individual mice, we observed periodic variations in the touch screen pressing frequency over time, which mostly cancelled out between individual mice. Similar variations seen in rats have been discussed to be a consequence of sensitization and habituation to stimulus or reward²⁹⁰. Very likely, they are also caused by changes in satiation and wakefulness over the course of several hours. In fact, key to successful training in our hands was the long duration of the individual training sessions of at least ten hours. This long time span comprised several phases of high and low activity levels, the latter indicative of sleep, which is known to be important for memory consolidation^{160, 162-164, 166, 167, 291}. Moreover, performing training during night time was important, because of higher motor activity and increased

exploratory behavior of mice, which are nocturnal animals²⁹². To ensure that mice collected their reward immediately after making a choice, it was essential to start training with long delays of 2 min between subsequent trials. This way, mice formed a habit of executing a fixed sequence of actions (e. g. [choice and immediate reward retrieval](#)), which was maintained during subsequent shortening of the intertrial delay down to 20 s during the food retrieval sessions. A correct choice was followed by immediate food retrieval in 97.7% of all cases in good performers. Even though we did not punish mice for incorrect choices, waiting during the intertrial delay time frequently elicited strong exploratory and touch screen pressing behavior, suggesting that mice may experience the waiting time as a punishment that induces avoidance behavior of non-target gratings, acting in synergy with the reward-based preference of the target stimulus.

By design of the task, there was a delay between the mouse's choice and food reward collection. To overcome such delays, click sounds are successfully used as secondary reinforcers (e. g. [an auditory stimulus predicting a reward](#)) for operant conditioning ([clicker training](#)) of animals, among them rodents²⁹³. This strategy was implemented in our operant conditioning setup: The release of the food pellet was accompanied by a click sound such that the mouse received immediate feedback about its performance. Consistent with this, mice less frequently walked to the food retrieval site if they made a wrong choice. This behavior is probably influenced by the habenula which suppresses motor behavior when an animal fails to obtain a reward²⁷⁸.

6.2.4 Elusive role of V1 in visual perceptual learning and memory

A number of brain areas, such as prefrontal cortex²⁹⁴⁻²⁹⁶, the medial temporal lobe^{295, 297-300}, and extrastriate cortex^{301, 302}, some of which receive input from visual cortex, are involved in memory formation, storage and retrieval. Whether early sensory cortical areas, such as V1, are involved in memory storage, is highly controversial. Some models of visual perceptual learning propose that difficult tasks requiring an increased signal-to-noise ratio for accurate discrimination cause permanent changes in low sensory areas¹²². However, little direct evidence has been provided for an involvement of V1 in learning¹²³. In order to reliably

identify and quantify learning-induced plasticity in V₁, we measured changes in neuronal response properties in individual V₁ neurons after learning of a visual discrimination task. This approach was made possible by the recent development of the genetically encoded calcium indicator GCaMP₃²²⁷.

6.2.5 Repeated calcium imaging of orientation tuning in individual neurons using GCaMP₃

In order to investigate changes in individual neurons induced by orientation discrimination learning, we repeatedly performed calcium imaging of the same neuron through a permanent cranial window over twelve days using the genetically encoded calcium indicator GCaMP₃. In individual neurons, orientation preference was relatively stable over time, consistent with previous reports^{233, 234}. The distribution of orientation preference in mouse V₁, however, is highly variable between individual animals. At the same time, learning-induced changes in V₁ neurons are potentially small, as suggested by the results from Schoups and colleagues¹²³. Following individual neurons over time and particularly during learning circumvents these issues and allows a precise quantification and characterization of learning-induced functional plasticity.

Genetically expressed calcium indicators are suitable tools for repeated calcium imaging of individual neurons. GCaMP₃ is the best genetically expressed calcium indicator available to date (with the newer version GCaMP₅ showing some improvement compared to GCaMP₃ according to preliminary data from our and other labs). Compared to the synthetic indicator OGB₁-AM, however, much fewer neurons were responsive to moving grating stimuli in anesthetized mice. While 69% were responsive using OGB₁-AM, only about 3 – 5% were responsive using GCaMP₃. Moreover, only 4% of all responsive neurons were non-selective to orientation in the GCaMP₃ dataset. In contrast, based on our data obtained with the synthetic indicator OGB₁-AM, we would expect a fraction of approximately 35% non-selective neurons. Apparently, using the genetically encoded indicator GCaMP₃, most of the calcium responses of the very broadly tuned neurons appear as sharply tuned or escape our detection. As previously shown, inhibitory neurons constitute a major population of

broadly tuned neurons in mouse visual cortex^{25, 47, 48} (but see also Runyan and colleagues⁵¹). Niell and Stryker showed that stimulus-driven firing rates of inhibitory neurons are typically higher than those of excitatory neurons²⁵. Thus, the detection limit of GCaMP3 in the range of small numbers of action potentials²²⁷ is not an issue here. The human synapsin-1 promoter we used for GCaMP3 expression drives protein expression in both excitatory and, under some conditions even preferentially³⁰³, inhibitory neurons (personal communication, Georg Keller). Thus, the most likely explanation for the discrepancy between the fractions of orientation-selective neurons assessed with GCaMP3 and OGB1-AM is provided by the differential calcium buffering mechanisms in GABAergic and excitatory neurons³⁰⁴. Due to this differential calcium buffering, activity-evoked calcium transients in inhibitory neurons might lay outside the dynamic range of the GCaMP3 calcium indicator. Along those lines, also the tuning widths assessed with GCaMP3 ranging from 16.8° to 105.7° (1/99 percentiles, median: 23.9°) were much narrower compared to the median tuning width measured with OGB1-AM (40.0°). Most likely, due to the above mentioned detection limit of GCaMP3, small responses to stimuli which weakly drive the neurons are not detected. In addition, the issue of broadly tuned neuropil signals contaminating neuronal signals is circumvented by sparser GCaMP3 labeling.

6.2.6 Adapted training paradigm for repeated calcium imaging

For permanent cranial window implantation and GCaMP3 expression, several experimental and temporal constraints exist. First, relatively strong bone growth in juvenile mice limits the stability of the cranial window preparation. Second, reactive gliosis following window implant surgery declines with a delay of a few weeks^{305, 306}. Finally, sufficient GCaMP3 expression using a viral vector²²⁷ takes at least two weeks. Therefore, we performed repeated calcium imaging in adult mice. Adult animals have been shown to perform worse than juvenile animals in learning tasks^{86, 307}. To partially compensate for this age-related decline in learning capacity, adult mice were housed in groups of four in an enriched environment providing a running wheel for voluntary motor activity. Both environmental enrichment and especially voluntary motor activity have beneficial effects on neuronal cell survival, plasticity and learning^{82, 86, 88-90, 308, 309}.

GCaMP3 expression levels were mostly stable over twelve days, granting a stable baseline GCaMP3 fluorescence and comparability of stimulus-elicited fluorescence changes in individual neurons measured in four subsequent imaging experiments spaced by four days each. Tailored to the imaging schedule, we used a compressed training paradigm lasting only 3.5 days. Performance varied strongly between mice, due to age and shorter training, and ranged between chance level and 83% accuracy (Fig. 24b). This wide range of performances among individual mice provided a strong advantage in allowing direct correlation of task performance with changes in neuronal function and demonstrating the functional relevance of the overall moderate learning-induced changes observed in V1 neurons.

6.2.7 Increased stability of orientation preference during training

Individual neurons in V1 of good performers showed, by trend, larger baseline variability in orientation preference before training, consistent with the idea of structural and functional plasticity determining the capacity for learning and memory^{77, 123-125, 310, 311}. Interestingly, the variability in orientation preference was by trend reduced in good performers during training. Along this line, an increased capacity for behavioral learning during a sensitive period was associated with higher spine dynamics in frontal cortex of zebrafishes. Subsequent instructive experience rapidly stabilized and strengthened these dynamic spines³¹². At a first glance both observations speak against the idea that learning induces plasticity. However, while neuronal plasticity is certainly indispensable for forming new memories^{289, 300, 311, 313, 314}, the brain at the same time has to ensure sufficient stability^{168, 315} in order to maintain the ability of decoding incoming essential information, which is the orientation of visual features during absolving an orientation discrimination task. This increased stability of orientation preference during learning underlines the role of V1 neurons as part of a feedforward infrastructure, gating information flow to higher visual areas as described by hierarchical models^{137, 138} of the visual system. In this context, orientation-selective V1 neurons might be regarded as part of an indexing system providing a feature reference on orientation during learning of an orientation discrimination task along the lines of models describing V1 as an indexing system for perceptual binding¹³⁶ of disparate types of information that are analyzed in separate visual areas¹³¹.

6.2.8 Functional changes in individual neurons during training

Very likely, V1 function in visual perceptual learning is not limited to the basic functions discussed above. What speaks against a purely infrastructural role, is several functional modifications occurring during training in individual neurons. These functional modifications are strong predictors for the overall performance of the mice in solving the orientation discrimination task. However, it is unclear whether these different levels of performance reflect differences in learning capacity, that is, less plasticity, or learning speed, that is slower plasticity. In the first case, changes observed in good performers should be absent or reversed in bad performers whereas in the second scenario, changes observed in good performers should precede changes found in bad performers. The fact that functional changes observed in individual neurons, such as changes in tuning width and response amplitude, are inverse in good and bad performers (Fig. 28a) rather argue for the first scenario. Those functional changes were specific both for the training period and for the orientation preference of the respective neurons in relation to the target orientation. While a stabilized orientation preference representation during training might increase the reliability of orientation detection, functional changes in response amplitude could reflect modulated weighting of incoming visual information about oriented contours. Task-specific selective re-weighting of visual input, is thought to permit memory formation during perceptual learning¹⁴⁸⁻¹⁵⁰ and might correspond to the assignment of behavioral relevance to sensory stimuli. Consistent with this idea, changes in response amplitude are thought to reflect saliency of a visual stimulus^{183, 316}. Applying this interpretation to our results, we may have observed here an increased saliency of the target orientation and a decreased saliency of nearby orientations. Potential re-weighting very likely involves top-down feedback signaling and may be due to synaptic^{310, 314, 317} or intrinsic^{216, 223} plasticity. Interestingly, while amplitude changes in neurons tuned to orientations nearby the stimulus were negatively correlated with task performance, these changes showed a positive correlation with the mice's ability of discriminating two similar orientations. Thus, fine and coarse orientation discrimination learning may require differential re-weighting of visual inputs. Therefore, competing for the same resources in V1, for example

opposing functional changes in the same neuronal population, fine and coarse orientation discrimination might be conflicting tasks to learn.

In addition to amplitude changes, very clear changes in tuning width were observed, again exclusively during training and this time in neurons preferring orientations orthogonal to the target orientation. We observed this effect both in acute calcium imaging experiments using OGB1-AM after a prolonged training over three weeks and in individual neurons during chronic calcium imaging experiments using GCaMP3. Therefore, this effect is not likely attributable to a longer exposure of orthogonal target-non-target pairs compared to narrow-angled pairs during stepwise increase of task complexity. This very robust effect on tuning width was predictive of accuracy in solving the task. A broader tuning in neurons preferring orthogonal orientations might be the consequence of the above-discussed potential increased weighting of target orientation signaling, probably eliciting higher neuronal activity. Local excitatory input to neurons in mouse V1 displaying diverse orientation preferences⁴³ can influence tuning width depending on input strength. The more two connected neurons differ in preferred orientation, the stronger this effect should be. The functional benefit of a broadening in tuning width of orthogonal preference can be a facilitated categorization of grating orientations into ‘target’ and ‘non-target’ orientation. A categorization based on the activity in two neuronal subpopulations, namely neurons preferring the target and neurons preferring a broad range of near-orthogonal orientations, should be less precise the narrower the angle between target and non-target is. In accordance with this, we observed a decreased accuracy for narrow angles between target and non-target grating. In further support of this view, facilitated categorization and increasing feedforward feature separation is predicted by the reverse hierarchy theory of perceptual learning¹²².

The categorization hypothesis is underlined by our finding that most neurons gaining orientation selectivity during training were tuned to either the target or the orthogonal orientation (Fig. 31a). Analysis of orientation preference in this population of neurons in individual mice revealed that this bimodal distribution was not due to the horizontal bias inherent to the distribution of orientation preference in mouse visual cortex^{22, 118}. These neurons gaining orientation selectivity during training could theoretically be newly recruited

from a pool of silent or non-orientation-selective neurons. However, as low neuronal activity is hardly detected with GCaMP3²²⁷, this measured gain in orientation selectivity, which was in most cases accompanied by a gain in responsiveness, could as well be explained by an amplified or additional synaptic input to orientation-selective neurons during training, lifting weakly responsive neurons above the detection threshold. Very likely, these neurons gaining orientation selectivity are not a correlate of long-term memory, as they lose orientation selectivity again after the offset of training at a much higher frequency compared to neurons showing stable orientation selectivity from the beginning.

Based on previous reports of functional changes during perceptual learning in monkey V1 and V4^{123, 124}, a steepening in the tuning curve of neurons tuned to orientations nearby the rewarded orientation are to be expected. We observed this effect during training by trend for neurons with a differential preferred orientation of 22.5° (Fig. 30). However, the effect was very weak. Interestingly, after the offset of training, we observed a significantly narrowed tuning width in neurons preferring the target orientation in good performers. As tuning width did not systematically change in these neurons during training, we can exclude a “reversal effect”. Still, it is unclear, whether the decrease in tuning width is causally linked to the training offset or just coincident, reflecting a later phase of learning or memory consolidation. Yet, because of the delayed appearance of the effect, it has – of all observed functional changes – the highest potential to represent a permanent memory trace.

6.2.9 Reward coding in V1

The correlation between functional changes in single neurons and task performance in individual mice suggests a role of V1 in memory formation during reward-based learning. Reliable association between a visual stimulus and a reward alters activity in visual cortex of rats¹⁹³ and humans¹⁹⁴. Interestingly, an eye-specific reward timing prediction was recently demonstrated in rat V1¹⁹³. Reward timing activity even persisted outside the task context, pointing to long-lasting, context-independent functional modifications during learning¹⁹³. Also in humans, reward leads to a task- and spatially specific increase in V1 activity³¹⁸. While these data strongly support a close association between reward signaling and visual signals in

V₁, a direct anatomical link between the reward circuit (Fig. 3) and V₁ has not been demonstrated yet (even though there is some evidence for dopaminergic input to cat V₁³¹⁹). However, close connections between higher visual areas and the reward circuit have been described, providing an indirect link between those areas and V₁ through top-down feedback connections in the visual system¹⁹⁰. Low-level reward-related visual learning can take place even in the absence of conscious perception¹⁹⁹ indicating an additional direct link between the reward circuit and lower visual areas circumventing higher visual areas. A potential pathway for this may run in parallel to the primary sensory thalamocortical projections and involves the lateral posterior and the supragenulate nucleus in the thalamus¹⁹⁰.

6.2.10 Learning-related plasticity in V₁

Taken together, primary visual cortex apparently is involved in memory formation at various levels, consistent with observations in other primary sensory cortical areas^{211, 212}. While, not surprisingly, V₁ is relevant as infrastructure for bottom-up information flow, indicated by a stabilized representation of orientation preference during learning, it seems to have additional functional impact in weighting incoming visual information. This process cannot be explained without close feedback interactions between V₁ and both higher visual areas and the reward circuit. In this context, our data support the view of the reverse hierarchy theory of perceptual learning, according to which optimized classification of visual stimuli is implemented resulting in an increasingly separated representation of the classified stimuli ('target' and 'non-target') in higher visual cortical areas. In the future, it will be very interesting to investigate, how the changes we observed in V₁ during learning are causally linked to functional modifications observed in extrastriate visual and prefrontal cortex during visual perceptual learning^{120, 122-125}, for example enhanced neuronal representation of the diagnostic features during categorization learning in inferior temporal cortex³²⁰. While a permissive or enhancing role of V₁ in memory formation is very likely, it remains elusive whether memory contents are stored in V₁. Long-term changes in V₁, which could represent memory traces, have been reported¹⁹³. We have identified a delayed training-induced decrease in tuning width in neurons preferring the target orientation which potentially might

be a memory correlate. Whether this is in fact the case, however, has to be investigated in subsequent studies.

6.3 Synopsis - experience-dependent and learning-induced plasticity in V1 neurons

In summary, I demonstrated the high adaptability of V1 in both an experience-dependent and a learning context in my thesis. Instructed by visual experience, V1 neurons undergo functional plasticity, specifically, changes in orientation preference and/or response amplitude. Thereby, feature detection in a visual environment with given feature statistics is optimized. In visual perceptual learning, coding of relevant information in individual V1 neurons is revealed. The reference parameter, on which the mouse has to rely in order to successfully solve an orientation discrimination task, is orientation preference. The representation of orientation preference is stabilized during training. At the same time, informative functional changes in amplitude and tuning width are induced. These changes are predictive of successful learning and possibly reflect an optimized categorization of behaviorally relevant visual stimuli. Thus, in undergoing vital functional modifications during experience-dependent plasticity and learning of a visual task, V1 neurons promote proper detection and interpretation of features in the visual environment.

References

- 1Gilbert, C.D. & Wiesel, T.N. Functional-organization of the visual-cortex. Progress in Brain Research 58, 209-218 (1983).
- 2.....Covey, A. & Stoerig, P. The neurobiology of blindsight. Trends in Neurosciences 14, 140-145 (1991).
- 3.....Garey, L.J. & Powell, T.P.S. Experimental study of termination of lateral geniculo-cortical pathway in cat and monkey. Proceedings of the Royal Society of London Series B-Biological Sciences 179, 41-63 (1971).
- 4Peters, A. & Feldman, M.L. Projection of lateral geniculate-nucleus to area 17 of rat cerebral-cortex .1. General description. J. Neurocytol. 5, 63-84 (1976).
- 5.....Gilbert, C.D. & Wiesel, T.N. Morphology and intra-cortical projections of functionally characterized neurons in the cat visual-cortex. Nature 280, 120-125 (1979).
- 6Gilbert, C.D. & Kelly, J.P. Projections of cells in different layers of cats visual-cortex. J. Comp. Neurol. 163, 81-105 (1975).
- 7.....Douglas, R.J. & Martin, K.A.C. Neuronal circuits of the neocortex. Annu. Rev. Neurosci. 27, 419-451 (2004).
- 8Holländer, H. Origin of corticotectal projections in cat. Exp. Brain Res. 21, 433-439 (1974).
- 9Hübener, M. & Bolz, J. Morphology of identified projection neurons in layer-5 of rat visual-cortex. Neuroscience Letters 94, 76-81 (1988).
- 10Lund, J.S., Lund, R.D., Hendrickson, A.E., Bunt, A.H. & Fuchs, A.F. Origin of efferent pathways from primary visual-cortex, area 17, of macaque monkey as shown by retro-grade transport of horseradish-peroxidase. J. Comp. Neurol. 164, 287-303 (1975).
- 11Albus, K. & Donat-Oliver, F. Cells of origin of occipito-pontine projection in cat - functional properties and intracortical location. Exp. Brain Res. 28, 167-174 (1977).

References

- 12Hirsch, J.A., Gallagher, C.A., Alonso, J.M. & Martinez, L.M. Ascending projections of simple and complex cells in layer 6 of the cat striate cortex. *J. Neurosci.* 18, 8086-8094 (1998).
- 13.....Tombol, T., Hajdu, F. & Somogyi, G. Identification of golgi picture of layer-6 cortico-geniculate projection neurons. *Exp. Brain Res.* 24, 107-110 (1975).
- 14Metin, C., Godement, P. & Imbert, M. The primary visual-cortex in the mouse - receptive-field properties and functional-organization. *Exp. Brain Res.* 69, 594-612 (1988).
- 15.....Wang, Q.X. & Burkhalter, A. Area map of mouse visual cortex. *J. Comp. Neurol.* 502, 339-357 (2007).
- 16Marshel, J.H., Garrett, M.E., Nauhaus, I. & Callaway, E.M. Functional specialization of seven mouse visual cortical areas. *Neuron* 72, 1040-1054 (2011).
- 17Schuett, S., Bonhoeffer, T. & Hübener, M. Mapping retinotopic structure in mouse visual cortex with optical imaging. *J. Neurosci.* 22, 6549-6559 (2002).
- 18Wiesel, T.N., Hubel, D.H. & Lam, D.M.K. Autoradiographic demonstration of ocular-dominance columns in monkey striate cortex by means of transneuronal transport. *Brain Res.* 79, 273-279 (1974).
- 19Horton, J.C. & Hedleywhyte, E.T. Mapping of cytochrome-oxidase patches and ocular dominance columns in human visual-cortex. *Philos. Trans. R. Soc. Lond. Ser. B-Biol. Sci.* 304, 255-272 (1984).
- 20.....Shatz, C.J., Lindstrom, S. & Wiesel, T.N. Distribution of afferents representing right and left eyes in cats visual-cortex. *Brain Res.* 131, 103-116 (1977).
- 21Law, M.I., Zahs, K.R. & Stryker, M.P. Organization of primary visual-cortex (area-17) in the ferret. *J. Comp. Neurol.* 278, 157-180 (1988).
- 22.....Dräger, U.C. Receptive-fields of single cells and topography in mouse visual-cortex. *J. Comp. Neurol.* 160, 269-289 (1975).
- 23.....Hübener, M. Mouse visual cortex. *Curr. Opin. Neurobiol.* 13, 413-420 (2003).
- 24.....Andermann, M.L., Kerlin, A.M., Roumis, D.K., Glickfeld, L.L. & Reid, R.C. Functional specialization of mouse higher visual cortical areas. *Neuron* 72, 1025-1039 (2011).
- 25.....Niell, C.M. & Stryker, M.P. Highly selective receptive fields in mouse visual cortex. *J. Neurosci* 28, 7520-7536 (2008).
- 26.....Ohzawa, I., DeAngelis, G.C. & Freeman, R.D. Encoding of binocular disparity by complex cells in the cat's visual cortex. *J. Neurophysiol.* 77, 2879-2909 (1997).
- 27.....Hubel, D.H. & Wiesel, T.N. Receptive fields and functional architecture of monkey striate cortex. *J. Physiol.-London* 195, 215-& (1968).

-
- 28.....Hubel, D.H. & Wiesel, T.N. Receptive fields, binocular interaction and functional architecture in cats visual cortex. *J. Physiol.-London* 160, 106-154 (1962).
- 29.....Chapman, B., Zahs, K.R. & Stryker, M.P. Relation of cortical cell orientation selectivity to alignment of receptive-fields of the geniculocortical afferents that arborize within a single orientation column in ferret visual-cortex. *J. Neurosci.* 11, 1347-1358 (1991).
- 30.....Bonhoeffer, T. & Grinvald, A. Iso-orientation domains in cat visual-cortex are arranged in pinwheel-like patterns. *Nature* 353, 429-431 (1991).
- 31.....Ohki, K., et al. Highly ordered arrangement of single neurons in orientation pinwheels. *Nature* 442, 925-928 (2006).
- 32.....Hübener, M., Shoham, D., Grinvald, A. & Bonhoeffer, T. Spatial relationships among three columnar systems in cat area 17. *J. Neurosci.* 17, 9270-9284 (1997).
- 33.....Swindale, N.V., Shoham, D., Grinvald, A., Bonhoeffer, T. & Hübener, M. Visual cortex maps are optimized for uniform coverage. *Nat. Neurosci.* 3, 822-826 (2000).
- 34.....Ohki, K., Chung, S., Ch'ng, Y.H., Kara, P. & Reid, R.C. Functional imaging with cellular resolution reveals precise micro-architecture in visual cortex. *Nature* 433, 597-603 (2005).
- 35.....Sohya, K., Kameyama, K., Yanagawa, Y., Obata, K. & Tsumoto, T. GABAergic neurons are less selective to stimulus orientation than excitatory neurons in layer II/III of visual cortex, as revealed by *in vivo* functional Ca²⁺ imaging in transgenic mice. *J. Neurosci.* 27, 2145-2149 (2007).
- 36.....Reid, R.C. & Alonso, J.M. Specificity of monosynaptic connections from thalamus to visual-cortex. *Nature* 378, 281-284 (1995).
- 37.....Ferster, D., Chung, S. & Wheat, H. Orientation selectivity of thalamic input to simple cells of cat visual cortex. *Nature* 380, 249-252 (1996).
- 38.....Sillito, A.M. Contribution of inhibitory mechanisms to receptive-field properties of neurons in striate cortex of cat. *J. Physiol.-London* 250, 305-329 (1975).
- 39.....Sato, H., Katsuyama, N., Tamura, H., Hata, Y. & Tsumoto, T. Mechanisms underlying direction selectivity of neurons in the primary visual-cortex of the macaque. *J. Neurophysiol.* 74, 1382-1394 (1995).
- 40.....Ringach, D.L., Hawken, M.J. & Shapley, R. Dynamics of orientation tuning in macaque V1: The role of global and tuned suppression. *J. Neurophysiol.* 90, 342-352 (2003).
- 41.....Bosking, W.H., Zhang, Y., Schofield, B. & Fitzpatrick, D. Orientation selectivity and the arrangement of horizontal connections in tree shrew striate cortex. *J. Neurosci.* 17, 2112-2127 (1997).
-

References

- 42.....Gilbert, C.D. & Wiesel, T.N. Columnar specificity of intrinsic horizontal and cortico-cortical connections in cat visual-cortex. *J. Neurosci.* 9, 2432-2442 (1989).
- 43.....Ko, H., et al. Functional specificity of local synaptic connections in neocortical networks. *Nature* 473, 87-U100 (2011).
- 44Liu, B.-h., et al. Broad inhibition sharpens orientation selectivity by expanding input dynamic range in mouse simple cells. *Neuron* 71, 542-554 (2011).
- 45.....Monier, C., Chavane, F., Baudot, P., Graham, L.J. & Fregnac, Y. Orientation and direction selectivity of synaptic inputs in visual cortical neurons: A diversity of combinations produces spike tuning. *Neuron* 37, 663-680 (2003).
- 46Anderson, J.S., Carandini, M. & Ferster, D. Orientation tuning of input conductance, excitation, and inhibition in cat primary visual cortex. *J. Neurophysiol.* 84, 909-926 (2000).
- 47.....Kerlin, A.M., Andermann, M.L., Berezovskii, V.K. & Reid, R.C. Broadly tuned response properties of diverse inhibitory neuron subtypes in mouse visual cortex. *Neuron* 67, 858-871 (2010).
- 48Liu, B.H., et al. Visual receptive field structure of cortical inhibitory neurons revealed by two-photon imaging guided recording. *J. Neurosci.* 29, 10520-10532 (2009).
- 49Hofer, S.B., et al. Differential connectivity and response dynamics of excitatory and inhibitory neurons in visual cortex. *Nat. Neurosci.* 14, 1045-U1146 (2011).
- 50.....Gilbert, C.D. Laminar differences in receptive-field properties of cells in cat primary visual-cortex. *J. Physiol.-London* 268, 391-421 (1977).
- 51Runyan, C.A., et al. Response features of parvalbumin-expressing interneurons suggest precise roles for subtypes of inhibition in visual cortex. *Neuron* 67, 847-857 (2010).
- 52.....Niell, C.M. & Stryker, M.P. Modulation of visual responses by behavioral state in mouse visual cortex. *Neuron* 65, 472-479 (2010).
- 53.....Szuts, T.A., et al. A wireless multi-channel neural amplifier for freely moving animals. *Nat. Neurosci.* 14, 263-U363 (2011).
- 54.....Rocheffort, N.L., et al. Development of direction selectivity in mouse cortical neurons. *Neuron* 71, 425-432 (2011).
- 55.....Barlow, H.B. & Pettigrew, J.D. Lack specificity of neurones in visual cortex young kittens. *J. Physiol.-London* 218, P98-& (1971).
- 56.....Blakemore, C. & van Sluyters, R.C. Innate and environmental factors in development of kittens visual-cortex. *J. Physiol.-London* 248, 663-716 (1975).

-
- 57.....Hubel, D.H. & Wiesel, T.N. Receptive fields of cells in striate cortex of very young, visually inexperienced kittens. *J. Neurophysiol.* 26, 994-1002 (1963).
- 58.....Chapman, B. & Stryker, M.P. Development of orientation selectivity in ferret visual-cortex and effects of deprivation. *J. Neurosci.* 13, 5251-5262 (1993).
- 59.....White, L.E., Coppola, D.M. & Fitzpatrick, D. The contribution of sensory experience to the maturation of orientation selectivity in ferret visual cortex. *Nature* 411, 1049-1052 (2001).
- 60Gödecke, I., Kim, D.S., Bonhoeffer, T. & Singer, W. Development of orientation preference maps in area 18 of kitten visual cortex. *Eur. J. Neurosci.* 9, 1754-1762 (1997).
- 61Crair, M.C., Gillespie, D.C. & Stryker, M.P. The role of visual experience in the development of columns in cat visual cortex. *Science* 279, 566-570 (1998).
- 62.....Wiesel, T.N. & Hubel, D.H. Single-cell responses in striate cortex of kittens deprived of vision in 1 eye. *J. Neurophysiol.* 26, 1003-1017 (1963).
- 63.....Gordon, J.A. & Stryker, M.P. Experience-dependent plasticity of binocular responses in the primary visual cortex of the mouse. *J. Neurosci.* 16, 3274-3286 (1996).
- 64Wang, B.S., Sarnaik, R. & Cang, J. Critical period plasticity matches binocular orientation preference in the visual cortex. *Neuron* 65, 246-256 (2010).
- 65.....Li, Y., Fitzpatrick, D. & White, L.E. The development of direction selectivity in ferret visual cortex requires early visual experience. *Nat. Neurosci.* 9, 676-681 (2006).
- 66Li, Y., Van Hooser, S.D., Mazurek, M., White, L.E. & Fitzpatrick, D. Experience with moving visual stimuli drives the early development of cortical direction selectivity. *Nature* 456, 952-956 (2008).
- 67.....Hubel, D.H. & Wiesel, T.N. Period of susceptibility to physiological effects of unilateral eye closure in kittens. *J. Physiol.-London* 206, 419-& (1970).
- 68Huang, Z.J., et al. BDNF regulates the maturation of inhibition and the critical period of plasticity in mouse visual cortex. *Cell* 98, 739-755 (1999).
- 69Fagiolini, M. & Hensch, T.K. Inhibitory threshold for critical-period activation in primary visual cortex. *Nature* 404, 183-186 (2000).
- 70.....Fagiolini, M., et al. Separable features of visual cortical plasticity revealed by N-methyl-D-aspartate receptor 2A signaling. *Proc. Natl. Acad. Sci. U. S. A.* 100, 2854-2859 (2003).
- 71Morales, B., Choi, S.Y. & Kirkwood, A. Dark rearing alters the development of GABAergic transmission in visual cortex. *J. Neurosci.* 22, 8084-8090 (2002).
-

References

- 72.....Kirkwood, A., Rioult, M.G. & Bear, M.F. Experience-dependent modification of synaptic plasticity in visual cortex. *Nature* 381, 526-528 (1996).
- 73.....Philpot, B.D., Espinosa, J.S. & Bear, M.F. Evidence for altered NMDA receptor function as a basis for metaplasticity in visual cortex. *J. Neurosci.* 23, 5583-5588 (2003).
- 74.....Antonini, A., Fagiolini, M. & Stryker, M.P. Anatomical correlates of functional plasticity in mouse visual cortex. *J. Neurosci.* 19, 4388-4406 (1999).
- 75.....Sawtell, N.B., et al. NMDA receptor-dependent ocular dominance plasticity in adult visual cortex. *Neuron* 38, 977-985 (2003).
- 76.....Tagawa, Y., Kanold, P.O., Majdan, M. & Shatz, C.J. Multiple periods of functional ocular dominance plasticity in mouse visual cortex. *Nat. Neurosci.* 8, 380-388 (2005).
- 77.....Hofer, S.B., Mrsic-Flogel, T.D., Bonhoeffer, T. & Hübener, M. Prior experience enhances plasticity in adult visual cortex. *Nat. Neurosci.* 9, 127-132 (2006).
- 78.....Feldman, D.E. Synaptic mechanisms for plasticity in neocortex. in *Annu. Rev. Neurosci.* 33-55 (2009).
- 79.....Rosenzweig, M.R. Environmental complexity cerebral change and behavior. *American Psychologist* 21, 321-& (1966).
- 80.....Rosenzweig, M.R., Bennett, E.L., Hebert, M. & Morimoto, H. Social grouping cannot account for cerebral effects of enriched environments. *Brain Res.* 153, 563-576 (1978).
- 81.....Sale, A., Berardi, N. & Maffei, L. Enrich the environment to empower the brain. *Trends in Neurosciences* 32, 233-239 (2009).
- 82.....Rampon, C., et al. Effects of environmental enrichment on gene expression in the brain. *Proc. Natl. Acad. Sci. U. S. A.* 97, 12880-12884 (2000).
- 83.....Keyvani, K., Sachser, N., Witte, O.W. & Paulus, W. Gene expression profiling in the intact and injured brain following environmental enrichment. *Journal of Neuropathology and Experimental Neurology* 63, 598-609 (2004).
- 84.....Cancedda, L., et al. Acceleration of visual system development by environmental enrichment. *J. Neurosci.* 24, 4840-4848 (2004).
- 85.....Kirkwood, A., Lee, H.K. & Bear, M.F. Coregulation of long-term potentiation and experience-dependent synaptic plasticity in visual-cortex by age and experience. *Nature* 375, 328-331 (1995).
- 86.....Sale, A., et al. Enriched environment and acceleration of visual system development. *Neuropharmacology* 47, 649-660 (2004).
- 87.....Bartoletti, A., Medini, P., Berardi, N. & Maffei, L. Environmental enrichment prevents effects of dark-rearing in the rat visual cortex. *Nat. Neurosci.* 7, 215-216 (2004).

-
- 88Sale, A., et al. Environmental enrichment in adulthood promotes amblyopia recovery through a reduction of intracortical inhibition. *Nat. Neurosci.* 10, 679-681 (2007).
- 89Kempermann, G., Kuhn, H.G. & Gage, F.H. More hippocampal neurons in adult mice living in an enriched environment. *Nature* 386, 493-495 (1997).
- 90Bennett, J.C., McRae, P.A., Levy, L.J. & Frick, K.M. Long-term continuous, but not daily, environmental enrichment reduces spatial memory decline in aged male mice. *Neurobiology of Learning and Memory* 85, 139-152 (2006).
- 91Blakemore, C. & Cooper, G.F. Modification of visual cortex by experience. *Brain Res.* 31, 366 (1971).
- 92.....Hirsch, H.V.B. & Spinelli, D.N. Visual experience modifies distribution of horizontally and vertically oriented receptive fields in cats. *Science* 168, 869-871 (1970).
- 93.....Chapman, B. & Bonhoeffer, T. Overrepresentation of horizontal and vertical orientation preferences in developing ferret area 17. *Proc. Natl. Acad. Sci. U. S. A.* 95, 2609-2614 (1998).
- 94Coppola, D.M., White, L.E., Fitzpatrick, D. & Purves, D. Unequal representation of cardinal and oblique contours in ferret visual cortex. *Proc. Natl. Acad. Sci. U. S. A.* 95, 2621-2623 (1998).
- 95.....Müller, T., et al. An analysis of orientation and ocular dominance patterns in the visual cortex of cats and ferrets. *Neural Comput.* 12, 2573-2595 (2000).
- 96Coppola, D.M., Purves, H.R., McCoy, A.N. & Purves, D. The distribution of oriented contours in the real world. *Proc. Natl. Acad. Sci. U. S. A.* 95, 4002-4006 (1998).
- 97.....Betsch, B.Y., Einhauser, W., Kording, K.P. & König, P. The world from a cat's perspective - statistics of natural videos. *Biol. Cybern.* 90, 41-50 (2004).
- 98Wark, R.C. & Peck, C.K. Behavioral consequences of early visual exposure to contours of a single orientation. *Dev. Brain Res.* 5, 218-221 (1982).
- 99Hirsch, H.V.B. Visual perception in cats after environmental surgery. *Exp. Brain Res.* 15, 405-423 (1972).
- 100Li, B.W., Peterson, M.R. & Freeman, R.D. Oblique effect: A neural basis in the visual cortex. *J. Neurophysiol.* 90, 204-217 (2003).
- 101.....Berkley, M.A., Kitterle, F. & Watkins, D.W. Grating visibility as a function of orientation and retinal eccentricity. *Vision Res.* 15, 239-244 (1975).
- 102Campbell, F.W. & Kulikows.Jj. Orientational selectivity of human visual system. *J. Physiol.-London* 187, 437-& (1966).
-

References

- 103Bouma, H. & Andriess, J. Perceived orientation of isolated line segments. *Vision Res.* 8, 493-500 (1968).
- 104Whitaker, D. & McGraw, P.V. Long-term visual experience recalibrates human orientation perception. *Nat. Neurosci.* 3, 13-13 (2000).
- 105Blakemore, C. & Cooper, G.F. Development of brain depends on visual environment. *Nature* 228, 477-478 (1970).
- 106Rauschecker, J.P. & Singer, W. The effects of early visual experience on the cat's visual cortex and their possible explanation by Hebb synapses. *J. Physiol.-London* 310, 215-239 (1981).
- 107Blasdel, G.G., Mitchell, D.E., Muir, D.W. & Pettigrew, J.D. Physiological and behavioral study in cats of effect of early visual experience with contours of a single orientation. *J. Physiol.-London* 265, 615-636 (1977).
- 108Sengpiel, F., Stawinski, P. & Bonhoeffer, T. Influence of experience on orientation maps in cat visual cortex. *Nat. Neurosci.* 2, 727-732 (1999).
- 109O'Hara, K., Miyashita, M. & Tanaka, S. Experience-dependent orientation plasticity in the visual cortex of rats chronically exposed to a single orientation. *Neurosci. Res.* 58, 86-90 (2007).
- 110Stryker, M.P., Sherk, H., Leventhal, A.G. & Hirsch, H.V.B. Physiological consequences for cat's visual cortex of effectively restricting early visual experience with oriented contours. *J. Neurophysiol.* 41, 896-909 (1978).
- 111Sengpiel, F., et al. Intrinsic and environmental factors in the development of functional maps in cat visual cortex. *Neuropharmacology* 37, 607-621 (1998).
- 112Rauschecker, J.P. Instructive changes in the kitten's visual cortex and their limitation. *Exp. Brain Res.* 48, 301-305 (1982).
- 113Crozier, R.A., Wang, Y., Liu, C.H. & Bear, M.F. Deprivation-induced synaptic depression by distinct mechanisms in different layers of mouse visual cortex. *Proc. Natl. Acad. Sci. U. S. A.* 104, 1383-1388 (2007).
- 114Mataga, N., Mizuguchi, Y. & Hensch, T.K. Experience-dependent pruning of dendritic spines in visual cortex by tissue plasminogen activator. *Neuron* 44, 1031-1041 (2004).
- 115Fregnac, Y., Shulz, D., Thorpe, S. & Bienenstock, E. A cellular analog of visual cortical plasticity. *Nature* 333, 367-370 (1988).
- 116Schuett, S., Bonhoeffer, T. & Hübner, M. Pairing-induced changes of orientation maps in cat visual cortex. *Neuron* 32, 325-337 (2001).

-
- 117Yao, H. & Dan, Y. Stimulus timing-dependent plasticity in cortical processing of orientation. *Neuron* 32, 315-323 (2001).
- 118Frenkel, M.Y., et al. Instructive effect of visual experience in mouse visual cortex. *Neuron* 51, 339-349 (2006).
- 119Dan, Y. & Poo, M.M. Spike timing-dependent plasticity: From synapse to perception. *Physiol. Rev.* 86, 1033-1048 (2006).
- 120Sasaki, Y., Nanez, J.E. & Watanabe, T. Advances in visual perceptual learning and plasticity. *Nat. Rev. Neurosci.* 11, 53-60 (2010).
- 121Dayan, P. & Niv, Y. Reinforcement learning: The good, the bad and the ugly. *Curr. Opin. Neurobiol.* 18, 185-196 (2008).
- 122Ahissar, M. & Hochstein, S. The reverse hierarchy theory of visual perceptual learning. *Trends in Cognitive Sciences* 8, 457-464 (2004).
- 123Schoups, A., Vogels, R., Qian, N. & Orban, G. Practising orientation identification improves orientation coding in V1 neurons. *Nature* 412, 549-553 (2001).
- 124Raiguel, S., Vogels, R., Mysore, S.G. & Orban, G.A. Learning to see the difference specifically alters the most informative V4 neurons. *J. Neurosci.* 26, 6589-6602 (2006).
- 125Adab, H.Z. & Vogels, R. Practicing coarse orientation discrimination improves orientation signals in macaque cortical area V4. *Curr. Biol.* 21, 1661-1666 (2011).
- 126Felleman, D.J. & Van Essen, D.C. Distributed hierarchical processing in the primate cerebral cortex. *Cerebral Cortex* 1, 1-47 (1991).
- 127Salin, P.A. & Bullier, J. Corticocortical connections in the visual-system - structure and function. *Physiol. Rev.* 75, 107-154 (1995).
- 128Holmes, G. Disturbances of vision by cerebral lesions. *Br J Ophthalmol* 2, 353-384 (1918).
- 129Maunsell, J.H.R. & Newsome, W.T. Visual processing in monkey extrastriate cortex. *Annu. Rev. Neurosci.* 10, 363-401 (1987).
- 130Wang, Q.X., Gao, E.Q. & Burkhalter, A. Gateways of Ventral and Dorsal Streams in Mouse Visual Cortex. *J. Neurosci.* 31, 1905-1918 (2012).
- 131Tong, F. Primary visual cortex and visual awareness. *Nat. Rev. Neurosci.* 4, 219-229 (2003).
- 132Murray, E.A., Bussey, T.J. & Saksida, L.M. Visual perception and memory: A new view of medial temporal lobe function in primates and rodents. in *Annu. Rev. Neurosci.* 99-122 (2007).
-

References

- 133.....Harris, J.A., Petersen, R.S. & Diamond, M.E. The cortical distribution of sensory memories. *Neuron* 30, 315-318 (2001).
- 134Harrison, S.A. & Tong, F. Decoding reveals the contents of visual working memory in early visual areas. *Nature* 458, 632-635 (2009).
- 135.....Barone, P., Batardiere, A., Knoblauch, K. & Kennedy, H. Laminar distribution of neurons in extrastriate areas projecting to visual areas V1 and V4 correlates with the hierarchical rank and indicates the operation of a distance rule. *J. Neurosci.* 20, 3263-3281 (2000).
- 136Treisman, A.M. & Gelade, G. Feature-integration theory of attention. *Cogn. Psychol.* 12, 97-136 (1980).
- 137.....Rees, G., Kreiman, G. & Koch, C. Neural correlates of consciousness in humans. *Nat. Rev. Neurosci.* 3, 261-270 (2002).
- 138Crick, F. & Koch, C. Are we aware of neural activity in primary visual-cortex. *Nature* 375, 121-123 (1995).
- 139Zeki, S. Localization and globalization in conscious vision. *Annu. Rev. Neurosci.* 24, 57-86 (2001).
- 140Zeki, S.M. Color coding in superior temporal sulcus of rhesus-monkey visual-cortex. *Proceedings of the Royal Society B-Biological Sciences* 197, 195-223 (1977).
- 141Gross, C.G., Bender, D.B. & RochaMir, Ce. Visual receptive fields of neurons in infero-temporal cortex of monkey. *Science* 166, 1303-& (1969).
- 142Leopold, D.A. & Logothetis, N.K. Multistable phenomena: Changing views in perception. *Trends in Cognitive Sciences* 3, 254-264 (1999).
- 143Pollen, D.A. Feature article on the neural correlates of visual perception. *Cerebral Cortex* 9, 4-19 (1999).
- 144Lamme, V.A.F. & Roelfsema, P.R. The distinct modes of vision offered by feedforward and recurrent processing. *Trends in Neurosciences* 23, 571-579 (2000).
- 145Bullier, J. Integrated model of visual processing. *Brain Research Reviews* 36, 96-107 (2001).
- 146Baars, B.J. In the theatre of consciousness. Global Workspace Theory, a rigorous scientific theory of consciousness. *Journal of Consciousness Studies* 4, 292-309 (1997).
- 147Wolfe, J.M. Moving towards solutions to some enduring controversies in visual search. *Trends in Cognitive Sciences* 7, 70-76 (2003).

-
- 148Doshier, B.A. & Lu, Z.L. Perceptual learning reflects external noise filtering and internal noise reduction through channel reweighting. *Proc. Natl. Acad. Sci. U. S. A.* 95, 13988-13993 (1998).
- 149Doshier, B.A. & Lu, Z.L. Mechanisms of perceptual learning. *Vision Res.* 39, 3197-3221 (1999).
- 150Petrov, A.A., Doshier, B.A. & Lu, Z.L. The dynamics of perceptual learning: An incremental reweighting model. *Psychological Review* 112, 715-743 (2005).
- 151Karni, A. & Sagi, D. The time-course of learning a visual skill. *Nature* 365, 250-252 (1993).
- 152.....Liu, Z.L. Perceptual learning in motion discrimination that generalizes across motion directions. *Proc. Natl. Acad. Sci. U. S. A.* 96, 14085-14087 (1999).
- 153.....Xiao, L.-Q., et al. Complete transfer of perceptual learning across retinal locations enabled by double training. *Curr. Biol.* 18, 1922-1926 (2008).
- 154Yang, T.M. & Maunsell, J.H.R. The effect of perceptual learning on neuronal responses in monkey visual area V4. *J. Neurosci.* 24, 1617-1626 (2004).
- 155.....Ahissar, M. & Hochstein, S. Attentional control of early perceptual-learning. *Proc. Natl. Acad. Sci. U. S. A.* 90, 5718-5722 (1993).
- 156Shiu, L.P. & Pashler, H. Improvement in line orientation discrimination is retinally local but dependent on cognitive set. *Perception & Psychophysics* 52, 582-588 (1992).
- 157.....Ahissar, M. & Hochstein, S. Task difficulty and the specificity of perceptual learning. *Nature* 387, 401-406 (1997).
- 158Lu, H.J., Qian, N. & Liu, Z.L. Learning motion discrimination with suppressed MT. *Vision Res.* 44, 1817-1825 (2004).
- 159Seitz, A.R., et al. Task-specific disruption of perceptual learning. *Proc. Natl. Acad. Sci. U. S. A.* 102, 14895-14900 (2005).
- 160Stickgold, R. Sleep-dependent memory consolidation. *Nature* 437, 1272-1278 (2005).
- 161.....Frank, M.G., Issa, N.P. & Stryker, M.P. Sleep enhances plasticity in the developing visual cortex. *Neuron* 30, 275-287 (2001).
- 162Karni, A., Tanne, D., Rubenstein, B.S., Askenasy, J.J.M. & Sagi, D. Dependence on rem-sleep of overnight improvement of a perceptual skill. *Science* 265, 679-682 (1994).
- 163Gais, S., Plihal, W., Wagner, U. & Born, J. Early sleep triggers memory for early visual discrimination skills. *Nat. Neurosci.* 3, 1335-1339 (2000).
-

References

- 164Stickgold, R., James, L. & Hobson, J.A. Visual discrimination learning requires sleep after training. *Nat. Neurosci.* 3, 1237-1238 (2000).
- 165Schwartz, S., Maquet, P. & Frith, C. Neural correlates of perceptual learning: A functional MIR study of visual texture discrimination. *Proc. Natl. Acad. Sci. U. S. A.* 99, 17137-17142 (2002).
- 166Walker, M.P., Stickgold, R., Jolesz, F.A. & Yoo, S.S. The functional anatomy of sleep-dependent visual skill learning. *Cerebral Cortex* 15, 1666-1675 (2005).
- 167Yotsumoto, Y., et al. Location-specific cortical activation changes during sleep after training for perceptual learning. *Curr. Biol.* 19, 1278-1282 (2009).
- 168Grossberg, S. How does a brain build a cognitive code. *Psychological Review* 87, 1-51 (1980).
- 169Ahissar, M. Perceptual training: A tool for both modifying the brain and exploring it. *Proc. Natl. Acad. Sci. U. S. A.* 98, 11842-11843 (2001).
- 170Knight, R.T., Staines, W.R., Swick, D. & Chao, L.L. Prefrontal cortex regulates inhibition and excitation in distributed neural networks. *Acta Psychologica* 101, 159-178 (1999).
- 171Gilbert, C.D. & Sigman, M. Brain states: Top-down influences in sensory processing. *Neuron* 54, 677-696 (2007).
- 172.....Tsushima, Y., Seitz, A.R. & Watanabe, T. Task-irrelevant learning occurs only when the irrelevant feature is weak. *Curr. Biol.* 18, R516-R517 (2008).
- 173.....Moran, J. & Desimone, R. Selective attention gates visual processing in the extrastriate cortex. *Science* 229, 782-784 (1985).
- 174.....Vidyasagar, T.R. Gating of neuronal responses in macaque primary visual cortex by an attentional spotlight. *Neuroreport* 9, 1947-1952 (1998).
- 175.....Ito, M. & Gilbert, C.D. Attention modulates contextual influences in the primary visual cortex of alert monkeys. *Neuron* 22, 593-604 (1999).
- 176Roelfsema, P.R., Lamme, V.A.F. & Spekreijse, H. Object-based attention in the primary visual cortex of the macaque monkey. *Nature* 395, 376-381 (1998).
- 177.....Watanabe, T., et al. Task-dependent influences of attention on the activation of human primary visual cortex. *Proc. Natl. Acad. Sci. U. S. A.* 95, 11489-11492 (1998).
- 178Gandhi, S.P., Heeger, D.J. & Boynton, G.M. Spatial attention affects brain activity in human primary visual cortex. *Proc. Natl. Acad. Sci. U. S. A.* 96, 3314-3319 (1999).
- 179Brefczynski, J.A. & DeYoe, E.A. A physiological correlate of the 'spotlight' of visual attention. *Nat. Neurosci.* 2, 370-374 (1999).

-
- 180Somers, D.C., Dale, A.M., Seiffert, A.E. & Tootell, R.B.H. Functional MRI reveals spatially specific attentional modulation in human primary visual cortex. *Proc. Natl. Acad. Sci. U. S. A.* 96, 1663-1668 (1999).
- 181Saenz, M., Buracas, G.T. & Boynton, G.M. Global effects of feature-based attention in human visual cortex. *Nat. Neurosci.* 5, 631-632 (2002).
- 182Super, H., Spekreijse, H. & Lamme, V.A.F. Two distinct modes of sensory processing observed in monkey primary visual cortex (V1). *Nat. Neurosci.* 4, 304-310 (2001).
- 183Lee, T.S., Yang, C.F., Romero, R.D. & Mumford, D. Neural activity in early visual cortex reflects behavioral experience and higher-order perceptual saliency. *Nat. Neurosci.* 5, 589-597 (2002).
- 184Mehta, A.D., Ulbert, I. & Schroeder, C.E. Intermodal selective attention in monkeys. I: Distribution and timing of effects across visual areas. *Cerebral Cortex* 10, 343-358 (2000).
- 185Ress, D., Backus, B.T. & Heeger, D.J. Activity in primary visual cortex predicts performance in a visual detection task. *Nat. Neurosci.* 3, 940-945 (2000).
- 186Seitz, A. & Watanabe, T. A unified model for perceptual learning. *Trends in Cognitive Sciences* 9, 329-334 (2005).
- 187Schultz, W. Multiple reward signals in the brain. *Nat. Rev. Neurosci.* 1, 199-207 (2000).
- 188Schultz, W., Tremblay, L. & Hollerman, J.R. Reward processing in primate orbitofrontal cortex and basal ganglia. *Cerebral Cortex* 10, 272-283 (2000).
- 189Schultz, W. Behavioral dopamine signals. *Trends in Neurosciences* 30, 203-210 (2007).
- 190Komura, Y., et al. Retrospective and prospective coding for predicted reward in the sensory thalamus. *Nature* 412, 546-549 (2001).
- 191LeDoux, J.E., Farb, C.R. & Romanski, L.M. Overlapping projections to the amygdala and striatum from auditory processing areas of the thalamus and cortex. *Neuroscience Letters* 134, 139-144 (1991).
- 192Linke, R., De Lima, A.D., Schwegler, H. & Pape, H.C. Direct synaptic connections of axons from superior colliculus with identified thalamo-amygdaloid projection neurons in the rat: Possible substrates of a subcortical visual pathway to the amygdala. *J. Comp. Neurol.* 403, 158-170 (1999).
- 193Shuler, M.G. & Bear, M.F. Reward timing in the primary visual cortex. *Science* 311, 1606-1609 (2006).
- 194Serences, J.T. Value-based modulations in human visual cortex. *Neuron* 60, 1169-1181 (2008).
-

References

- 195Sidman, M., Brady, J.V., Boren, J.J., Conrad, D.G. & Schulman, A. Reward schedules and behavior maintained by intracranial self-stimulation. *Science* 122, 830-831 (1955).
- 196Garris, P.A., et al. Dissociation of dopamine release in the nucleus accumbens from intracranial self-stimulation. *Nature* 398, 67-69 (1999).
- 197Seitz, A., Lefebvre, C., Watanabe, T. & Jolicoeur, P. Requirement for high-level processing in subliminal learning. *Curr. Biol.* 15, R753-R755 (2005).
- 198Shibata, K., Yamagishi, N., Ishii, S. & Kawato, M. Boosting perceptual learning by fake feedback. *Vision Res.* 49, 2574-2585 (2009).
- 199Seitz, A.R., Kim, D. & Watanabe, T. Rewards evoke learning of unconsciously processed visual stimuli in adult humans. *Neuron* 61, 700-707 (2009).
- 200Rangel, A., Camerer, C. & Montague, P.R. A framework for studying the neurobiology of value-based decision making. *Nat. Rev. Neurosci.* 9, 545-556 (2008).
- 201Daw, N.D., Niv, Y. & Dayan, P. Uncertainty-based competition between prefrontal and dorsolateral striatal systems for behavioral control. *Nat. Neurosci.* 8, 1704-1711 (2005).
- 202Yin, H.H., Knowlton, B.J. & Balleine, B.W. Blockade of NMDA receptors in the dorso-medial striatum prevents action-outcome learning in instrumental conditioning. *Eur. J. Neurosci.* 22, 505-512 (2005).
- 203Valentin, V.V., Dickinson, A. & O'Doherty, J.P. Determining the neural substrates of goal-directed learning in the human brain. *J. Neurosci.* 27, 4019-4026 (2007).
- 204Balleine, B.W. Neural bases of food-seeking: Affect, arousal and reward in corticostriatal limbic circuits. *Physiology & Behavior* 86, 717-730 (2005).
- 205Pessiglione, M., Seymour, B., Flandin, G., Dolan, R.J. & Frith, C.D. Dopamine-dependent prediction errors underpin reward-seeking behaviour in humans. *Nature* 442, 1042-1045 (2006).
- 206Killcross, S. & Coutureau, E. Coordination of actions and habits in the medial prefrontal cortex of rats. *Cerebral Cortex* 13, 400-408 (2003).
- 207Yin, H.H. & Knowlton, B.J. The role of the basal ganglia in habit formation. *Nat. Rev. Neurosci.* 7, 464-476 (2006).
- 208Rohles, F.H. & Coy, R. A miniaturized operant conditioning chamber for behavioral research in the upper atmosphere. U S a F Wright Air Developm Cent Tech Note 59, 1-7 (1959).
- 209Rohles, F.H. & Grunzke, M.E. Sustained operant behavior in mice. A model for behavioral research in biosatellites. U S a F Wright Air Developmt Cent Tech Note, 59 (1959).

-
- 210Uchida, N. & Mainen, Z.F. Speed and accuracy of olfactory discrimination in the rat. *Nat. Neurosci.* 6, 1224-1229 (2003).
- 211 Bao, S.W., Chang, E.F., Woods, J. & Merzenich, M.M. Temporal plasticity in the primary auditory cortex induced by operant perceptual learning. *Nat. Neurosci.* 7, 974-981 (2004).
- 212 Ganguly, K. & Kleinfeld, D. Goal-directed whisking increases phase-locking between vibrissa movement and electrical activity in primary sensory cortex in rat. *Proc. Natl. Acad. Sci. U. S. A.* 101, 12348-12353 (2004).
- 213 Kepecs, A., Uchida, N., Zariwala, H.A. & Mainen, Z.F. Neural correlates, computation and behavioural impact of decision confidence. *Nature* 455, 227-U255 (2008).
- 214 Zeeb, F.D., Robbins, T.W. & Winstanley, C.A. Serotonergic and dopaminergic modulation of gambling behavior as assessed using a novel rat gambling task. *Neuropsychopharmacology* 34, 2329-2343 (2009).
- 215 Viana, D.S., Gordo, I., Sucena, E. & Moita, M.A.P. Cognitive and motivational requirements for the emergence of cooperation in a rat social game. *PLoS One* 5 (2010).
- 216 Saar, D., Grossman, Y. & Barkai, E. Reduced after-hyperpolarization in rat piriform cortex pyramidal neurons is associated with increased learning capability during operant conditioning. *Eur. J. Neurosci.* 10, 1518-1523 (1998).
- 217 Seroussi, Y., Brosh, I. & Barkai, E. Learning-induced reduction in post-burst after-hyperpolarization (AHP) is mediated by activation of PKC. *Eur. J. Neurosci.* 16, 965-969 (2002).
- 218 Saar, D. & Barkai, E. Long-term modifications in intrinsic neuronal properties and rule learning in rats. *Eur. J. Neurosci.* 17, 2727-2734 (2003).
- 219 Alkon, D.L. Calcium-mediated reduction of ionic currents - a biophysical memory trace. *Science* 226, 1037-1045 (1984).
- 220 Antonov, I., Antonova, I., Kandel, E.R. & Hawkins, R.D. The contribution of activity-dependent synaptic plasticity to classical conditioning in *Aplysia*. *J. Neurosci.* 21, 6413-6422 (2001).
- 221 Brons, J.F. & Woody, C.D. Long-term changes in excitability of cortical-neurons after pavlovian conditioning and extinction. *J. Neurophysiol.* 44, 605-615 (1980).
- 222 Moyer, J.R., Thompson, L.T. & Disterhoft, J.F. Trace eyeblink conditioning increases CA1 excitability in a transient and learning-specific manner. *J. Neurosci.* 16, 5536-5546 (1996).
- 223 Zhang, W. & Linden, D.J. The other side of the engram: Experience-driven changes in neuronal intrinsic excitability. *Nat. Rev. Neurosci.* 4, 885-900 (2003).
-

References

- 224.....Denk, W., Strickler, J.H. & Webb, W.W. 2-photon laser scanning fluorescence microscopy. *Science* 248, 73-76 (1990).
- 225.....Helmchen, F. & Denk, W. Deep tissue two-photon microscopy. *Nature Methods* 2, 932-940 (2005).
- 226.....Stosiek, C., Garaschuk, O., Holthoff, K. & Konnerth, A. *In vivo* two-photon calcium imaging of neuronal networks. *Proc. Natl. Acad. Sci. U. S. A.* 100, 7319-7324 (2003).
- 227.....Tian, L., et al. Imaging neural activity in worms, flies and mice with improved GCaMP calcium indicators. *Nature Methods* 6, 875-U113 (2009).
- 228.....Berridge, M.J., Lipp, P. & Bootman, M.D. The versatility and universality of calcium signalling. *Nat. Rev. Mol. Cell Biol.* 1, 11-21 (2000).
- 229.....Tsien, R.W. & Tsien, R.Y. Calcium channels stores and oscillations. in Palade, G. E. 715-760 (1990).
- 230.....Orbach, H.S., Cohen, L.B. & Grinvald, A. Optical mapping of electrical-activity in rat somatosensory and visual-cortex. *J. Neurosci.* 5, 1886-1895 (1985).
- 231.....Grewe, B.F., Langer, D., Kasper, H., Kampa, B.M. & Helmchen, F. High-speed *in vivo* calcium imaging reveals neuronal network activity with near-millisecond precision. *Nature Methods* 7, 399-U391 (2010).
- 232.....Hendel, T., et al. Fluorescence changes of genetic calcium indicators and OGB-1 correlated with neural activity and calcium *in vivo* and *in vitro*. *J. Neurosci.* 28, 7399-7411 (2008).
- 233.....Andermann, M.L., Kerlin, A.M. & Reid, R.C. Chronic cellular imaging of mouse visual cortex during operant behavior and passive viewing. *Frontiers in Cellular Neuroscience* 4 (2010).
- 234.....Mank, M., et al. A genetically encoded calcium indicator for chronic *in vivo* two-photon imaging. *Nat Methods* 5, 805-811 (2008).
- 235.....Nimmerjahn, A., Kirchhoff, F., Kerr, J.N. & Helmchen, F. Sulforhodamine 101 as a specific marker of astroglia in the neocortex *in vivo*. *Nat Methods* 1, 31-37 (2004).
- 236.....Holtmaat, A., et al. Long-term, high-resolution imaging in the mouse neocortex through a chronic cranial window. *Nat Protoc* 4, 1128-1144 (2009).
- 237.....Trachtenberg, J.T., et al. Long-term *in vivo* imaging of experience-dependent synaptic plasticity in adult cortex. *Nature* 420, 788-794 (2002).
- 238.....Weibull, W. A statistical distribution function of wide applicability. *Journal of Applied Mechanics-Transactions of the Asme* 18, 293-297 (1951).

-
- 239.....Harvey, L.O. Efficient estimation of sensory thresholds. *Behav. Res. Methods Instr. Comput.* 18, 623-632 (1986).
- 240Brainard, D.H. The Psychophysics Toolbox. *Spatial Vis.* 10, 433-436 (1997).
- 241Stryker, M.P. & Sherk, H. Modification of cortical orientation selectivity in cat by restricted visual experience - re-examination. *Science* 190, 904-906 (1975).
- 242.....Trachtenberg, J.T., Trepel, C. & Stryker, M.P. Rapid extragranular plasticity in the absence of thalamocortical plasticity in the developing primary visual cortex. *Science* 287, 2029-2032 (2000).
- 243.....Liu, C.H., Heynen, A.J., Shuler, M.G.H. & Bear, M.F. Cannabinoid receptor blockade reveals parallel plasticity mechanisms in different layers of mouse visual cortex. *Neuron* 58, 340-345 (2008).
- 244Webster, M.A. & Devalois, R.L. Relationship between spatial-frequency and orientation tuning of striate-cortex cells. *J. Opt. Soc. Am. A-Opt. Image Sci. Vis.* 2, 1124-1132 (1985).
- 245.....Jones, J.P., Stepnoski, A. & Palmer, L.A. The two-dimensional spectral structure of simple receptive-fields in cat striate cortex. *J. Neurophysiol.* 58, 1212-1232 (1987).
- 246Fregnac, Y. & Imbert, M. Early development of visual cortical-cells in normal and dark-reared kittens - relationship between orientation selectivity and ocular dominance. *J. Physiol.-London* 278, 27-44 (1978).
- 247.....Fagiolini, M., Pizzorusso, T., Berardi, N., Domenici, L. & Maffei, L. Functional post-natal-development of the rat primary visual-cortex and the role of visual experience - dark rearing and monocular deprivation. *Vision Res.* 34, 709-720 (1994).
- 248Bevins, R.A. & Besheer, J. Object recognition in rats and mice: a one-trial non-matching-to-sample learning task to study 'recognition memory'. *Nat. Protoc.* 1, 1306-1311 (2006).
- 249.....Karmarkar, U.R. & Dan, Y. Experience-dependent plasticity in adult visual cortex. *Neuron* 52, 577-585 (2006).
- 250.....Frick, K.M. & Gresack, J.E. Sex differences in the behavioral response to spatial and object novelty in adult C57BL/6 mice. *Behav. Neurosci.* 117, 1283-1291 (2003).
- 251.....Dalla, C. & Shors, T.J. Sex differences in learning processes of classical and operant conditioning. *Physiology & Behavior* 97, 229-238 (2009).
- 252.....McNaughton, B.L., Barnes, C.A. & O'Keefe, J. The contributions of position, direction, and velocity to single unit-activity in the hippocampus of freely-moving rats. *Exp. Brain Res.* 52, 41-49 (1983).
-

References

- 253.....Leutgeb, S., Leutgeb, J.K., Treves, A., Moser, M.B. & Moser, E.I. Distinct ensemble codes in hippocampal areas CA3 and CA1. *Science* 305, 1295-1298 (2004).
- 254.....McNaughton, B.L., Battaglia, F.P., Jensen, O., Moser, E.I. & Moser, M.B. Path integration and the neural basis of the 'cognitive map'. *Nat. Rev. Neurosci.* 7, 663-678 (2006).
- 255.....Blasdel, G.G. & Salama, G. Voltage-sensitive dyes reveal a modular organization in monkey striate cortex. *Nature* 321, 579-585 (1986).
- 256.....Chapman, B., Stryker, M.P. & Bonhoeffer, T. Development of orientation preference maps in ferret primary visual cortex. *J. Neurosci.* 16, 6443-6453 (1996).
- 257.....Martinez, L.M., et al. Receptive field structure varies with layer in the primary visual cortex. *Nat. Neurosci.* 8, 372-379 (2005).
- 258.....Kim, I.J., Zhang, Y.F., Yamagata, M., Meister, M. & Sanes, J.R. Molecular identification of a retinal cell type that responds to upward motion. *Nature* 452, 478-U411 (2008).
- 259.....Huberman, A.D., et al. Genetic identification of an on-off direction-selective retinal ganglion cell subtype reveals a layer-specific subcortical map of posterior motion. *Neuron* 62, 327-334 (2009).
- 260.....Kay, J.N., et al. Retinal ganglion cells with distinct directional preferences differ in molecular identity, structure, and central projections. *J. Neurosci.* 31, 7753-7762 (2011).
- 261.....Freeman, R.D. & Pettigrew, J.D. Alteration of visual-cortex from environmental asymmetries. *Nature* 246, 359-360 (1973).
- 262.....Gordon, B. & Presson, J. Orientation deprivation in cat - what produces the abnormal-cells. *Exp. Brain Res.* 46, 144-146 (1982).
- 263.....Tanaka, S., Tani, T., Ribot, J. & Yamazaki, T. Chronically mountable goggles for persistent exposure to single orientation. *J. Neurosci. Methods* 160, 206-214 (2007).
- 264.....Singer, W., Freeman, B. & Rauschecker, J. Restriction of visual experience to a single orientation affects the organization of orientation columns in cat visual-cortex - a study with deoxyglucose. *Exp. Brain Res.* 41, 199-215 (1981).
- 265.....Tieman, S.B. & Hirsch, H.V.B. Exposure to lines of only one orientation modifies dendritic morphology of cells in the visual-cortex of the cat. *J. Comp. Neurol.* 211, 353-362 (1982).
- 266.....De Paola, V., et al. Cell type-specific structural plasticity of axonal branches and boutons in the adult neocortex. *Neuron* 49, 861-875 (2006).
- 267.....Holtmaat, A., Wilbrecht, L., Knott, G.W., Welker, E. & Svoboda, K. Experience-dependent and cell-type-specific spine growth in the neocortex. *Nature* 441, 979-983 (2006).

-
- 268Hirsch, H.V.B., Leventhal, A.G., McCall, M.A. & Tieman, D.G. Effects of exposure to lines of one or two orientations on different cell-types in striate cortex of cat. *J. Physiol.-London* 337, 241-255 (1983).
- 269Kameyama, K., et al. Difference in binocularity and ocular dominance plasticity between GABAergic and excitatory cortical neurons. *J Neurosci* 30, 1551-1559 (2010).
- 270.....Gandhi, S.P., Yanagawa, Y. & Stryker, M.P. Delayed plasticity of inhibitory neurons in developing visual cortex. *Proc. Natl. Acad. Sci. U. S. A.* 105, 16797-16802 (2008).
- 271.....Coleman, P.D., Flood, D.G., Whitehead, M.C. & Emerson, R.C. Spatial sampling by dendritic trees in visual-cortex. *Brain Res.* 214, 1-21 (1981).
- 272.....Schiltz, C., et al. Neuronal mechanisms of perceptual learning: Changes in human brain activity with training in orientation discrimination. *Neuroimage* 9, 46-62 (1999).
- 273.....Erllich, J.C., Bialek, M. & Brody, C.D. A Cortical Substrate for Memory-Guided Orienting in the Rat. *Neuron* 72, 330-343 (2011).
- 274.....Wiest, M.C., Thomson, E., Pantoja, J. & Nicolelis, M.A.L. Changes in S1 neural responses during tactile discrimination learning. *J. Neurophysiol.* 104, 300-312 (2010).
- 275.....Malkki, H.A.I., Donga, L.A.B., De Groot, S.E., Battaglia, F.P. & Pennartz, C.M. Appetitive operant conditioning in mice: heritability and dissociability of training stages. *Frontiers in Behavioral Neuroscience* 4 (2010).
- 276.....Brooks, S.P., Pask, T., Jones, L. & Dunnett, S.B. Behavioural profiles of inbred mouse strains used as transgenic backgrounds. II. cognitive tests. *Genes Brain Behav.* 4, 307-317 (2005).
- 277.....Skinner, B.F. Phylogeny and ontogeny of behavior. *Science* 153, 1205-1213 (1966).
- 278.....Hikosaka, O. The habenula: from stress evasion to value-based decision-making. *Nat. Rev. Neurosci.* 11, 503-513 (2010).
- 279.....Papini, M.R. & Overmier, J.B. Partial-reinforcement and autoshaping of the pigeons key-peck behavior. *Learning and Motivation* 16, 109-123 (1985).
- 280Cowan, N. & Morey, C.C. Visual working memory depends on attentional filtering. *Trends in Cognitive Sciences* 10, 139-141 (2006).
- 281de Fockert, J.W., Rees, G., Frith, C.D. & Lavie, N. The role of working memory in visual selective attention. *Science* 291, 1803-1806 (2001).
- 282.....Freund, G. & Walker, D.W. Operant conditioning in mice. *Life Science Part 1 Physiology & Pharmacology* 11, 905-914 (1972).
- 283.....Bushnell, P.J. Detection of visual signals by rats: effects of signal intensity, event rate, and task type. *Behav. Processes* 46, 141-150 (1999).
-

References

- 284Ennaceur, A. & Delacour, J. A new one-trial test for neurobiological studies of memory in rats .1. Behavioral-data. *Behav. Brain Res.* 31, 47-59 (1988).
- 285.....Dere, E., Huston, J.P. & De Souza Silva, M.A. The pharmacology, neuroanatomy and neurogenetics of one-trial object recognition in rodents. *Neurosci. Biobehav. Rev.* 31, 673-704 (2007).
- 286Dudchenko, P.A. An overview of the tasks used to test working memory in rodents. *Neurosci. Biobehav. Rev.* 28, 699-709 (2004).
- 287.....Hammond, R.S., Tull, L.E. & Stackman, R.W. On the delay-dependent involvement of the hippocampus in object recognition memory. *Neurobiology of Learning and Memory* 82, 26-34 (2004).
- 288Clark, R.E., Zola, S.M. & Squire, L.R. Impaired recognition memory in rats after damage to the hippocampus. *J. Neurosci.* 20, 8853-8860 (2000).
- 289Winters, B.D., Saksida, L.M. & Bussey, T.J. Object recognition memory: Neurobiological mechanisms of encoding, consolidation and retrieval. *Neurosci. Biobehav. Rev.* 32, 1055-1070 (2008).
- 290McSweeney, F.K., Hinson, J.M. & Cannon, C.B. Sensitization-habituation may occur during operant conditioning. *Psychol. Bull.* 120, 256-271 (1996).
- 291Rasch, B. & Born, J. Maintaining memories by reactivation. *Curr. Opin. Neurobiol.* 17, 698-703 (2007).
- 292.....van Oortmerssen, G.A. Biological significance, genetics and evolutionary origin of variability in behaviour within and between inbred strains of mice (*mus-musculus*) - behaviour genetic study. *Behaviour* 38, 1-92 (1971).
- 293.....Kelleher, R.T. & Gollub, L.R. A review of positive conditioned reinforcement. *Jour Exptl Analysis Behavior* 5, 543-597 (1962).
- 294Miller, E.K., Erickson, C.A. & Desimone, R. Neural mechanisms of visual working memory in prefrontal cortex of the macaque. *J. Neurosci.* 16, 5154-5167 (1996).
- 295.....Ranganath, C., Cohen, M.X., Dam, C. & D'Esposito, M. Inferior temporal, prefrontal, and hippocampal contributions to visual working memory maintenance and associative memory retrieval. *J. Neurosci.* 24, 3917-3925 (2004).
- 296Miyashita, Y. & Hayashi, T. Neural representation of visual objects: encoding and top-down activation. *Curr. Opin. Neurobiol.* 10, 187-194 (2000).
- 297.....Milner, B. The medial temporal-lobe amnesic syndrome. *Psychiatric Clinics of North America* 28, 599-+ (2005).

-
- 298Miyashita, Y. Neuronal correlate of visual associative long-term memory in the primate temporal cortex. *Nature* 335, 817-820 (1988).
- 299Quiroga, R.Q., Kreiman, G., Koch, C. & Fried, I. Sparse but not 'Grandmother-cell' coding in the medial temporal lobe. *Trends in Cognitive Sciences* 12, 87-91 (2008).
- 300.....Griffiths, S., et al. Expression of long-term depression underlies visual recognition memory. *Neuron* 58, 186-194 (2008).
- 301Lee, H., Simpson, G.V., Logothetis, N.K. & Rainer, G. Phase locking of single neuron activity to theta oscillations during working memory in monkey extrastriate visual cortex. *Neuron* 45, 147-156 (2005).
- 302.....Nikolic, D. & Singer, W. Creation of visual long-term memory. *Perception & Psychophysics* 69, 904-912 (2007).
- 303.....Nathanson, J.L., Yanagawa, Y., Obata, K. & Callaway, E.M. Preferential labeling of inhibitory and excitatory cortical neurons by endogenous tropism of adeno-associated virus and lentivirus vectors. *Neuroscience* 161, 441-450 (2009).
- 304.....Lee, S.H., Rosenmund, C., Schwaller, B. & Neher, E. Differences in Ca²⁺ buffering properties between excitatory and inhibitory hippocampal neurons from the rat. *J. Physiol.-London* 525, 405-418 (2000).
- 305.....Keck, T., et al. Massive restructuring of neuronal circuits during functional reorganization of adult visual cortex. *Nat Neurosci* 11, 1162-1167 (2008).
- 306.....Xu, H.-T., Pan, F., Yang, G. & Gan, W.-B. Choice of cranial window type for *in vivo* imaging affects dendritic spine turnover in the cortex. *Nat. Neurosci.* 10, 549-551 (2007).
- 307.....Lowy, A.M., et al. Discrimination-learning requiring different memory components in rats - age and neurochemical comparisons. *Behav. Neurosci.* 99, 638-651 (1985).
- 308.....van Praag, H., Christie, B.R., Sejnowski, T.J. & Gage, F.H. Running enhances neurogenesis, learning, and long-term potentiation in mice. *Proc Natl Acad Sci U S A* 96, 13427-13431 (1999).
- 309.....van Praag, H., Kempermann, G. & Gage, F.H. Running increases cell proliferation and neurogenesis in the adult mouse dentate gyrus. *Nat Neurosci* 2, 266-270 (1999).
- 310Yuste, R. & Bonhoeffer, T. Morphological changes in dendritic spines associated with long-term synaptic plasticity. *Annu. Rev. Neurosci.* 24, 1071-1089 (2001).
- 311Hofer, S.B., Mrsic-Flogel, T.D., Bonhoeffer, T. & Hübener, M. Experience leaves a lasting structural trace in cortical circuits. *Nature* 457, 313-U314 (2009).
-

References

- 312.....Roberts, T.F., Tschida, K.A., Klein, M.E. & Mooney, R. Rapid spine stabilization and synaptic enhancement at the onset of behavioural learning. *Nature* 463, 948-U123 (2010).
- 313.....Messinger, A., Squire, L.R., Zola, S.M. & Albright, T.D. Neuronal representations of stimulus associations develop in the temporal lobe during learning. *Proc. Natl. Acad. Sci. U. S. A.* 98, 12239-12244 (2001).
- 314Chklovskii, D.B., Mel, B.W. & Svoboda, K. Cortical rewiring and information storage. *Nature* 431, 782-788 (2004).
- 315.....Ogasawara, H., Doi, T. & Kawato, M. Systems biology perspectives on cerebellar long-term depression. *Neurosignals* 16, 300-317 (2008).
- 316Zhang, X., Zhaoping, L., Zhou, T. & Fang, F. Neural activities in V1 create a bottom-up saliency map. *Neuron* 73, 183-192 (2012).
- 317.....Xu, T., et al. Rapid formation and selective stabilization of synapses for enduring motor memories. *Nature* 462, 915-U108 (2009).
- 318Weil, R.S., et al. Rewarding feedback after correct visual discriminations has both general and specific influences on visual cortex. *J. Neurophysiol.* 104, 1746-1757 (2010).
- 319Parkinson, D. Evidence for a dopaminergic innervation of cat primary visual-cortex. *Neuroscience* 30, 171-179 (1989).
- 320.....Sigala, N. & Logothetis, N.K. Visual categorization shapes feature selectivity in the primate temporal cortex. *Nature* 415, 318-320 (2002).
- 321.....Levelt, C.N. & Hübener, M. Critical-period plasticity in the visual cortex. *Annu. Rev. Neurosci.* 35, 309-330 (2012).

Acknowledgements

I thank Mark Hübener, my supervisor, for support in every scientific and non-scientific aspect. I enjoyed our extended discussions in an open, friendly, and cooperative atmosphere. Especially, I am grateful for Mark's open-minded view on my ideas, giving me freedom to develop and implement my own approaches. At the same time, he directed my awareness to inconsistencies and pitfalls. Whenever possible, he took his time and readily gave me advice both on my projects and my future career.

To Tobias Bonhoeffer, our head of department, I am thankful for his helpful comments in a number of discussions particularly when preparing my paper manuscript. Furthermore, I thank him for his advice and support regarding my future career. He conveyed a collaborative, friendly and enjoyable atmosphere to the lab by promoting retreats and joint adventures.

I am deeply grateful to my parents, who have been standing behind me and supporting me throughout all ups and downs of life. They have always believed in me. Providing me a solid basis to build my life upon, they are the foundation of everything that I have achieved. Therefore, I dedicate this thesis to them.

For all his help and support, particularly during the initial phase of my PhD project, I owe my deep gratitude to Marcus Leinweber, who also was a close collaborator during parts of my second thesis project.

I thank Max Sperling, Volker Staiger und Frank Voss. They provided me with technical support and valuable advice, whenever needed. Moreover, I am grateful to Gabriele Künzel, Heinz Brandstetter, and the whole animal house team, who were very cooperative and open to the implementation of stripe rearing and environmental enrichment in the animal house.

Acknowledgements

I appreciate their competent and reliable work. To the machine shop staff, especially Mr. Wintersberger, I am thankful for close collaboration, valuable input and high quality work manufacturing the mouse goggles and other custom-made devices. I thank all lab members for discussions, advice, enjoyable lunch times and fun experiences.

For financial support, for funding of conferences and courses, for special training, and for the opportunity of meeting great scientists, I owe my deep gratitude to the Boehringer Ingelheim Fonds, particularly Claudia Walther, Monika Beutelspacher and Sandra Schedler. For support, training, and funding, I thank the International Max Planck Research School for Life Sciences.

